NUREG/CR-0516
TREE-1236
for the U.S. Nuclear Regulatory Commission

Steve Scott
NAI-1220

EXPERIMENT DATA REPORT FOR TEST RIA 1-1 (REACTIVITY INITIATED ACCIDENT TEST SERIES)

RUSSELL J. BUCKLAND CHRISTINE E. WHITE
DAVID G. ABBOTT

May 1979

7908140484

EG&G Idaho, Inc.

IDAHO NATIONAL ENGINEERING LABORATORY

DEPARTMENT OF ENERGY

IDAHO OPERATIONS OFFICE UNDER CONTRACT DE-AC07-76IDO1570

647 305

Available from
National Technical Information Service
Springfield, Virginia 22161
Price: Printed Copy A06; Microfiche $3.00

The price of this document for requesters outside the North American continent can be obtained from the National Technical Information Service.

NUREG/CR-0516
TREE-1236
R3

EXPERIMENT DATA REPORT

FOR TEST RIA 1-1

(REACTIVITY INITIATED ACCIDENT TEST SERIES)

Russell J. Buckland
David G. Abbott
Christine E. White

EG&G Idaho, Inc.
Idaho Falls, Idaho 83401

Published May 1979

PREPARED FOR THE
U.S. NUCLEAR REGULATORY COMMISSION
AND THE U.S. DEPARTMENT OF ENERGY
IDAHO OPERATIONS OFFICE
UNDER CONTRACT NO. EY-76-C-07-1570
NRC FIN NO. A6041

ABSTRACT

Recorded test data are presented for Test RIA 1-1 of the Thermal Fuels Behavior Program Reactivity Initiated Accident Test Series I. This test, conducted at the Power Burst Facility, was designed to characterize the response of unirradiated and preirradiated fuel rods during an RIA event conducted at boiling water reactor hot-startup coolant conditions, and to evaluate test instrumentation response during a power burst. The data, presented in the form of graphs in engineering units, have been analyzed only to the extent necessary to ensure they are reasonable and consistent. These uninterpreted data from Test RIA 1-1 are presented in advance of detailed analysis and interpretation.

SUMMARY

The Reactivity Initiated Accident (RIA) Test RIA 1-1 was completed October 7, 1978, as part of the Thermal Fuels Behavior Program conducted by EG&G Idaho, Inc. for the U.S. Nuclear Regulatory Commission. Test RIA 1-1 was the first of six planned tests of RIA Test Series I, and was designed to satisfy the following objectives:

(1) Characterize the response of unirradiated and preirradiated fuel rods during an RIA event conducted at boiling water reactor (BWR) hot-startup coolant conditions

(2) Evaluate test instrumentation response during a power burst.

The Power Burst Facility provided the neutron and coolant environment which simulates the postulated reactivity initiated accident for a BWR at hot-startup conditions. The test facility components included:

(1) A reactor vessel and driver core region to provide the neutron environment

(2) An in-pile tube in the center of the driver core to contain the test rods

(3) A pressurized water flow loop to provide the coolant environment in the in-pile tube.

The test train assembly consisted of four individually shrouded pressurized water reactor-type fuel rods which were positioned in the in-pile tube at driver core level. Two rods were preirradiated to burnups of approximately 4600 MWd/t, and two were unirradiated fuel rods.

The test procedure included: (a) nonnuclear heatups to establish the initial test coolant conditions, (b) a power calibration to calibrate test fuel rod power with reactor power, (c) a nuclear conditioning to promote fuel pellet cracking and relocation, and (d) a single power burst to a reactor power of about 24 000 MW to simulate an RIA event. Posttest examination of the test rods revealed that all four experienced cladding failure as a result of the power burst.

The PBF data acquisition and reduction system recorded measurements of the test rod shroud flow rates, test rod cladding elongation, test rod and coolant temperatures, coolant pressures, reactor power, and neutron flux within the in-pile tube.

The data obtained from this test have been subjected to a thorough review and subsequently categorized as qualified, restrained, trend, or failed data. The power burst data are presented in the main body of this report and power calibration and preconditioning data are included on the microfiche attached to the back cover.

CONTENTS

FIGURES

647 313

MICROFICHE ADDRESSES FOR TEST RIA 1-1

B1 Fuel temperature Rod 3, 0.79 m above fuel stack bottom.

C1 Plenum temperature in Fuel Rod 3.

D1 Cladding temperature Rod 1, 0.46 m above fuel stack bottom.

E1 Cladding temperature Rod 1, 0.79 m above fuel stack bottom.

F1 Cladding temperature Rod 3, 0.46 m above fuel stack bottom.

G1 Cladding temperature Rod 3, 0.79 m above fuel stack bottom.

H1 Pressure increase in Fuel Rod 1 plenum.

I1 Pressure increase in Fuel Rod 3 plenum.

647 317

J1 Fluid temperature of Fuel Rod 1 coolant inlet.

K1 Fluid temperature of Fuel Rod 2 coolant inlet.

L1 Fluid temperature of Fuel Rod 3 coolant inlet.

M1 Fluid temperature of Fuel Rod 4 coolant inlet.

N1 Fluid temperature of Fuel Rod 1 coolant outlet.

O1 Fluid temperature of Fuel Rod 2 coolant outlet.

P1 Fluid temperature of Fuel Rod 3 coolant outlet.

B2 Fluid temperature of Fuel Rod 4 coolant outlet.

C2 Differential temperature of Rod 1 coolant inlet and outlet.

D2 Differential temperature of Rod 2 coolant inlet and outlet.

E2 Differential temperature of Rod 3 coolant inlet and outlet.

F2 Differential temperature of Rod 4 coolant inlet and outlet.

G2 Absolute pressure in upper test assembly.

H2 Absolute pressure in upper test assembly.

I2 Absolute pressure in upper test assembly.

J2 Absolute pressure in Fuel Rod 1 shroud.

K2 Absolute pressure in Fuel Rod 2 shroud.

L2 Absolute pressure in Fuel Rod 3 shroud.

M2 Absolute pressure in Fuel Rod 4 shroud.

N2 Volumetric flow rate in Fuel Rod 1 shroud inlet.

O2 Volumetric flow rate in Fuel Rod 2 shroud inlet.

P2 Volumetric flow rate in Fuel Rod 3 shroud inlet.

B3 Volumetric flow rate in Fuel Rod 4 shroud inlet.

647 318

C3 Cladding elongation of Fuel Rod 1.

D3 Cladding elongation of Fuel Rod 2.

E3 Cladding elongation of Fuel Rod 4.

F3 Neutron flux in Quadrant 1, 0.09 m above fuel stack bottom.

G3 Neutron flux in Quadrant 1, 0.27 m above fuel stack bottom.

H3 Neutron flux in Quadrant 1, 0.46 m above fuel stack bottom.

I3 Neutron flux in Quadrant 1, 0.64 m above fuel stack bottom.

J3 Neutron flux in Quadrant 1, 0.82 m above fuel stack bottom.

K3 Neutron flux in Quadrant 3, 0.09 m above fuel stack bottom.

L3 Neutron flux in Quadrant 3, 0.27 m above fuel stack bottom.

M3 Neutron flux in Quadrant 3, 0.46 m above fuel stack bottom.

N3 Neutron flux in Quadrant 3, 0.64 m above fuel stack bottom.

O3 Neutron flux in Quadrant 3, 0.82 m above fuel stack bottom.

P3 Reactor power from Core Ionization Chamber TR 1.

B4 Reactor power from Core Ionization Chamber TR 2.

C4 Reactor power from Core Evacuation Chamber EV 1.

D4 Reactor power from Core Evacuation Chamber EV 2.

E4 Gross neutron rate of fission product Detector.

F4 Gross neutron rate of fission product detector system.

TABLES

EXPERIMENT DATA REPORT

FOR TEST RIA 1-1

(REACTIVITY INITIATED ACCIDENT TEST SERIES)

I. INTRODUCTION

The Thermal Fuels Behavior Program (TFBP) is one of several programs being conducted by the Water Reactor Research Directorate of EG&G Idaho, Inc., for the U.S. Nuclear Regulatory Commission. The TFBP performs an integral analytical and experimental study of the behavior of nuclear fuel rods under normal, off-normal, and accident conditions in light water reactors. Data from the TFBP experimental effort are used to determine the completeness and accuracy of analytical models developed to predict fuel rod behavior for a wide range of postulated reactor operating conditions.

The objectives of the TFBP Reactivity Initiated Accident (RIA) Test Series I are to determine fuel failure thresholds, modes, and consequences as functions of energy depositions, irradiation history, and fuel rod design. For the RIA Test Series I, the pressure, temperature, and flow rate of the coolant are typical of the hot-startup conditions in commercial boiling water reactors (BWRs). These conditions were selected in order to simulate the coolant conditions of the most severe RIA postulated – the BWR control rod drop accident during hot-startup conditions.

Test RIA 1-1 was the first of six planned RIA Series I tests to be performed in the Power Burst Facility (PBF) following the preliminary RIA Scoping Test (RIA-ST). Completed October 7, 1978, Test RIA 1-1 had the following specific objectives:

(1) Characterize the response of unirradiated and preirradiated fuel rods during an RIA event conducted at BWR hot-startup conditions

(2) Evaluate test instrumentation response during an RIA test.

The test train assembly comprised four individual rods, two preirradiated and two unirradiated, with each surrounded by a separate flow shroud. The test sequence consisted of (a) nonnuclear heatups to establish test coolant conditions, (b) a power calibration to calibrate test rod power with reactor power, (c) a preconditioning period to promote fuel pellet cracking and restructuring, and (d) a single power burst to attain a reactor peak power of about 24 000 MW.

This report presents the data from Test RIA 1-1 in a form readily usable by the nuclear community in advance of detailed analysis and interpretation. The data have been subjected to a thorough review and categorized as qualified, restrained, trend, or failed data.

Power burst data are presented in Section IV and power calibration and preconditioning data plots are included on microfiche attached to the back cover of this report.

Section II of this report presents the system configuration, procedures, initial test conditions, and events that are specific to Test RIA 1-1; Section III provides brief descriptions of test instrumentation; and Section IV presents information necessary for data interpretation. Appendix A describes the methods used in applying posttest corrective adjustments to the data and subsequent qualification; and Appendix B presents a guide to the uncertainty associated with the data.

II. SYSTEM AND EVENTS FOR TEST RIA 1-1

The following system configuration, procedures, and events are specific to Test RIA 1-1.

1. SYSTEM CONFIGURATION

The Power Burst Facility (PBF) is located at the Idaho National Engineering Laboratory. The PBF reactor, shown in Figure 1, is contained in an open tank reactor vessel and consists of a driver core and a flux trap. A pressurized water coolant flow loop provides a wide range of coolant conditions in the flux trap test space.

The PBF core is a right-circular annulus 1.3 m in diameter and 0.91 m in length, enclosing a centrally located vertical flux trap 0.21 m in diameter. This core has been designed for steady state and power burst operation. The core contains eight control rods for reactivity control during steady state operation. During power burst operation, the control rods and four additional transient rods dynamically control reactivity. Each of the control and transient rods consists of a stainless steel canister which contains a cylindrical annulus of boron carbide and is operated in an air-filled shroud. A cutaway view of the PBF core is shown in Figure 2.

An in-pile tube (IPT) fits in the central flux trap region and contains the test train assembly. The IPT is a thick-walled, Inconel 718, high strength pressure tube designed to contain the steady-state operating pressure and any pressure surges from test fuel rod failures. Any conceivable failure of the test fuel during the test (such as cladding failure, gross fuel melting, fuel-coolant interactions, fuel failure propagation, fission product release, or metal-water reactions) can be safely contained by the PBF IPT without damage to the driver core.

A flow tube is positioned inside the IPT to direct the coolant flow. Coolant flow enters the top of the IPT above the reactor core and flows down the annulus between the IPT wall and the flow tube. The flow reverses at the bottom, passes up through the test train assembly, and exits above the reactor core at the IPT outlet. The flow tube consists of an upper stainless steel section, a center zircaloy-2 section for neutron economy in the test fuel, and a lower catch basket section for a heat sink and collection of fuel fragments. A nitrogen gas annulus is provided between the IPT wall and aluminum core filler piece because of the temperature gradient between the two. A radial cross section of the IPT in the reactor core area is shown in Figure 3.

The loop coolant system provides cooling water for the IPT at controllable pressures, temperatures, and flow rates. For Test RIA 1-1, this system simulated the hot-startup coolant conditions of a BWR. The system includes a pressurizer, a pump, heat exchangers for removing the energy transferred to the coolant by the test fuel, a flow control valve,

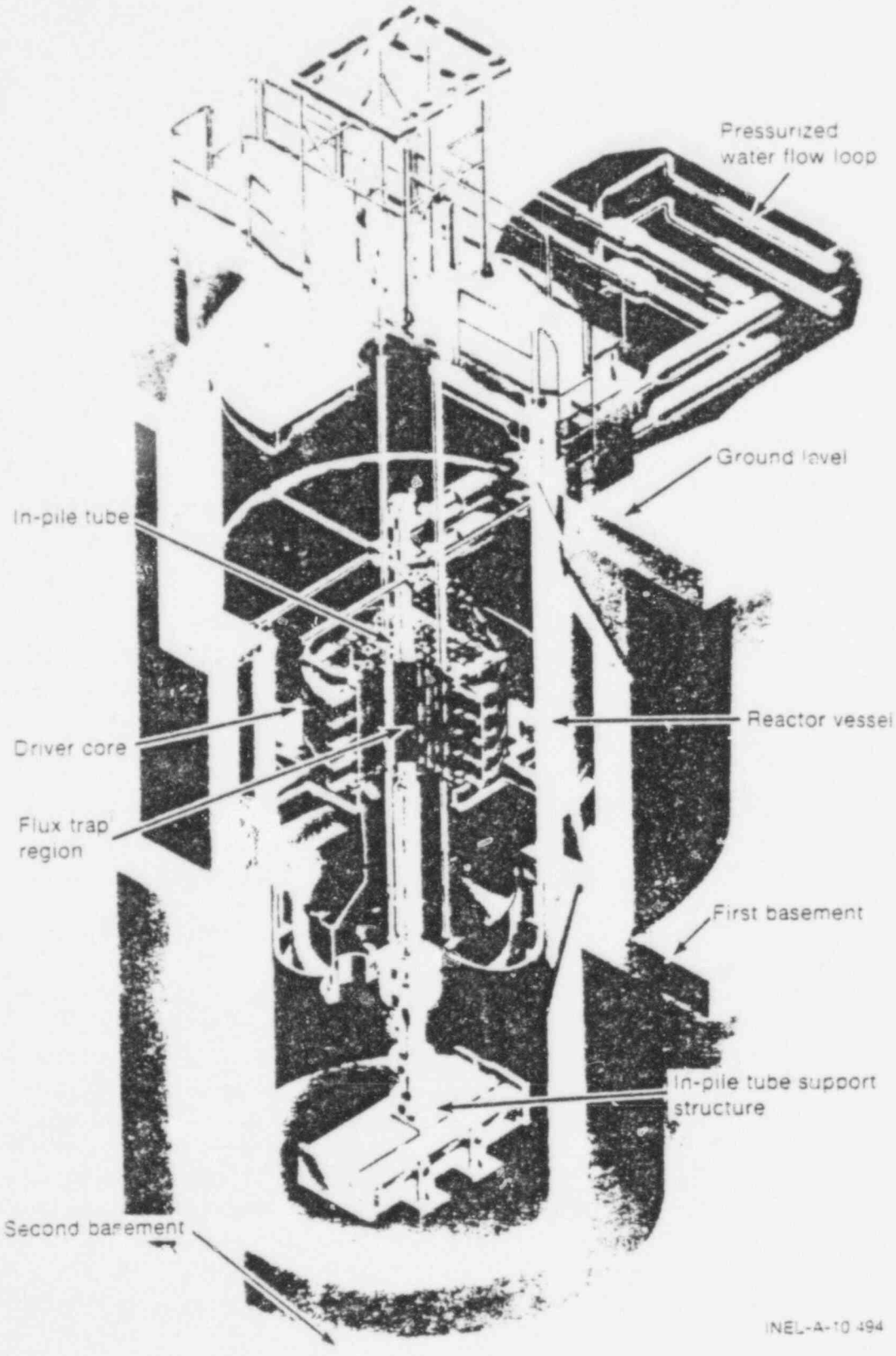

Fig. 1 Power Burst Facility reactor – cutaway view.

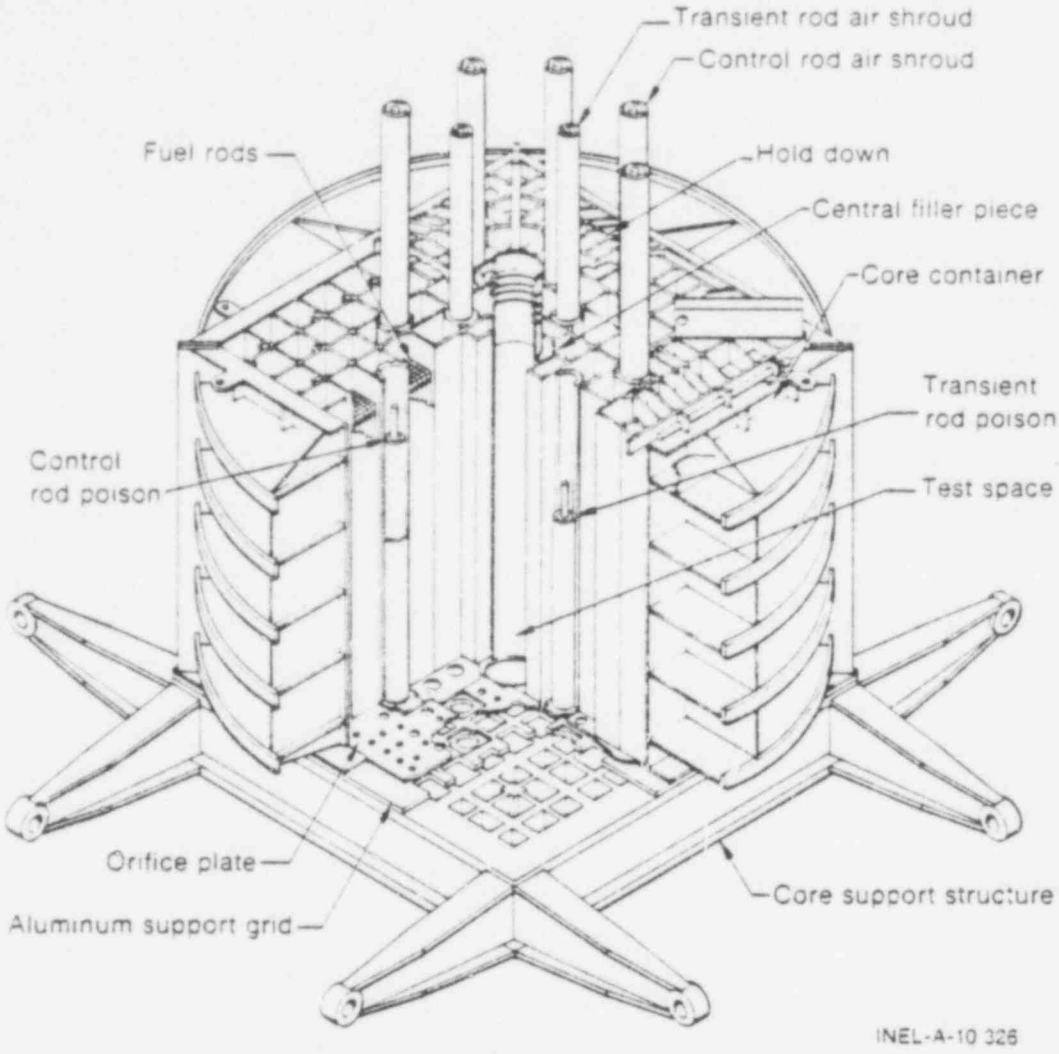

Fig. 2 Power Burst Facility core – cutaway view.

acoustic filters and thermal swell accumulators to attenuate any pressure surges from fuel failure, and electrical heaters to control the inlet temperature.

The Battelle Pacific Northwest Laboratory four-rod test train assembly was used for Test RIA 1-1. The test train assembly positions the test fuel rods in the driver core test space and provides support for a variety of test instrumentation hardware. Four independently shrouded fuel rods were rigidly secured at their top end to the assembly, but were free to expand axially downward. An axial cross section of Test RIA 1-1 test train assembly is shown in Figure 4, and Figure 5 is an orientation schematic of the test fuel rods.

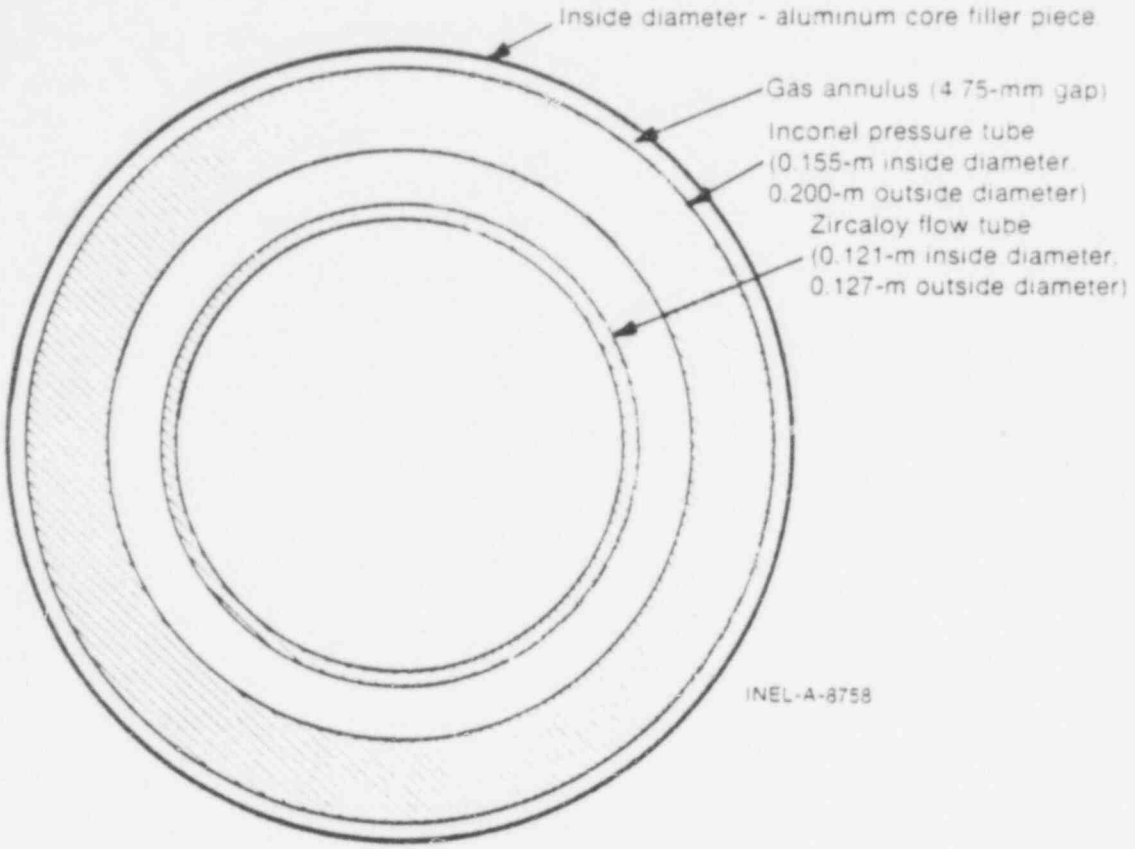

Fig. 3 Radial cross section of the PBF in-pile tube.

Five test fuel rods were used in Test RIA 1-1. Two MAPI[a] fuel rods, Rods 801-1 and 801-2, were previously irradiated to a burnup of approximately 4600 MWd/t in the Saxton Reactor[1]. Three unirradiated fuel rods, Rods 801-3, 801-4, and 801-5, were built by EG&G Idaho, Inc. Rod 801-4 was removed from the test assembly and replaced with Rod 801-5 after the power calibration and conditioning phases of the test were completed but prior to the power burst. The rod designations and burnups are given in Table I. The nominal design characteristics of these fuel rods are listed in Table II.

The top end cap was removed from Rod 801-1 and replaced with an end cap containing a pressure transducer. The rod was then backfilled with 77.7% helium and 22.3% argon to a pressure of 0.103 MPa. This gas mixture simulates the thermal conductivity of the fill gases, including fission gases in the MAPI fuel rods. Rod 801-2 was not opened prior to testing. Unirradiated Rods 801-3, 801-4, and 801-5 were backfilled with commercially pure helium to a pressure of 0.103 MPa.

a. The MAPI rods were built by Westinghouse Electric Co. and irradiated in the Saxton Reactor for the Mitsubishi Atomic Power Industries, Inc., Tokyo, Japan.

647 326

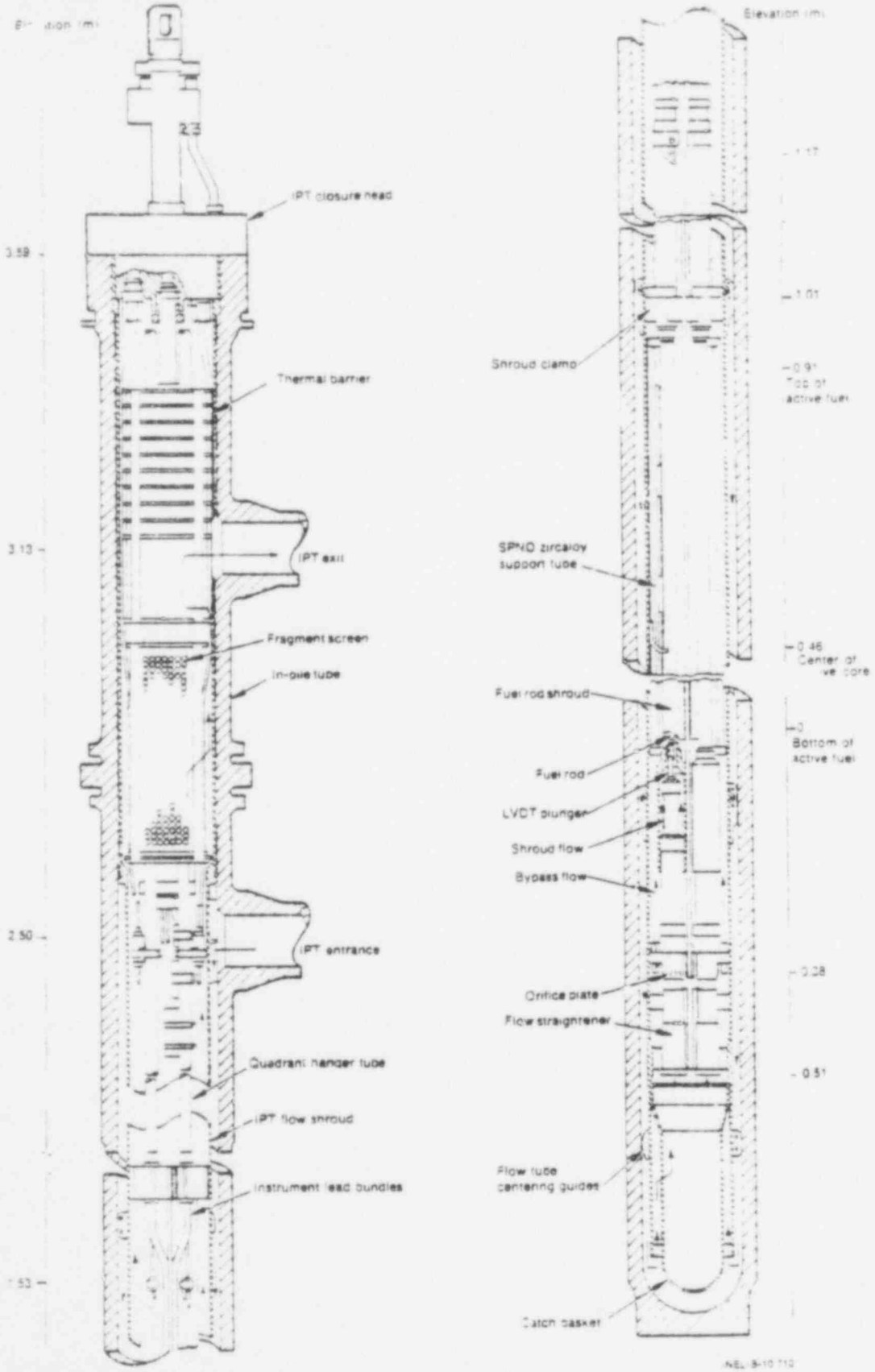

Fig. 4 Typ. RIA (+1 sec) fuel assembly axial cross section

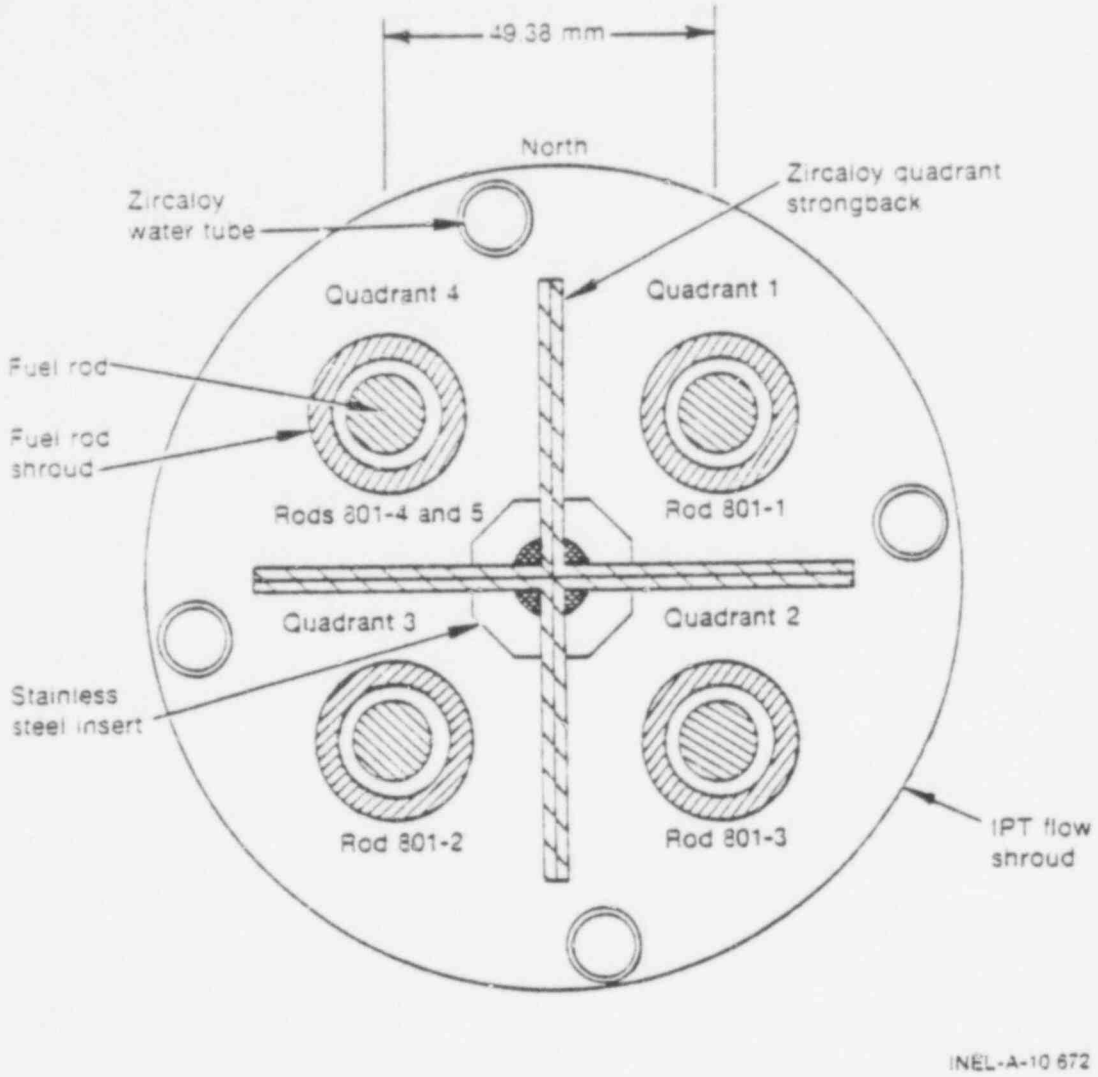

Fig. 5 Test fuel rod orientation schematic.

Individual zircaloy-4 flow shrouds, having a nominal inner diameter of 16.30 mm and an outer diameter of 22.60 mm, surrounded each rod. An orifice plate with a 6.95 ± 0.025-mm diameter hole was located below each shroud.

647 328

TABLE I

TEST RIA 1-1 ROD DESIGNATIONS AND BURNUP

Test RIA 1-1 Rod Identification	Westinghouse Electric Company Corresponding Rod Identification	Average Burnup (MWd/t)
801-1	M-42	4600
801-2	M-9	4650
801-3	958	Unirradiated
801-4	951	Unirradiated
801-5	950	Unirradiated

647 329

TABLE II

TEST RIA 1-1 FUEL ROD DESIGN CHARACTERISTICS

Characteristics	Irradiated Rods 801-1, -2[a]	Unirradiated Rods 801-3, -4, -5
Fuel		
Material	UO_2	UO_2
Pellet outside diameter (mm)	8.59	8.53
Pellet length (mm)	15.2	15.2
Pellet enrichment (wt%)	5.7	5.8
Density (% theoretical density)	94	94.5
Fuel stack length (m)	0.914	0.914
End configuration	Dished	Dished
Cladding		
Material	Zircaloy-4	Zircaloy-4
Tube outside diameter (mm)	9.99	9.93
Tube wall thickness (mm)	0.572	0.533
Yield strength (MPa)	570	570
Ultimate strength (MPa)	700	700
Fuel Rod		
Gas plenum length (mm)	45.7	45.7
Insulator pellets	None	None

a. Data are preirradiation values.

2. EXPERIMENT CONDUCT

Test RIA 1-1 comprised two heatup phases, a power calibration and preconditioning phase, and the power burst.

2.1 Heatup Phases

Prior to nuclear operation for both the power calibration and preconditioning phase and the power burst, the IPT system coolant conditions were established at 6.45 MPa pressure and 538 K IPT inlet temperature. The flow rate through each test rod shroud was adjusted to 0.76 l/s for the power calibration and preconditioning phases but was reduced to 0.085 l/s for the power burst.

The IPT system coolant chemistry requirements were established during both heatup phases and adjusted within the following limits:

pH range	5.7 to 10.2
Specific conductivity	1.4 to 48 μS/cm
Dissolved oxygen	Less than 0.1 ppm
Chlorides	Less than 0.15 ppm
Total suspended solids	Less than 1.0 ppm

Instrumentation calibrations were also performed throughout the heatup phases.

2.2 Power Calibration and Preconditioning Phase

The power calibration for Test RIA 1-1 served to calibrate the thermal-hydraulically determined test rod power with the reactor neutron detector chambers and the self-powered neutron detectors (SPNDs) mounted on the test train. The test rod power was calculated from a thermal balance using measurements of the coolant pressure, inlet temperatures, temperature increase across the test rod shroud, and the flow rate inside the shroud.

Test rod conditioning was accomplished by several cycles of reactor power changes. The power cycles promote fuel pellet cracking and relocation, and contribute to fission product inventory build up which improves cladding failure indication by the fission product detection system during the burst testing. The reactor core power history during the power calibration and preconditioning phases is summarized in Table III.

Following the completion of the power calibration and preconditioning phase, the test train assembly was removed from the IPT and test Rod 801-4 was removed and replaced with a fresh unirradiated rod, Rod 801-5. This exchange was made to provide a rod for

TABLE III

CORE POWER HISTORY DURING THE TEST RIA 1-1
POWER CALIBRATION AND PRECONDITIONING PHASE

Duration (minutes)	Reactor Power (MW)	Comments
	0	
6	0 to 1.0	Start of power calibration
8	1.0	
4	1.0 to 0	
	0	
8	0 to 2.5	
1	2.5	
9	2.5 to 5.0	
2	5.0	
10	5.0 to 7.5	
5	7.5	
12	7.5 to 11.6	
4	11.6	
12	11.6 to 15.1	
11	15.1	
15	15.1 to 18.6	
12	18.6	
13	18.6 to 22.0	
24	22.0	
40	22.0 to 25.5 to 0	Shutdown for plant adjustments
	0	
20	0 to 7.5	
4	7.5	
14	7.5 to 11.6	
5	11.6	
13	11.6 to 0	Shutdown for plant adjustments
	0	
20	0 to 7.5	
5	7.5	
10	7.5 to 11.6	

TABLE III (continued)

Duration (minutes)	Reactor Power (MW)	Comments
5	11.6	
8	11.6 to 15.1	
4	15.1	
8	15.1 to 18.6	
5	18.6	
9	18.6 to 22.0	
3	22.0	
8	22.0 to 25.5	
23	25.5	
6	25.5 to 27.0	
57	27.0	Power calibration completed
47	27.0 to 1.7	Additional preconditioning
3	1.7	
44	1.7 to 25.5	
60	25.5	
43	25.5 to 1.7	
5	1.7	
38	1.7 to 22.0	
60	22.0	
38	22.0 to 1.7	
13	1.7	
33	1.7 to 18.6	
17	18.6	
8	18.6 to 15.1	
4	15.1	
8	15.1 to 11.6	
4	11.6	
10	11.6 to 7.5	
2	7.5	
8	7.5 to 4.0	
2	4.0	
8	4.0 to 0	Preconditioning completed

posttest burnup analysis which had not received any pretransient irradiation. The total energy deposition during Test RIA 1-1 power burst will be determined from this burnup analysis later. The four flux wires mounted on the outer surface of each flow shroud were also replaced at this time.

2.3 Power Burst

The test train assembly was reinstalled in the IPT, test coolant conditions were established, and a single power burst to a peak power of about 24 000 MW with a reactor period of 3.1 ms was performed.

A reactivity balance method was used to initiate the power burst. This method provides assurance that the control and transient rods have not been grossly mispositioned and no potentially dangerous reactivity addition will be made. The sequence of events used to complete the power burst are shown in Figure 6 and described as follows:

(1) The control rods were withdrawn from their shutdown positions (Figure 6a) until criticality was achieved at about 100 W and the low power critical position of the control rods was determined (Figure 6b).

(2) From that position the control rods were further withdrawn until a reactor transient period of about 10 s was achieved. Then the reactor power was increased until the plant protection system was determined to be operating correctly. The control rods were then inserted until the reactor was subcritical.

(3) The transient rods were inserted into the core to a position calculated for the reactivity insertion required for the power burst (Figure 6c).

(4) The control rods were then withdrawn again to reestablish criticality at a low power level (Figure 6d). The reactivity inserted by the withdrawal of the control rods and the worth of the transient rods were compared for assurance that the increment of control rod withdrawal determined for the power burst was not grossly in error.

(5) The control rods were adjusted to the withdrawal position for the desired reactivity insertion.

(6) The transient rods were then fully inserted into the core (Figure 6e).

(7) To initiate the power burst, all four transient rods were ejected at a velocity of about 950 cm/s (Figure 6f). The power burst was

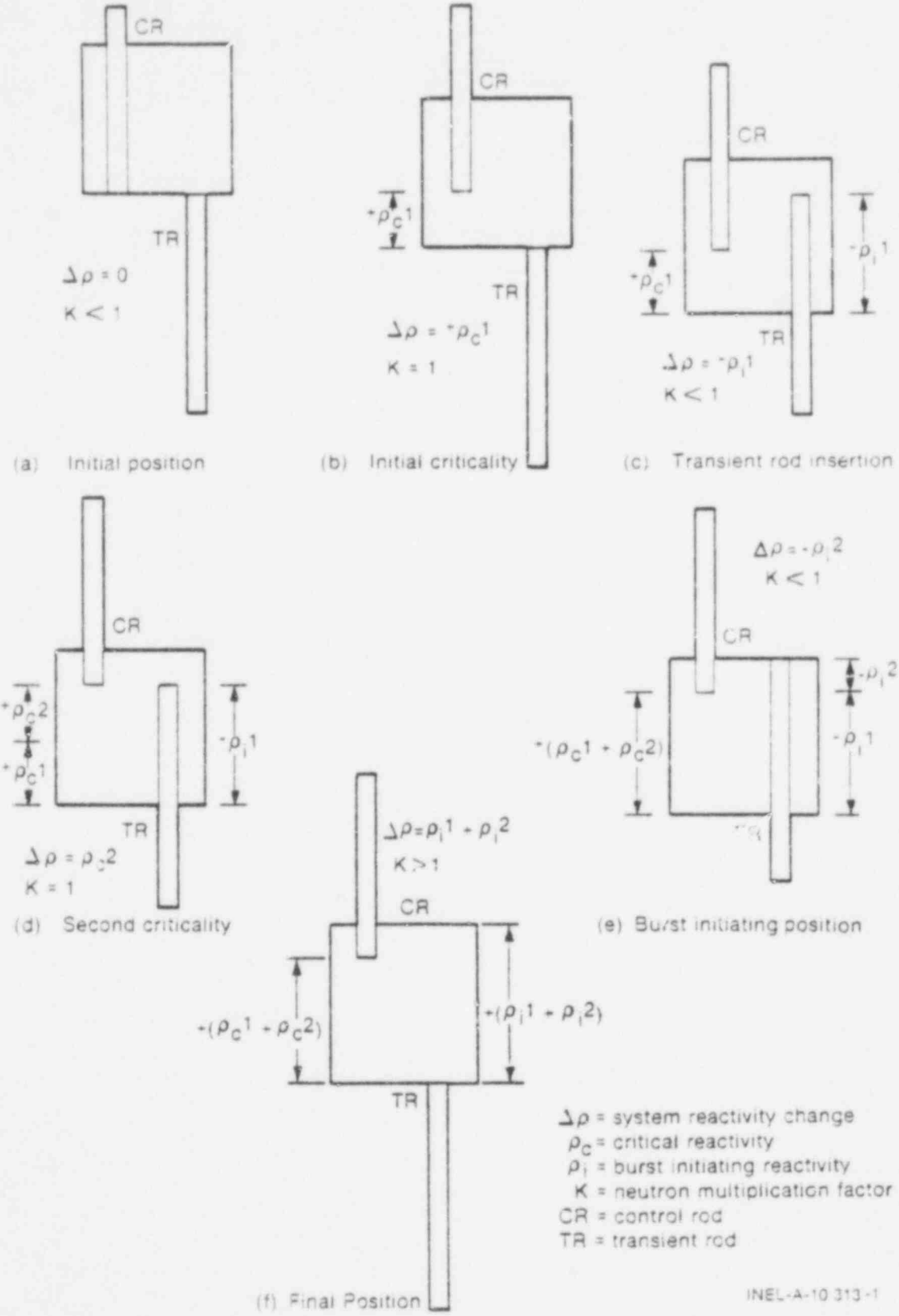

Fig. 6 Power burst testing sequence.

self-terminating by Doppler reactivity feedback which is capable of terminating the burst without primary dependence on mechanical systems. All eight control rods were completely inserted into the driver core immediately following the completion of the burst to provide a mechanical shutdown of the reactor.

Test rod instrumentation and the fission product detection system indicate that the test fuel experienced cladding failure. Posttest examination revealed that all four of the test fuel rods failed during or following the burst.

III. INSTRUMENTATION AND MEASUREMENTS

Instrumentation for Test RIA 1-1 was designed to aid in determining fuel rod response characteristics and failure mechanisms during an RIA event. The measurements presented in this report have been divided into three instrumentation sections: (a) fuel rod, (b) test train, and (c) plant.

1. FUEL ROD INSTRUMENTATION

Irradiated Rod 801-1 was instrumented for measurement of the internal gas pressure, cladding surface temperature, and cladding elongation. Unirradiated Rod 801-3 was fully instrumented for measurement of the internal gas pressure, cladding surface temperature, fuel centerline temperature, plenum temperature, and cladding elongation. Rods 801-2, 801-4, and 801-5 were instrumented only for cladding elongation.

The fuel rod instrumentation is further specified in the following description and the geometric orientation is shown in Figure 7. The measurement identifiers are included in parentheses and provide an abbreviated description of the measurement made, its orientation or position, and transducer manufacturer or range. The last two characters identify the measurement as a test train instrument (TT), a plant instrument (PT or FP, for fission product detection system), or a test rod number.

(1) One molybdenum-rhenium sheathed, tungsten-rhenium thermocouple (FUEL TMP 79 03) was located at 0.790 m above the bottom of the fuel stack of Rod 801-3 to measure the fuel centerline temperature.

(2) One EG&G Idaho, Inc., stainless steel sheathed, magnesia insulated, Type K therm couple (PLNM TMP 03) was located at the centerline of the spring in the upper plenum region of Rod 301-3 to measure the plenum gas temperature.

(3) Two EG&G Idaho, Inc., titanium sheathed, magnesia insulated, Type S (platinum/10% rhodium-platinum) cladding surface thermocouples with spaded junctions were installed on each of Rods 801-1 and 801-3. The thermocouples on irradiated Rod 801-1 were resistance welded to the cladding outer surface 0.46 m from the fuel stack bottom at 180-degree azimuthal orientation (CLAD TMP 46-18001), and 0.79 m from the fuel stack bottom at zero-degree azimuthal orientation (CLAD TMP 79-0 01). The unirradiated Rod 801-3 thermocouples were laser welded to the cladding outer surface 0.46 m from the fuel stack bottom at zero-degree azimuthal orientation

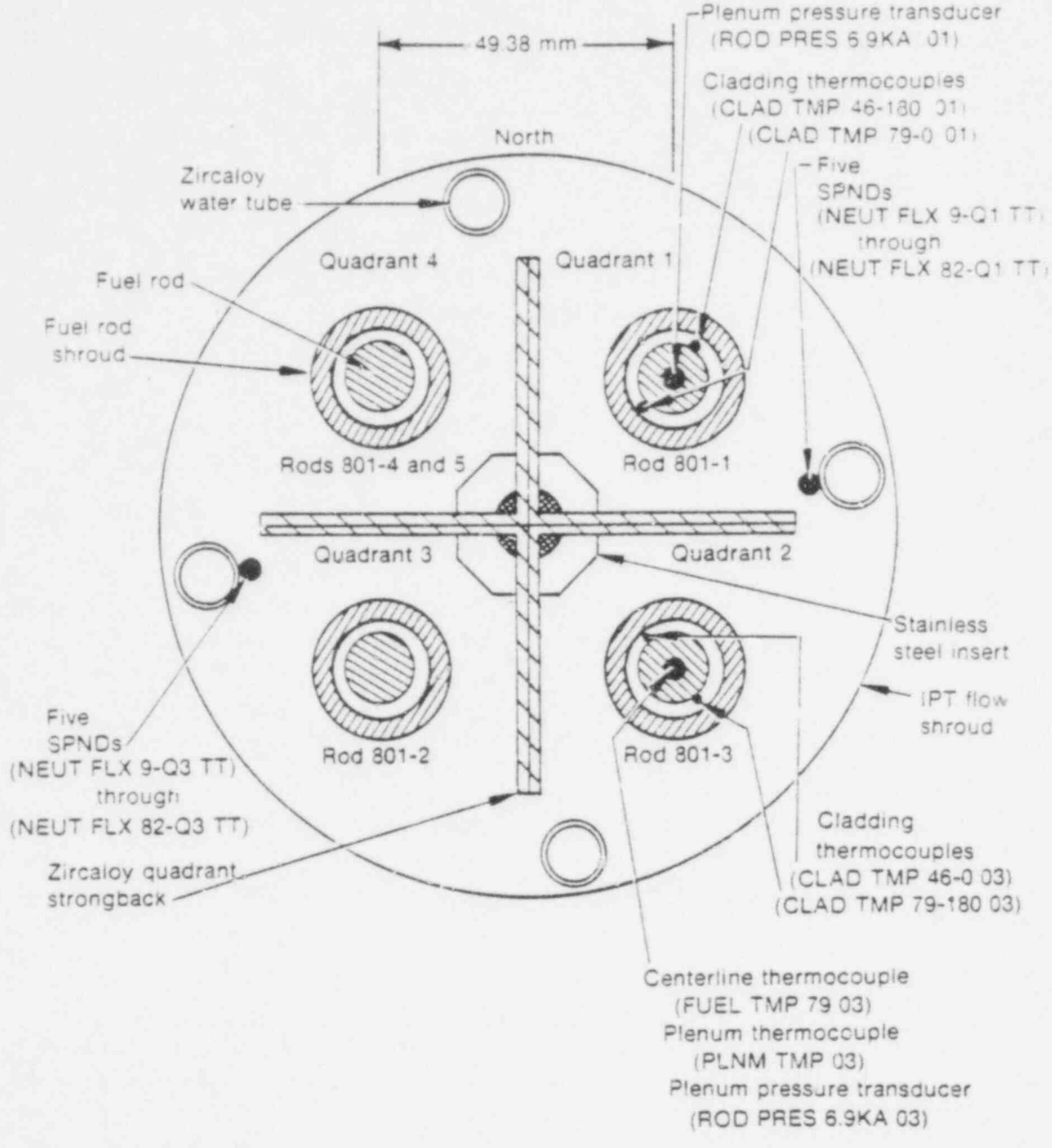

Fig. 7 Test fuel rod instrumentation orientation schematic.

(CLAD TMP 46-0 03), and 0.79 m from the fuel stack bottom at 180-degree azimuthal orientation (CLAD TMP 79-180 03). The zero-degree azimuthal position of each quadrant is toward the center of the assembly.

(4) One 6.9 MPa Kaman Sciences Corp. pressure transducer was mounted on Rods 801-1 (ROD PRES 6.9 KA 01) and 801-3 (ROD PRES 6.9 KA 03) to measure rod internal pressure in the upper plenum.

2. TEST TRAIN INSTRUMENTATION

The test train hardware provided support for a variety of measurement devices which primarily provided information on the coolant variables and neutron flux in the in-pile tube. The test train instrumentation is shown in Figure 8 and specified in the following description.

All of the test train thermocouples were stainless steel sheathed, magnesia insulated, and supplied by Control Products Corporation.

(1) A Chromel-Alumel, Type K, thermocouple was mounted at each fuel rod flow shroud inlet to measure the coolant inlet temperature (INLT TMP 01, 02, 03, 04/05).

(2) A Chromel-Alumel, Type K, thermocouple was mounted at each fuel rod flow shroud outlet to measure the coolant outlet temperature (OUT TEMP 01, 02, 03, 04/05).

(3) Two paired Chromel-Alumel, Type K thermocouples, one located at the fuel rod shroud inlet and the other at the outlet, measured the temperature rise in the coolant (DEL TEMP 01, 02, 03, 04/05).

(4) Three coolant pressure transducers, a 69-MPa EG&G Idaho, Inc., a 17.2-MPa Kaman Sciences Corp., and a 17.2-MPa Schaevitz Engineering, were located above the fuel rod flow shroud outlets in the upper test train to measure the transient pressure response and normal system pressure (SYS PRES 69 EG UTT) (SYS PRES 17 KA UTT) (SYS PRES SCHAV UTT).

(5) Four Kaman Sciences Corp., coolant pressure transducers were connected with tubing to the axial power peak location of the fuel rod flow shroud interiors to measure individual shroud transient pressure pulses generated during the burst and by fuel rod failure (SHRD PRES 17 KA 01, 02, 03, 04/05).

(6) A Flow Technology, Inc., turbine flowmeter, located at the inlet of each fuel rod flow shroud, measured the volumetric flow rate in each shroud (FLOWRATE INLET 01, 02, 03, 04/05).

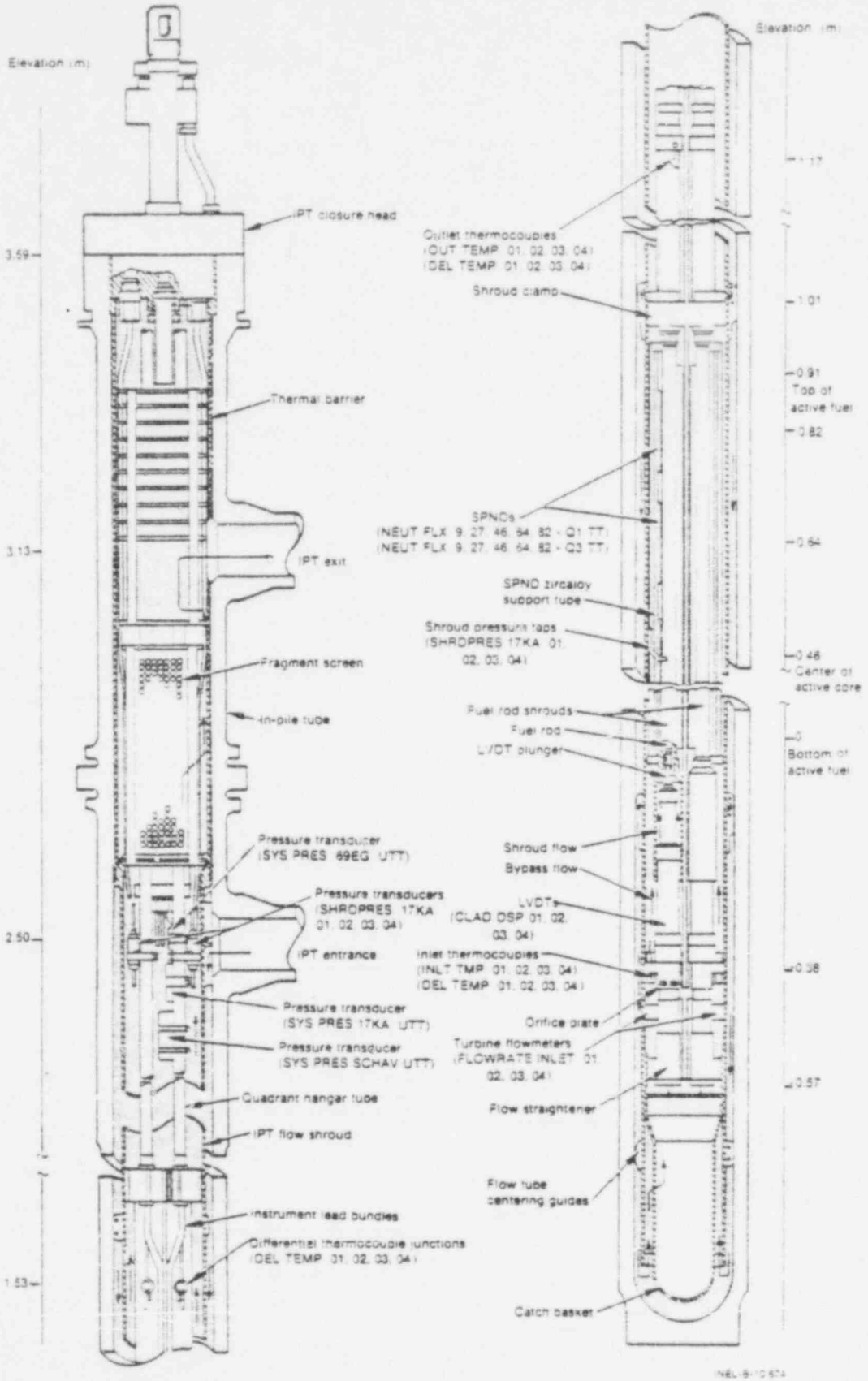

Fig. 8 Test train assembly axial cross section with instrumentation.

(7) An EG&G Idaho, Inc., variable differential transformer was mounted below the lower end of each fuel rod to measure the cladding axial elongation (CLAD DSP 01, 02, 03, 04/05).

(8) A flux wire was mounted on the outer surface of each fuel rod flow shroud at the 180-degree orientation to measure the integrated neutron flux. Flux wires with 0.51% cobalt and 99.49% aluminum content were used during the power calibration and preconditioning phase. These wires were removed and replaced with 100% cobalt wires before the transient power burst. The results of these measurements will not be presented in this report.

(9) Ten ARI Industries self-powered neutron detectors (SPNDs) were located in two vertical columns 180-degrees apart in Quadrants 1 and 3 to measure the relative neutron flux. The detector midpoints in each quadrant were located 0.09, 0.27, 0.46, 0.64, and 0.82 m above the bottom of the fuel stack (NEUT FLX 9, 27, 46, 64, 82 - Q1 TT) (NEUT FLX 9, 27, 46, 64, 82 - Q3 TT).

3. PLANT INSTRUMENTATION

The plant instrumentation included measurement of the PBF driver core power and the experimental loop coolant pressures. Ionization chambers sensitive to gamma and neutron radiation provided steady state and transient operating information, and their locations are shown in the driver core cross section, Figure 9. A simplified schematic diagram of the experimental loop showing the locations of pressure transducers and the fission product detectors is presented by Figure 10. The fission product detection system (FPDS) withdrew a continuous sample stream from the coolant loop near the IPT outlet and monitored the sample for fission products which would indicate test rod failure. The coolant transit time from the IPT to the detector locations was approximately 3.2 minutes. The plant instrumentation is specified in the following description.

(1) One 2.5- by 3.8-cm NaI crystal gamma ray detector was used to determine the gross gamma count rate in the sample line before, during, and after fission product release. The output from this detector was fed into two single channel analyzers. One analyzer (FP GAMMA NO. 1 FP) measured the gamma-ray intensity in the 150- to 3400-kev energy range and the other (FP GAMMA NO. 3 FP) in the 3400- to 6300-kev energy range.

(2) One 7.6- by 7.6-cm NaI crystal gamma ray detector (FP GAMMA NO. 2 FP) did not view the sample stream but measured the

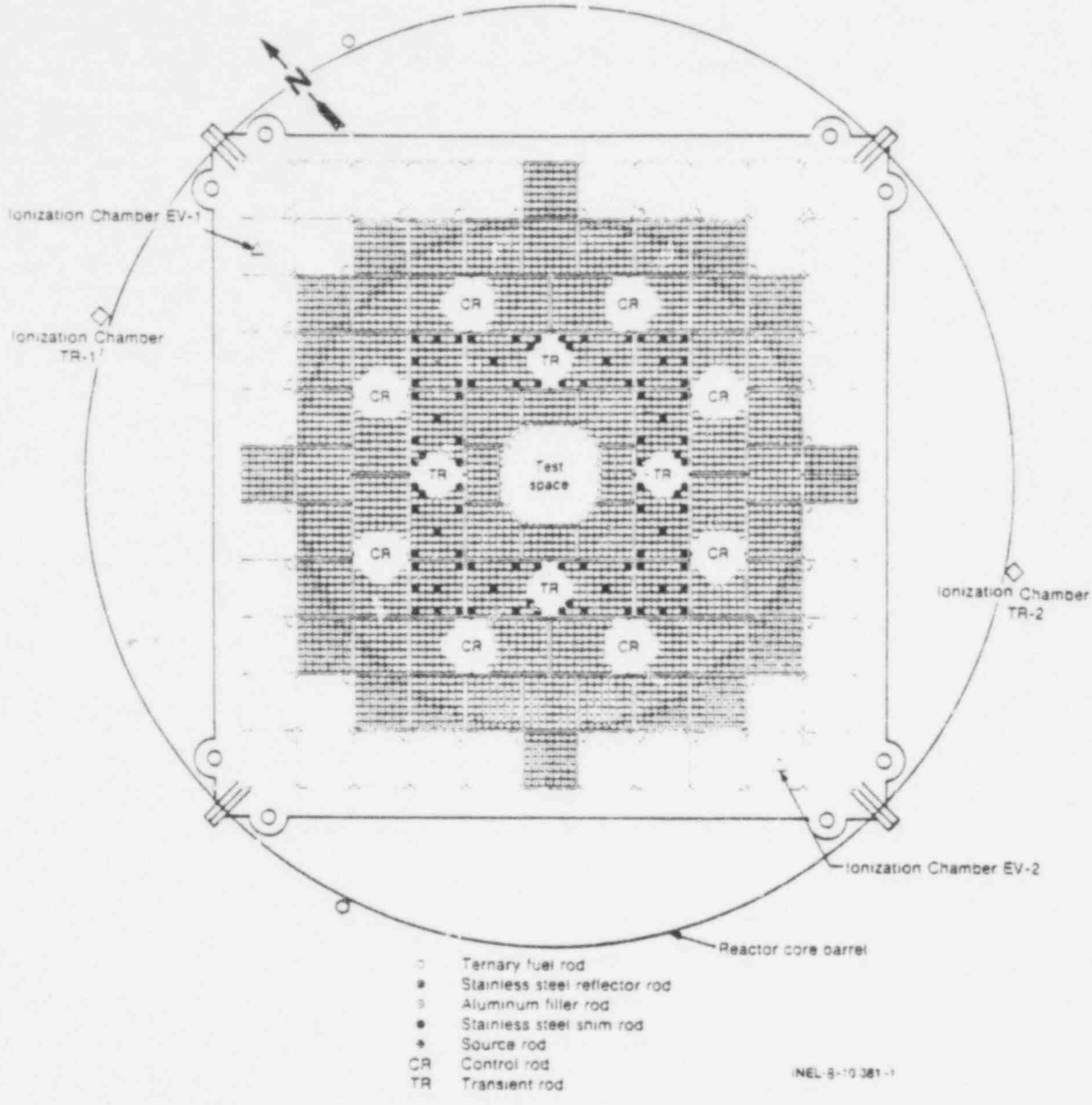

Fig. 9 Radial cross section of the PBF reactor core with ionization chamber locations.

effectiveness of the detector enclosure shielding against direct reactor radiation. This detector measured the gamma-ray intensity in the 150- to 6300-kev energy range.

(3) One BF_3 delayed neutron detector (FP NEUT FP) was used to detect delayed neutrons in the sample stream.

(4) Two Westinghouse Electric Corporation, WX-31994, nitrogen filled ionization chambers, TR-1 [(REAC POW 50TR1PT) low

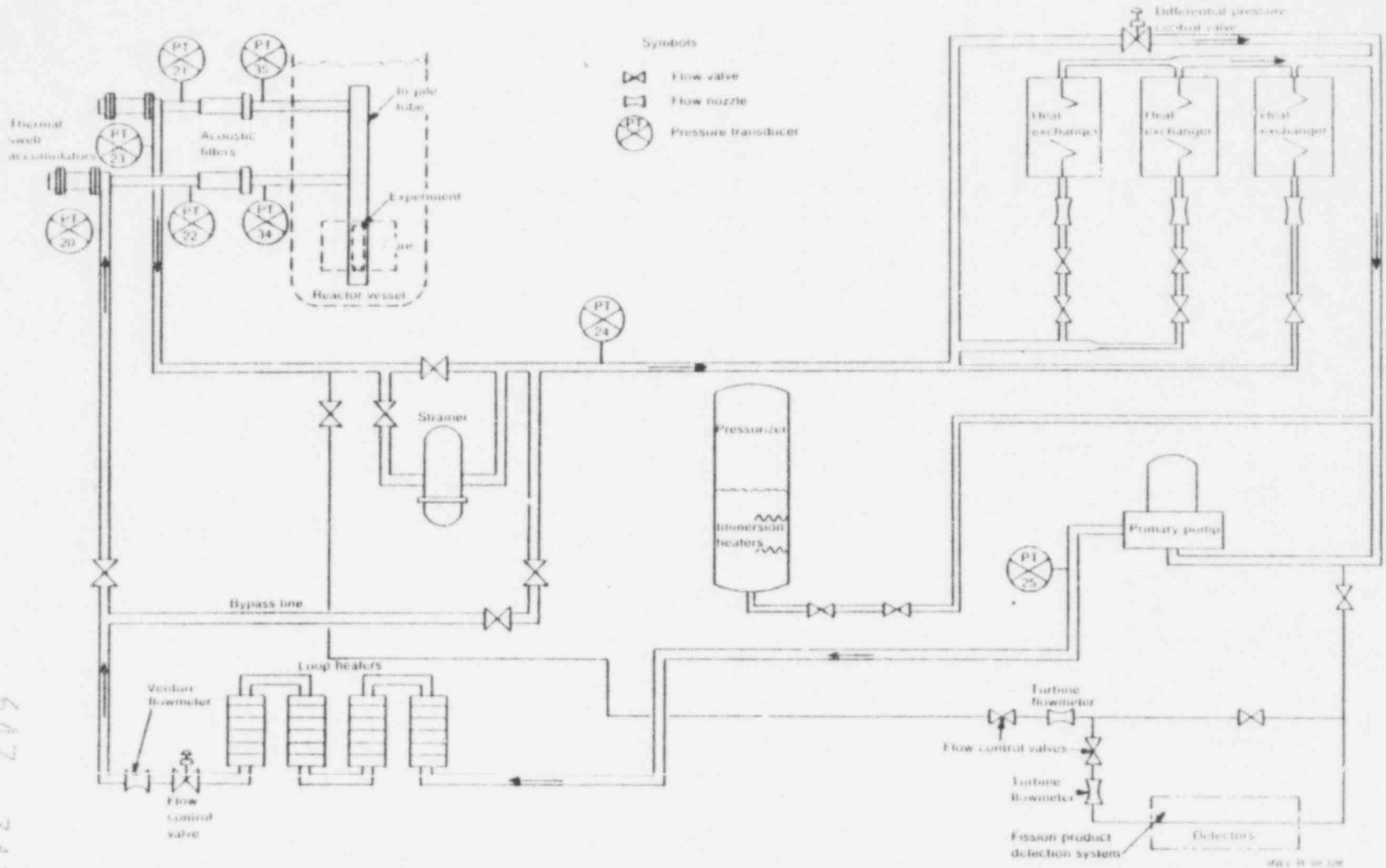

Fig. 10 Schematic of the PBF coolant loop system with pressure transducer and fission product detector locations.

range, (REAC POW 50KTR1PT) high range] and TR-2 [(REAC POW 50TR2PT) low range, (REAC POW 50KTR2PT) high range] were designed to measure power transients to 32 GW. Chambers TR-1 and TR-2 are located outside the core barrel at about 335 degrees and 145 degrees, respectively, from the reactor north.

(5) Two Westinghouse Electric Corporation, WX-31845, evacuated ionization chambers, EV-1 [(REAC POW 50EV1PT) low range, (REAC POW 50KEV1PT) high range] and EV-2 [(REAC POW 50EV2PT) low range, (REAC POW 50KEV2PT) high range] were designed to measure high power transients to 200 GW. Chambers EV-1 and EV-2 are located near the north and south corners, respectively, of the reactor core support structure.

(6) Three American Standard Norwood 103-MPa air-cooled pressure transducers, PT-22 (LOOPPRES 5-22 PT), PT-34 (LOOPPRES 5-34 PT), and PT-35 (LOOPPRES 5-35 PT) were to measure any large pressure surges in the coolant loop.

(7) Three American Standard Norwood 34.5-MPa air-cooled pressure transducers, PT-20 (LOOPPRES 5-20 PT), PT-21 (LOOPPRES 5-21 PT), and PT-23 (LOOPPRES 5-23 PT) were also measuring coolant loop pressure surges.

(8) Two Precise Sensors Inc., 34.5-MPa pressure transducers, PT-24 (LOOPPRES 5-24 PT) and PT-25 (LOOPPRES 5-25 PT) measured surges propagating further into the coolant loop piping.

IV. DATA PRESENTATION

The data from Test RIA 1-1 are presented with brief comment. The processing analysis has been performed only to the extent necessary to obtain appropriate engineering units and to ensure that the data are reasonable and consistent. All the data in this report were subjected to a thorough review by comparing instrument channel outputs with duplicate measurements, calculated parameter values, initial conditions, and pre- and postcalibration results. Appendix A describes the methods used to determine the adjustments that have been applied to the presented data and provides the basis for categorizing the data as follows:

(1) Qualified engineering unit data (QEUD) have been qualified to represent the variable being measured within specified uncertainty limits

(2) Restrained data – appear reasonable but are not within certainty limits, or data are not available from an independent channel for comparison

(3) Trend data – are suitable for illustrative purposes but probably not for numerical analysis

(4) Failed data – are irretrievable due to a transducer, signal conditioning, or data channel failure or inadequate rejection of extraneous noise, transients, or frequencies.

All detector analog ouput was digitized and recorded by the PBF data acquisition and reduction system (PBF/DARS). The PBF/DARS tape recording system was configured to record at four different bandwidths:

(1) dc to 10 Hz

(2) dc to 100 Hz

(3) dc to 5 kHz

(4) dc to 20 kHz.

Table IV lists all the measurements included in this report, specifies the measurement location and instrument type, indicates detector range and frequency response and PBF/DARS recording range and bandwidth, references the measurement to the corresponding figures, and lists the qualification category of each data segment. Data that have been fully qualified as QEUD have been so noted in the figure caption.

TABLE IV

DATA PRESENTATION FOR TEST RIA 1-1

Measurement	Location and Comments	Range		Frequency Response		Figure	Data Qualification[a]	
		Detector	Data Acquisition System	Detector	Data Acquisition System			
Fuel Rod								
FUEL IMP 79 03	Tungsten-rhenium thermocouple to measure fuel centerline temperature on Rod 801-3 located 79 cm above bottom of fuel stack.	500 to 2800 K	500 to 3000 K	350 Hz	100 Hz	11	From -5 to 0.4 s	QEUD
							0.4 to 40 s	Trend[b]
						B1		QEUD
PLNM IMP 03	Chromel-Alumel (Type K) thermocouple located in upper plenum of Rod 801-3 to measure temperature.	273 to 1309 K	0 to 1100 K	350 Hz	100 Hz	12		QEUD
						C1		QEUD
CLAD IMP 46-18001	Rhodium/platinum (Type S) thermocouple located on Rod 801-1, 46 cm above bottom of fuel stack, 180°, to measure cladding temperature.	478 to 1811 K	0 to 2250 K	350 Hz	100 Hz	13	From -0.5 to 0.4 s	QEUD
							0.4 to 2	Failed[b]
						14	From -5 to 0.4 s	QEUD
							0.4 to 25	Failed[b]
								QEUD
CLAD IMP 79-0 01	Type S thermocouple located on Rod 801-1, 79 cm above bottom of fuel stack, 0°, to measure cladding temperature.	478 to 1811 K	0 to 2250 K	350 Hz	100 Hz	15		QEUD
						16		QEUD
						E1		QEUD
CLAD IMP 46-0 03	Type S thermocouple located on Rod 801-3, 46 cm above bottom of fuel stack, 0°, to measure cladding temperature.	478 to 1811 K	0 to 2250 K	350 Hz	100 Hz	17	From -0.5 to 0.4 s	QEUD
							0.4 to 2 s	Failed[b]
						18	From -5 to 0.4 s	QEUD
							0.4 to 25 s	Failed[b]
						F1		QEUD
CLAD IMP 79-18003	Type S thermocouple located on Rod 801-3, 79 cm above bottom of fuel stack, 180°, to measure cladding temperature.	478 to 1811 K	0 to 2250 K	350 Hz	100 Hz	19		QEUD
						20		QEUD
						G1		QEUD
ROD PRES 6.9 KA 01	A 6.9-MPa Kaman Sciences Corp. pressure transducer to measure internal pressure in the upper plenum of Rod 801-1.	0 to 6.9 MPa	0 to 6.9 MPa	58 kHz	5 kHz	21		Trend[c]
						H1		Trend[c]

TABLE IV (continued)

Measurement	Location and Comments	Range: Detector	Range: Data Acquisition System	Frequency Response: Detector	Frequency Response: Data Acquisition System	Figure	Data Qualification[a]
Fuel Rod (continued)							
ROD PRES 6.9 KA 03	A 6.9-MPa Kaman Sciences Corp. pressure transducer to measure internal pressure in the upper plenum of Rod 801-3.	0 to 6.9 MPa	0 to 6.9 MPa	58 kHz	5 kHz	22 I1	Trend[c] Trend[c]
Test Train							
INLT TMP 01	Type K thermocouple located near the inlet of each flow shroud to measure coolant inlet temperature.	273 to 1309 K	300 to 1000 K	350 Hz	10 Hz	23 J1	QEUD QEUD
INLT TMP 02		273 to 1309 K	300 to 1000 K	350 Hz	10 Hz	24 K1	QEUD QEUD
INLT TMP 03		273 to 1309 K	300 to 1000 K	350 Hz	10 Hz	25 L1	QEUD QEUD
INLT TMP 05 04		273 to 1309 K	300 to 1000 K	350 Hz	10 Hz	26 M1	QEUD QEUD
OUT TEMP 01	Type K thermocouple located near the outlet of each flow shroud to measure coolant outlet temperature.	273 to 1309 K	300 to 1000 K	350 Hz	10 Hz	27 N1	QEUD QEUD
OUT TEMP 02		273 to 1309 K	300 to 1000 K	350 Hz	10 Hz	28 O1	QEUD QEUD
OUT TEMP 03		273 to 1309 K	300 to 1000 K	350 Hz	10 Hz	29 P1	QEUD QEUD
OUT TEMP 05 04		273 to 1309 K	300 to 1000 K	350 Hz	10 Hz	30 B2	QEUD QEUD
DEL TEMP 01	A pair of Type K thermocouples, one located at the inlet and one at the outlet of each rod flow shroud to measure the coolant temperature rise.	0 to 23 K	0 to 20 K	350 Hz	10 Hz	31 C2	QEUD QEUD
DEL TEMP 02		0 to 23 K	0 to 20 K	350 Hz	10 Hz	32 D2	QEUD Trend[d]
DEL TEMP 03		0 to 23 K	0 to 20 K	350 Hz	10 Hz	33 E2	QEUD Restrained[d]
DEL TEMP 05 04		0 to 23 K	0 to 20 K	350 Hz	10 Hz	34 F2	QEUD QEUD

TABLE IV (continued)

Measurement	Location and Comments	Range		Frequency Response			
		Detector	Data Acquisition System	Detector	Data Acquisition System	Figure	Data Qualification[a]
Test Train (continued)							
SYS PRES 69 EG UTT	A 69-MPa pressure transducer located above the flow shroud outlets to measure transient pressure response and normal system pressure.	0 to 69 MPa	0 to 69 MPa	35 kHz	20 kHz	G2	Power burst: Failed[e] Restrained[e]
SYS PRES 17 KA UTT	A 17-MPa pressure transducer located above the flow shroud outlets to measure transient pressure response and normal system pressure.	0 to 17.2 MPa	0 to 17 MPa	58 kHz	20 kHz	35 H2	Restrained[f] Restrained[f]
SYS PRES 5000V UTT	A 17-MPa pressure transducer located above the flow shroud outlets to measure transient pressure response and normal system pressure.	0 to 17.2 MPa	0 to 17 MPa	350 Hz	5 kHz	I2	Power burst: Failed[g] Restrained[f]
SHRD PRES 17 KA 01	A 17-MPa pressure transducer connected by tubing to the midpoint of each flow shroud to measure internal flow shroud transient pressure pulses resulting from fuel rod failure.	0 to 17.2 MPa	0 to 17 MPa	58 kHz	20 kHz	36 J2	Restrained[f,h] Restrained[f]
SHRD PRES 17 KA 02		0 to 17.2 MPa	0 to 17 MPa	58 kHz	20 kHz	K2	Power Burst: Failed Restrained[f]
SHRD PRES 17 KA 03		0 to 17.2 MPa	0 to 17 MPa	58 kHz	20 kHz	37 L2	Restrained[f] Restrained[f]
SHRD PRES 17 KA 05 04		0 to 17.2 MPa	0 to 17 MPa	58 kHz	20 kHz	38 M2	Restrained[f] Restrained[f]
FLOWRATE INLET 01	Turbine flowmeter located at each flow shroud inlet to measure volumetric coolant flow to each fuel rod.	0 to 0.82 l/s	0 to 0.82 l/s	120 Hz	100 Hz	39 40[i] N2	From -0.1 to -0.003 s: QEUD -0.003 to 0.3 s: Failed[j] From -2 to -0.003 s: QEUD -0.003 to 10 s: Failed[j] QEUD
FLOWRATE INLET 02		0 to 0.82 l/s	0 to 0.82 l/s	120 Hz	100 Hz	41 42[i] O2	From -0.1 to -0.003 s: QEUD -0.003 to 0.3 s: Failed[j] From -2 to -0.003 s: QEUD -0.003 to 10 s: Failed[j] QEUD

TABLE IV (continued)

Measurement		Location and Comments	Range		Frequency Response				
			Detector	Data Acquisition System	Detector	Data Acquisition System	Figure	Data Qualification[a]	
Test Train (continued)									
FLOWRATE INLET	03		0 to 0.82 l/s	0 to 0.82 l/s	120 Hz	100 Hz	43	From -0.1 to -0.003 s	QEUD
								-0.003 to 0.3 s	Failed[j]
							44[i]	From -2 to -0.003 s	QEUD
								-0.003 to 10 s	Failed[j]
							P2		QEUD
FLOWRATE INLET	05		0 to 0.82 l/s	0 to 0.82 l/s	120 Hz	100 Hz	45	From -0.1 to -0.003 s	QEUD
								-0.003 to 0.3 s	Failed[j]
							46[i]	From -2 to -0.003 s	QEUD
								-0.003 to 10 s	Failed[j]
	04						B3		QEUD
CLAD DSP	01	A linear variable differential transformer mounted at the lower end of each fuel rod to measure cladding axial elongation.	-12.7 to 12.7 mm	-5 to 25 mm	3.5 kHz	5 kHz	47		QEUD
							48		QEUD
							C3		QEUD
CLAD DSP	02		-12.7 to 12.7 mm	-5 to 25 mm	3.5 kHz	5 kHz	49		QEUD
							D3		QEUD
CLAD DSP	03		-12.7 to 12.7 mm	-5 to 25 mm	3.5 kHz	5 kHz			Failed[k]
CLAD DSP	05		-12.7 to 12.7 mm	-5 to 25 mm	3.5 kHz	5 kHz		Power burst	Failed[k]
	04						E3		Trend[l]
NEUT FLX 9-Q1	TT	Self powered neutron detector (SPND) located in Quadrant 1, 0.09 m above the bottom of the fuel stack to measure the relative neutron flux.	0 to 1 ma	10^{-8} to 1 ma	350 Hz	5 kHz		Power burst	Failed[g]
							F3		QEUD
NEUT FLX 27-Q1	TT	SPND in Quadrant 1, 0.27 m above bottom of fuel stack.	0 to 1 ma	10^{-8} to 1 ma	350 Hz	5 kHz		Power burst	Failed[g]
							G3		QEUD
NEUT FLX 46-Q1	TT	SPND in Quadrant 1, 0.46 m above bottom of fuel stack.	0 to 1 ma	10^{-8} to 1 ma	350 Hz	5 kHz	50		Restrained[m]
							H3		QEUD
NEUT FLX 64-Q1	TT	SPND in Quadrant 1, 0.64 m above bottom of fuel stack.	0 to 1 ma	10^{-8} to 1 ma	350 Hz	5 kHz	51		Restrained[m]
							I3		QEUD

TABLE IV (continued)

Measurement	Location and Comments	Range		Frequency Response			Data Qualification[a]
		Detector	Data Acquisition System	Detector	Data Acquisition System	Figure	
Test Train (continued)							
NEUT FLX 82-Q1 TT	SPND in Quadrant 1, 0.82 m above bottom of fuel stack.	0 to 1 ma	10^{-8} to 1 ma	350 Hz	5 kHz	J3	Power burst Failed[g] QE0D
NEUT FLX 9-Q3 TT	SPND in Quadrant 3, 0.09 m above bottom of fuel stack.	0 to 1 ma	10^{-8} to 1 ma	350 Hz	10 kHz	K3	Power burst n QE0D
NEUT FLX 27-Q3 TT	SPND in Quadrant 3, 0.27 m above bottom of fuel stack.	0 to 1 ma	10^{-8} to 1 ma	350 Hz	10 kHz	L3	Power burst n QE0D
NEUT FLX 46-Q3 TT	SPND in Quadrant 3, 0.46 m above bottom of fuel stack.	0 to 1 ma	10^{-8} to 1 ma	350 Hz	10 kHz	M3	Power burst n QE0D
NEUT FLX 64-Q3 TT	SPND in Quadrant 3, 0.64 m above bottom of fuel stack.	0 to 1 ma	10^{-8} to 1 ma	350 Hz	10 kHz	N3	Power burst n QE0D
NEUT FLX 82-Q3 TT	SPND in Quadrant 3, 0.82 m above bottom of fuel stack.	0 to 1 ma	10^{-8} to 1 ma	350 Hz	10 kHz	O3	Power burst n QE0D
Plant							
REAC POW 50IR1PT	Ionization chamber located outside the reactor core barrel about 335 degrees from the reactor north to measure reactor steady state power. Low range electronics.	0 to 32 GW	0 to 50 MW	>5 kHz	5 kHz	P3	Restrained[d]
REAC POW 50KIR1PT	High range electronics to measure reactor transient power.	0 to 32 GW	0 t 50 GW	>5 kHz	5 kHz	S2	QE0D
REAC POW 50IR2PT	Ionization chamber located outside the reactor core barrel about 145 degrees from the reactor north to measure reactor steady state power. Low range electronics.	0 to 32 GW	0 to 50 MW	>5 kHz	5 kHz	B4	Trend[l]

TABLE IV (continued)

Measurement	Location and Comments	Range		Frequency Response		Figure	Data Qualification[a]	
		Detector	Acquisition System	Detector	Data Acquisition System			
Plant (continued)								
REAC POW 50KTR2PT	High range electronics to measure reactor transient power.	0 to 32 GW	0 to 50 GW	>5 kHz	5 kHz			Failed[g]
REAC POW 50EV1PT	Evacuated ionization chamber located just outside the north corner of the reactor core to measure reactor steady state power. Low range electronics.	0 to 200 GW	0 to 50 MW	>5 kHz	5 kHz	C4		QEUD
REAC POW 50KEV1PT	High range electronics to measure reactor transient power.	0 to 200 GW	0 to 50 GW	>5 kHz	5 kHz	53		QEUD
REAC POW 50EV2PT	Evacuated ionization chamber located just outside the south corner of the reactor core to measure reactor steady state power. Low range electronics.	0 to 200 GW	0 to 50 MW	>5 kHz	5 kHz	D4		QEUD
REAC POW 50KEV2PT	High range electronics to measure reactor transient power.	0 to 200 GW	0 to 50 GW	>5 kHz	5 kHz	54		QEUD
FP GAMMA NO. 1 FP	An analyzer measuring gamma-ray intensity in the 150 to 3400 keV energy range from a 2.5- by 3.8-cm NaI crystal detector located in the fission product detection system.	10 to 10^6 cts	10 to 10^6 cts	--	10 Hz	55 E4		Trend[g] Trend[g]
FP GAMMA NO. 2 FP	An analyzer measuring gamma-ray intensity in the 150 to 6300 keV energy range from a 7.6- by 7.6-cm NaI crystal detector located in the fission product detection system.	10 to 10^6 cts	10 to 10^6 cts	--	10 Hz	56	Power Calibration	Trend[g] Failed[g]

TABLE IV (continued)

Measurement	Location and Comments	Range		Frequency Response			
		Detector	Data Acquisition System	Detector	Data Acquisition System	Figure	Data Qualification[a]
Plant (continued)							
FP GAMMA NO. 3 FP	An analyzer measuring gamma-ray intensity in the 3400 to 6300 keV energy range from the same detector used by FP GAMMA No. 1 FP.	10 to 10^6 cts	10 to 10^6cts	--	10 Hz		Failed[b]
FP NEBI FP	A BF_3 delayed neutron detector used to detect delayed neutrons in the fission product detection system sample stream.	10 to 10^6 cts	10 to 10^6cts	--	10 Hz	57 F4	Trend[c] Trend[c]
LOOP PRES 5-20 PT	Air cooled Norwood pressure transducers to measure coolant loop pressure surges.	0 to 34.5 MPa	0 to 34 MPa	--	100 Hz	58	Trend[d]
LOOP PRES 5-21 PT		0 to 34.5 MPa	0 to 34 MPa	--	100 Hz	59	Trend[d]
LOOP PRES 5-22 PT		0 to 103 MPa	0 to 34 MPa	--	100 Hz	60	Trend[d]
LOOP PRES 5-23 PT		0 to 34.5 MPa	0 to 34 MPa	--	100 Hz	61	Trend[d]
LOOP PRES 5-24 PT		0 to 34.5 MPa	0 to 34 MPa	--	100 Hz	62	Trend[d]
LOOP PRES 5-25 PT		0 to 34.5 MPa	0 to 34 MPa	--	100 Hz	63	Trend[d]
LOOP PRES 5-34 PT		0 to 103 MPa	0 to 34 MPa	--	100 HZ	64	Trend[d]
LOOP PRES 5-35 PT		0 to 103 MPa	0 to 34 MPa	--	100 Hz		Failed[b]

a. For all power calibration and preconditioning plots presented on microfiche, data were not recorded from 6.2 to 8.2 hours and from 11.1 to 12.0 hours. The reactor was at zero power during these intervals.

b. Visual examination revealed these thermocouple junctions to be effectively destroyed by the power burst.

c. The rod pressures were set to zero prior to nuc operation to give an indication of pressure increase. The uncertainty level is high due to very large offsets between similar channels.

d. The data display a strong negative time dependent drift.

e. The signal to noise ratio was too low.

f. These pressure measurements are restrained because of excessive hysteresis noted during hydrostatic tests. A preburst and prepower calibration offset has been applied to normalize the measurement to a calibrated loop pressure gage.

TABLE IV (continued)

g. Data acquisition system multiplexer failed.

h. These data have been treated with a 60 Hz low pass filter.

i. These plots are highly decimated and cannot be used as valid transient indications. They are presented to give steady state indication several seconds following the burst.

j. Probable flow oscillation and reversal occurred during the burst. Partial blocking was probable and apparent following the burst.

k. Transducer failure.

l. Data are very erratic.

m. Comparison of SPND currents with ionization chambers is not consistent with power calibration data.

n. Recording rate was too low for power burst operation.

o. Not calibrated to give numerical results for any measured parameter.

p. Data were inverted.

q. Large offset application and excessive hysteresis result in trend qualification.

The data graphs, Figures 11 through 64, for the power burst are presented on the subsequent pages of this report. Time zero for the power burst data is the time of peak reactor power. The power calibration and preconditioning data are included on microfiche which is attached to the back cover of this report. The scales selected for the graphs do not reflect the obtainable resolution of the data.

Appendix B is an analysis of selected data which provides a guide to the uncertainty associated with data measurements in the PBF system.

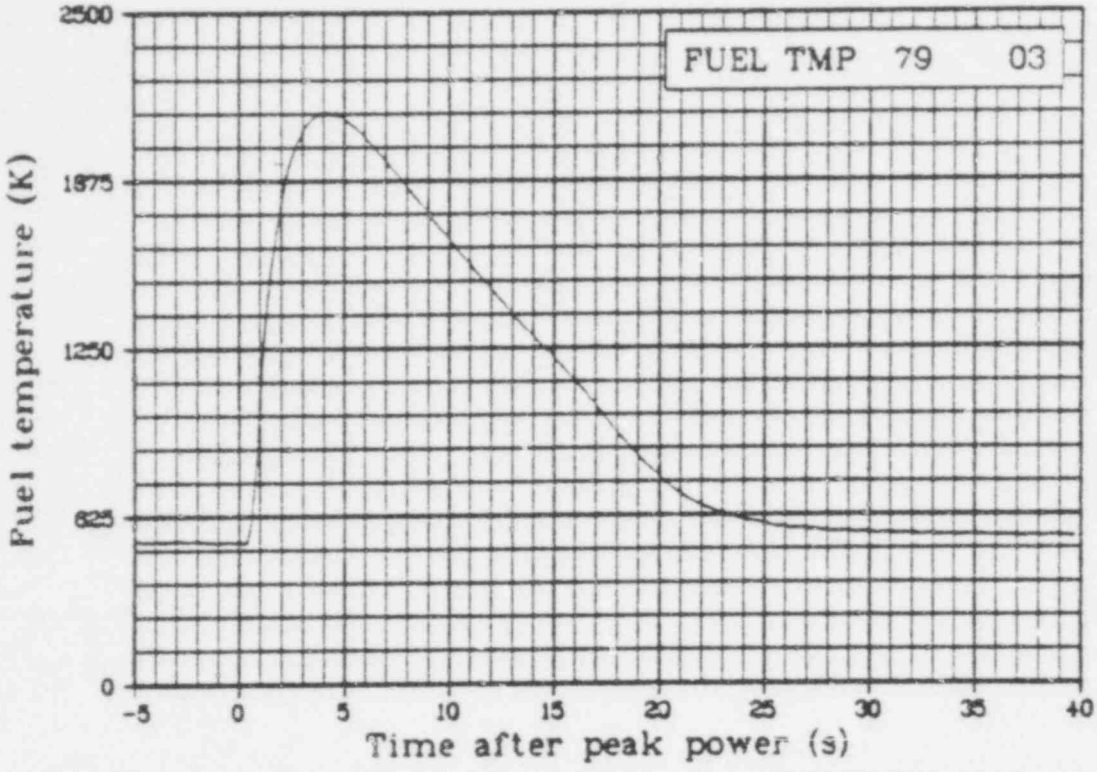

Fig. 11 Fuel centerline temperature in Rod 801-3, 0.79 m above fuel stack bottom (FUEL TMP 79 03), from -5 to 40 s.

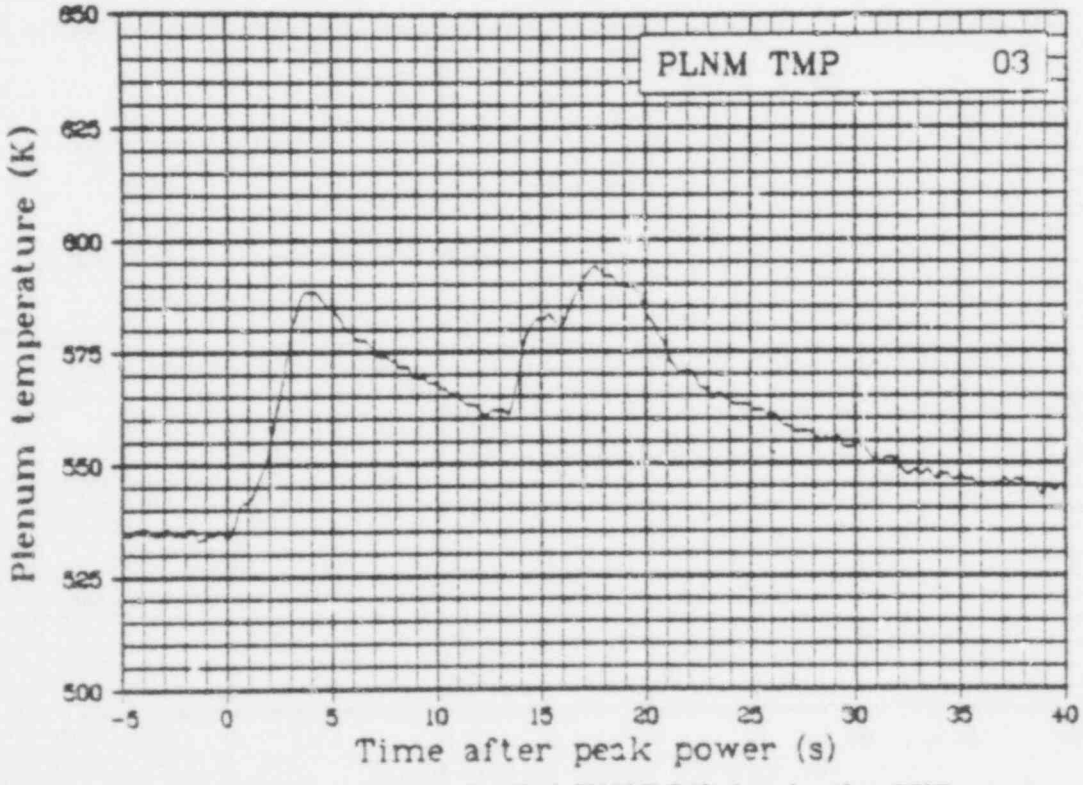

Fig. 12 Plenum temperature in Rod 801-3 (PLNM TMP 03), from -5 to 40 s. (QEUD)

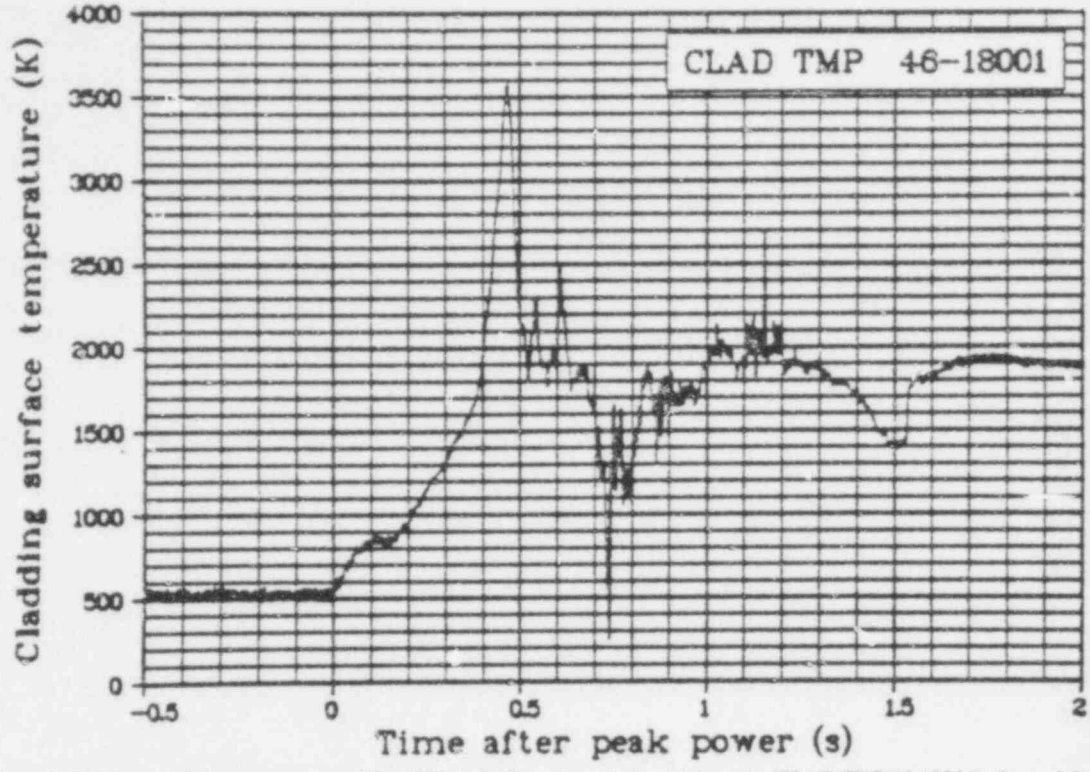

Fig. 13 Cladding surface temperature of Rod 801-1, 0.46 m above fuel stack bottom (CLAD TMP 46-18001), from -0.5 to 2 s.

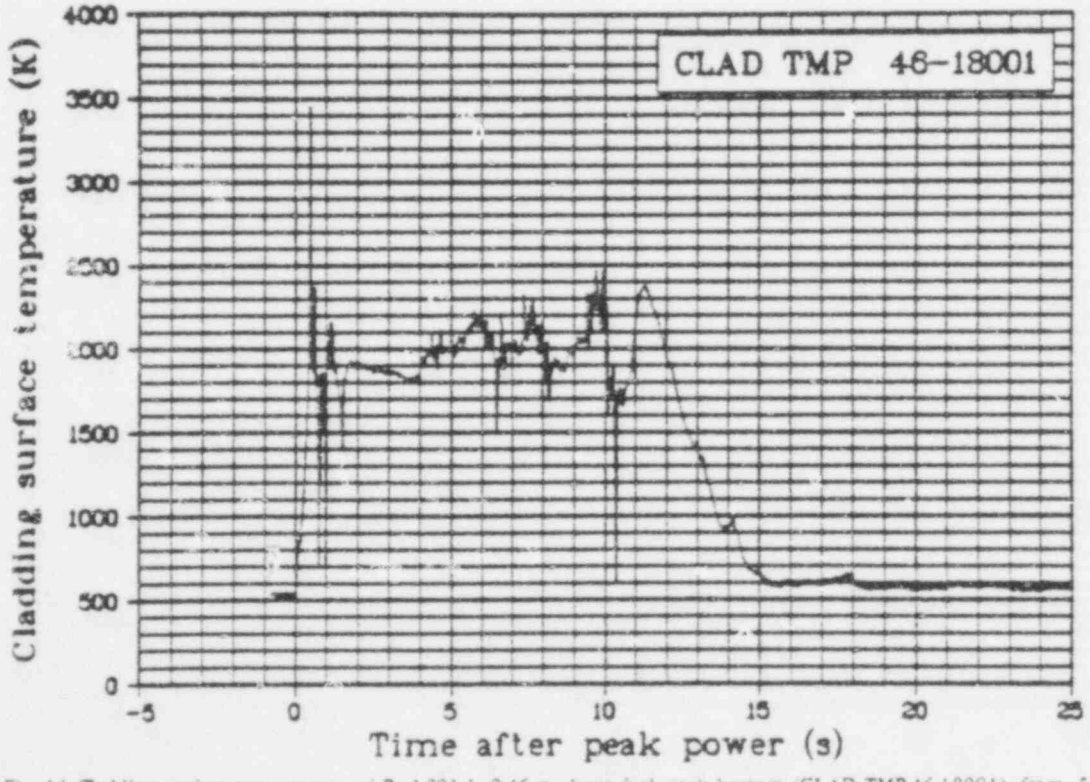

Fig. 14 Cladding surface temperature of Rod 801-1, 0.46 m above fuel stack bottom (CLAD TMP 46-18001), from -5 to 25 s.

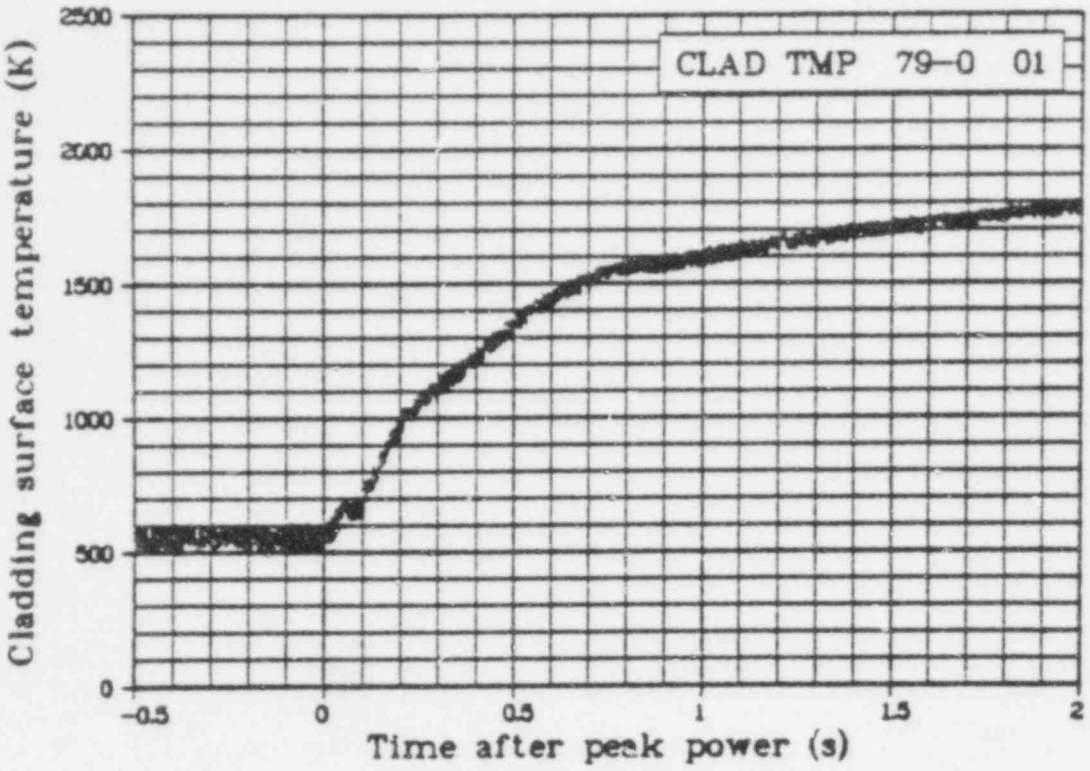

Fig. 15 Cladding surface temperature of Rod 801-1, 0.79 m above fuel stack bottom (CLAD TMP 79-0 01), from -0.5 to 2 s. (QEUD)

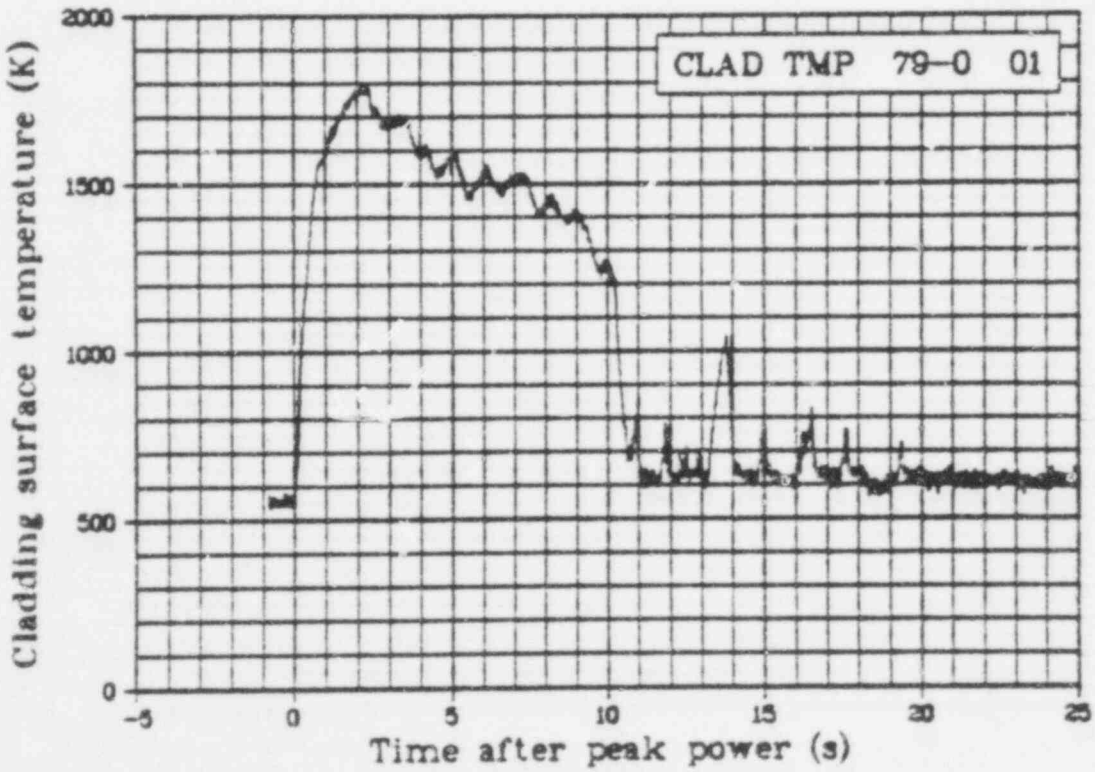

Fig. 16 Cladding surface temperature of Rod 801-1, 0.79 m above fuel stack bottom (CLAD TMP 79-0 01), from -5 to 25 s. (QEUD)

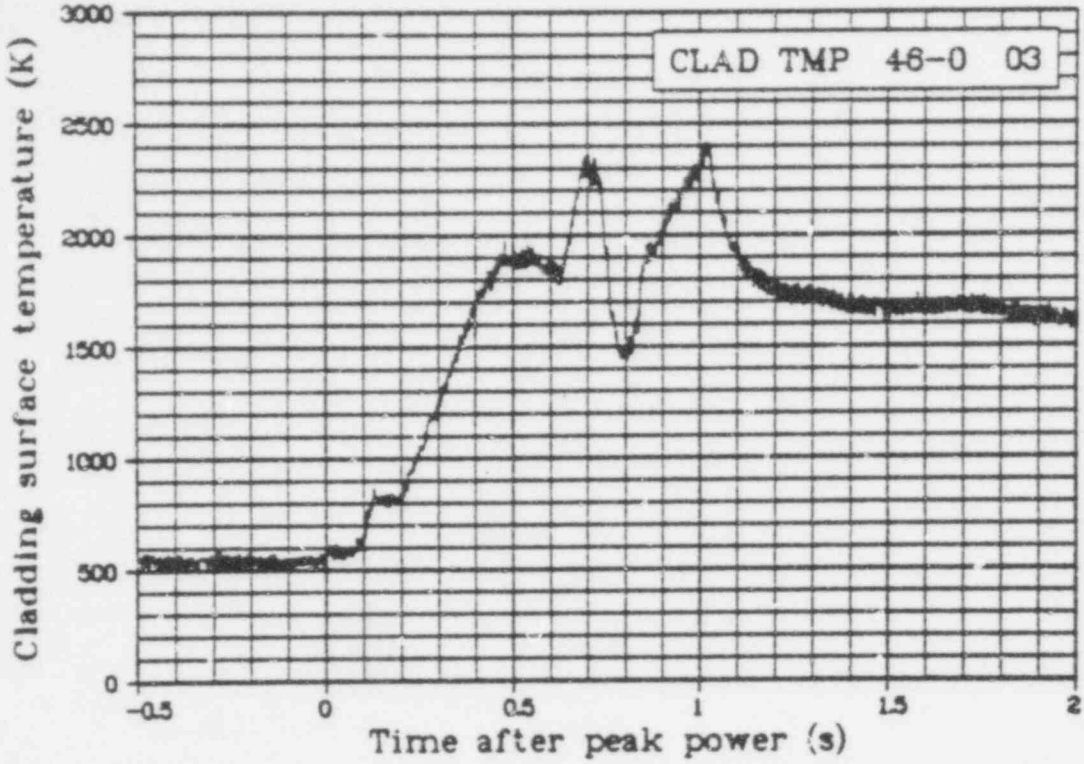

Fig. 17 Cladding surface temperature of Rod 801-3, 0.46 m above fuel stack bottom (CLAD TMP 46-0 03), from -0.5 to 2 s.

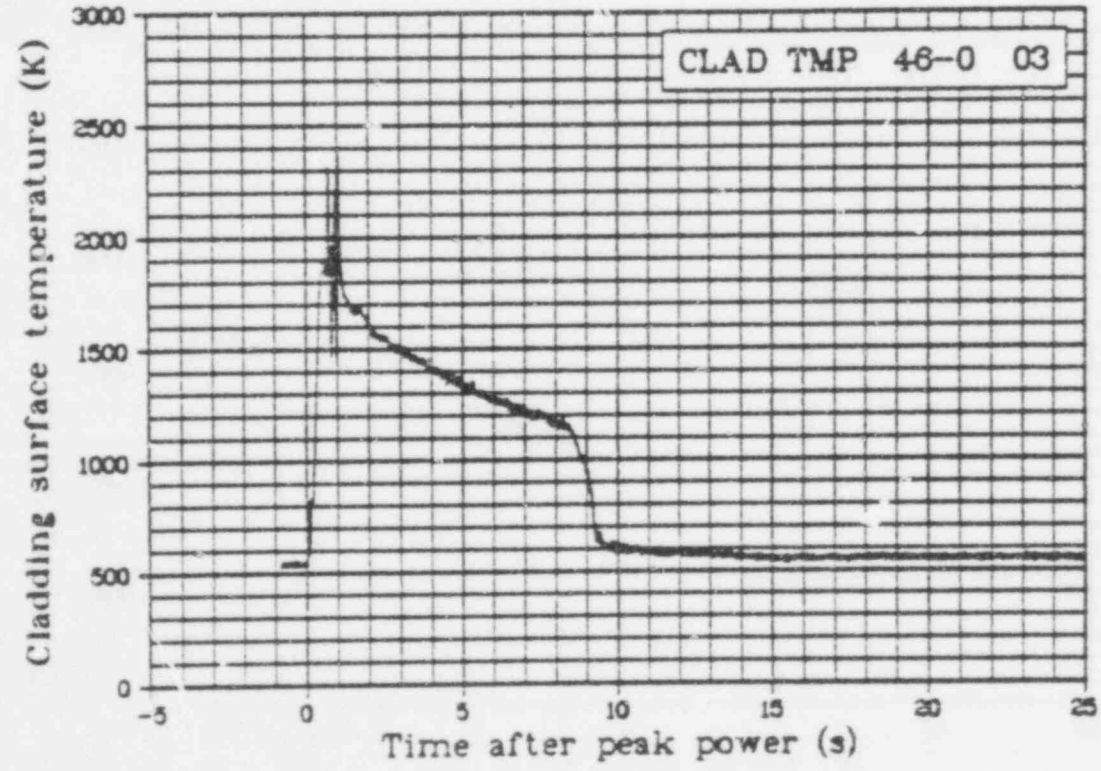

Fig. 18 Cladding surface temperature of Rod 801-3, 0.46 m above fuel stack bottom (CLAD TMP 46-0 03), from -5 to 25 s.

447 358

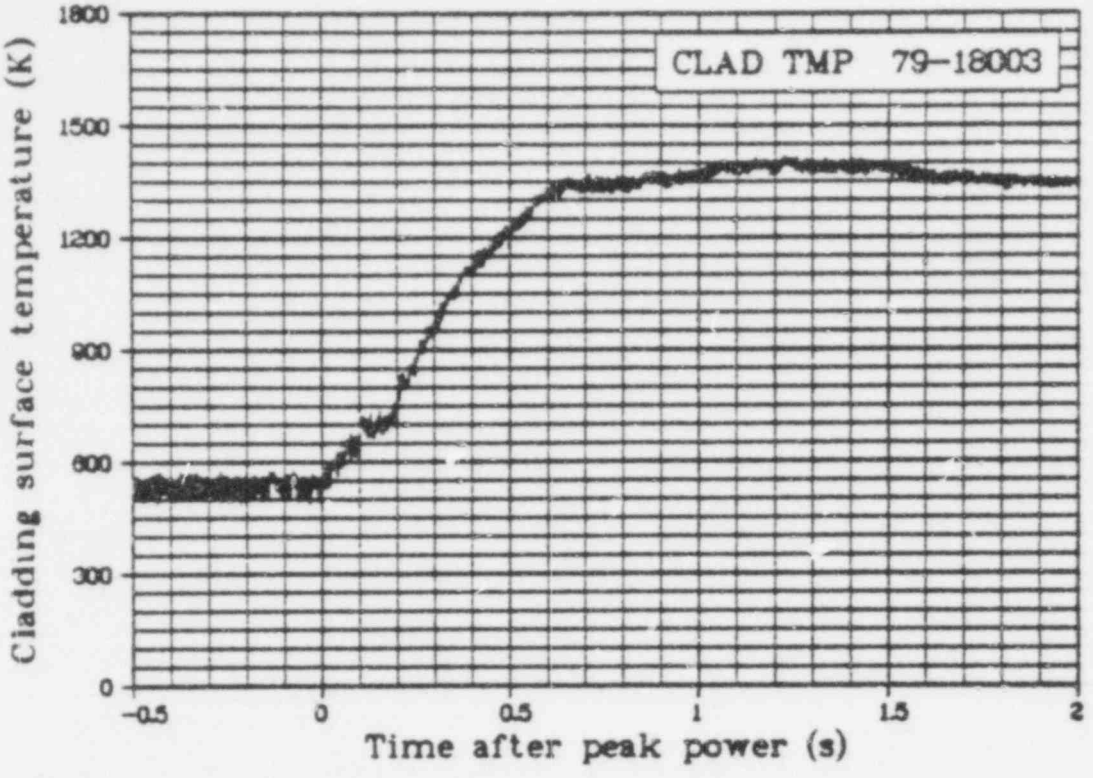

Fig. 19 Cladding surface temperature of Rod 801-3, 0.79 m above fuel stack bottom (CLAD TMP 79-18003), from -0.5 to 2 s. (QEUC)

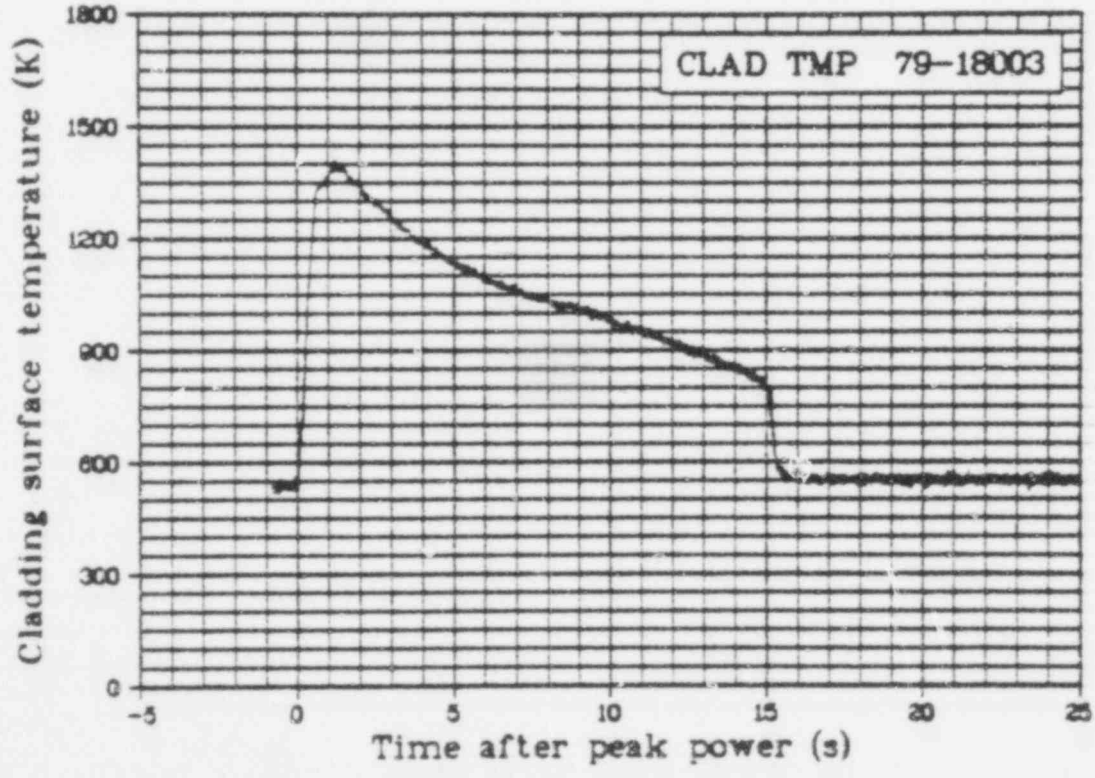

Fig. 20 Cladding surface temperature of Rod 801-3, 0.79 m above fuel stack bottom (CLAD TMP 79-18003), from -5 to 25 s. (QEUD)

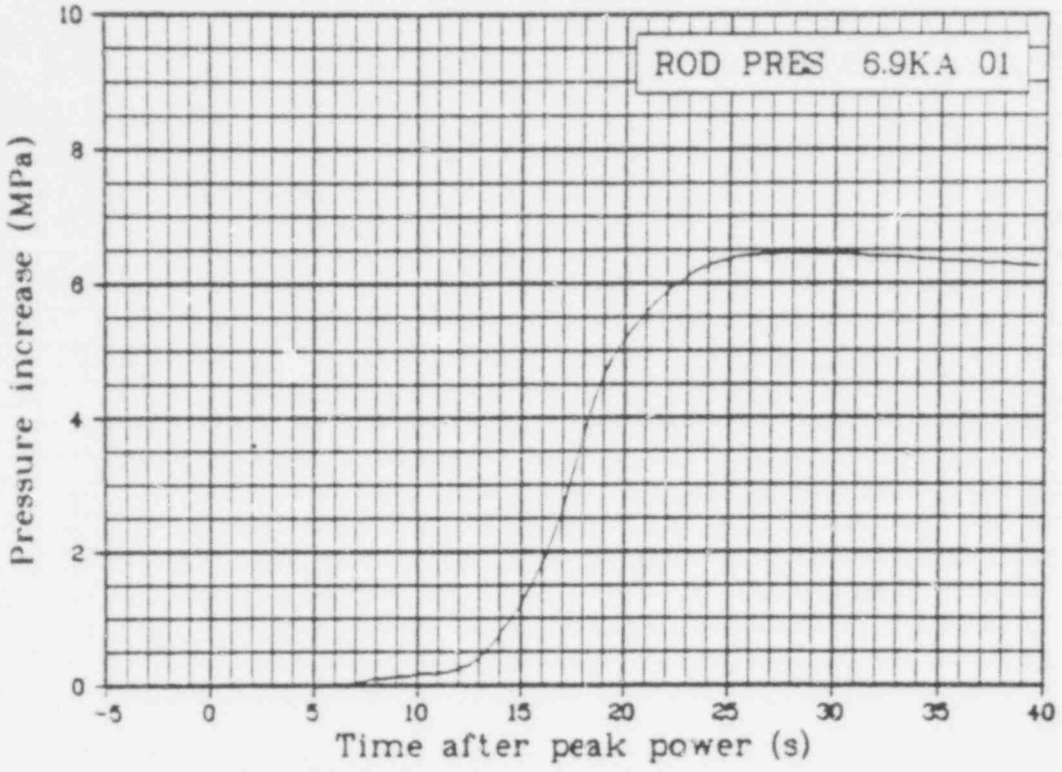

Fig. 21 Pressure increase in Rod 801-1 plenum (ROD PRES 6.9 KA 01), from -5 to 40 s.

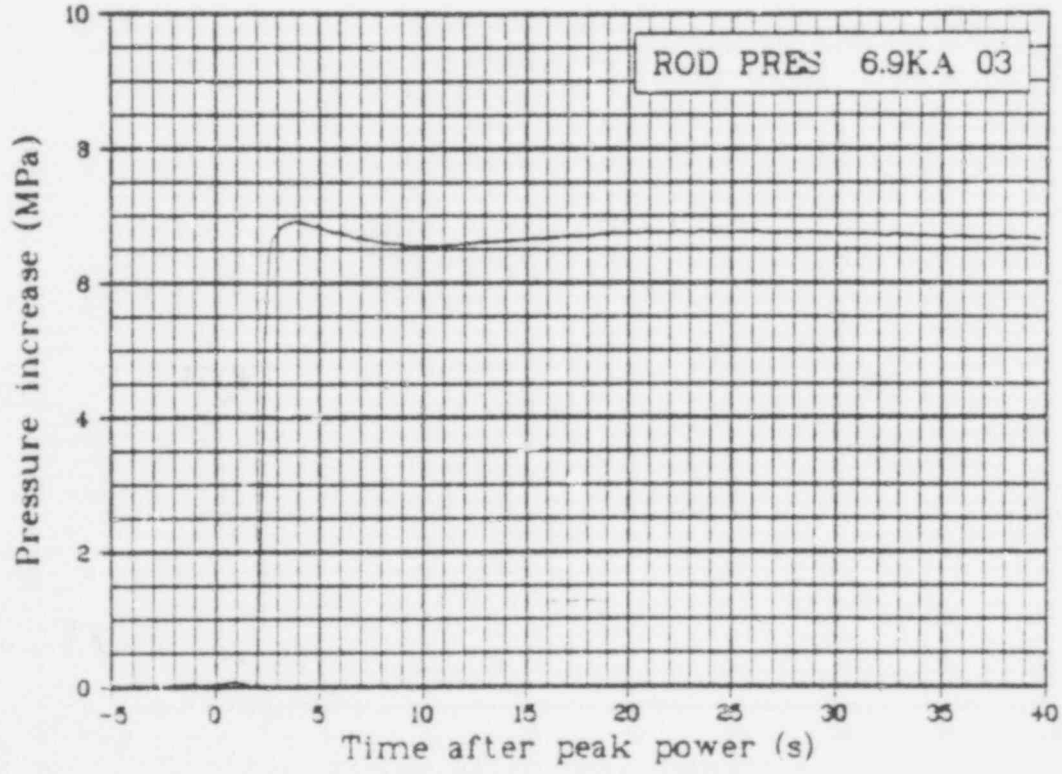

Fig. 22 Pressure increase in Rod 801-3 plenum (ROD PRES 6.9 KA 03), from -5 to 40 s.

CAT 760

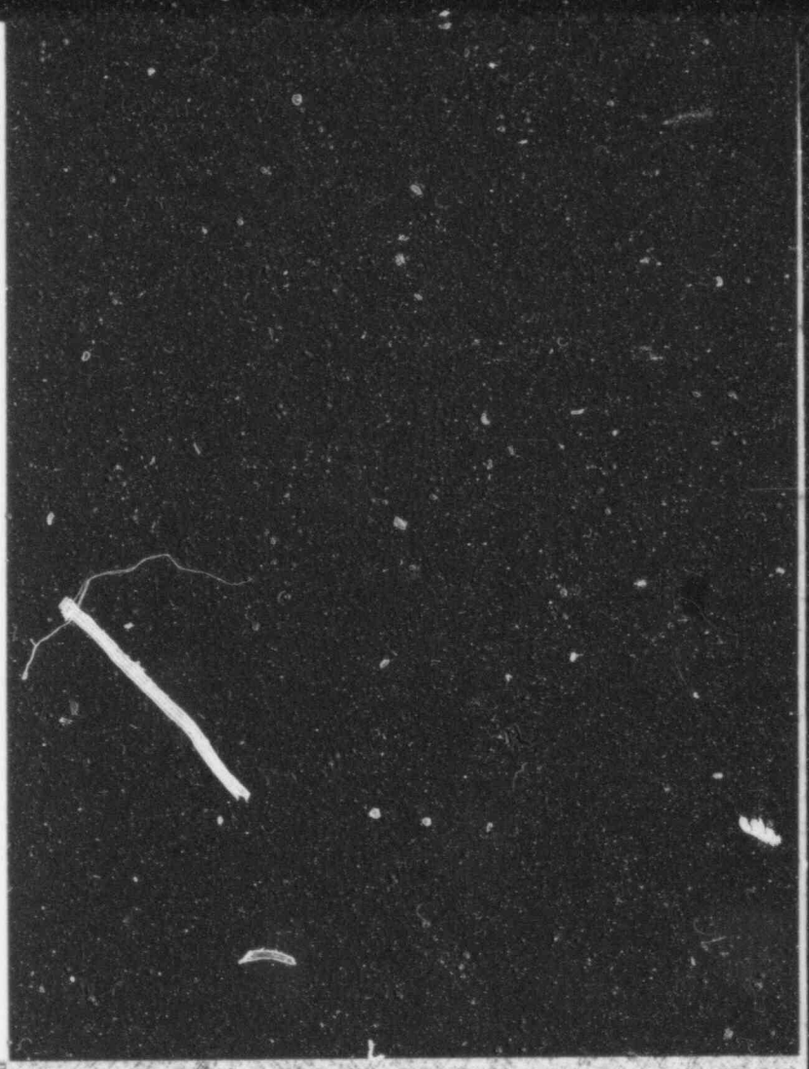

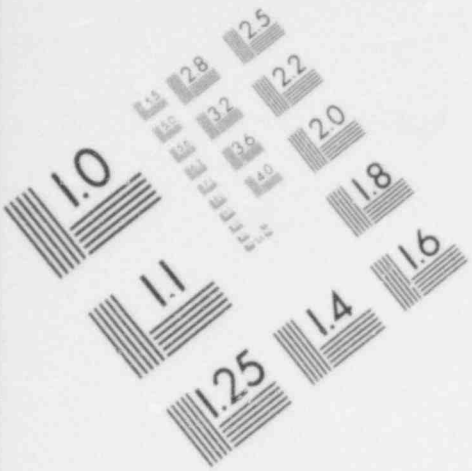

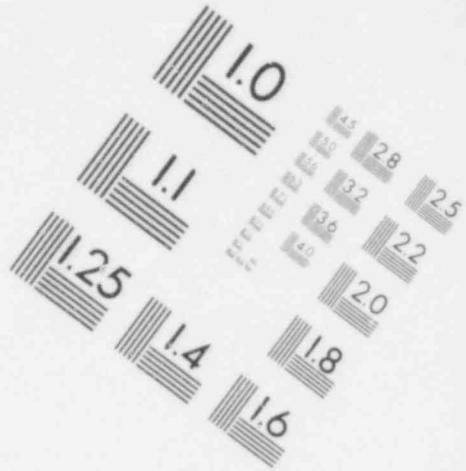

IMAGE EVALUATION TEST TARGET (MT-3)

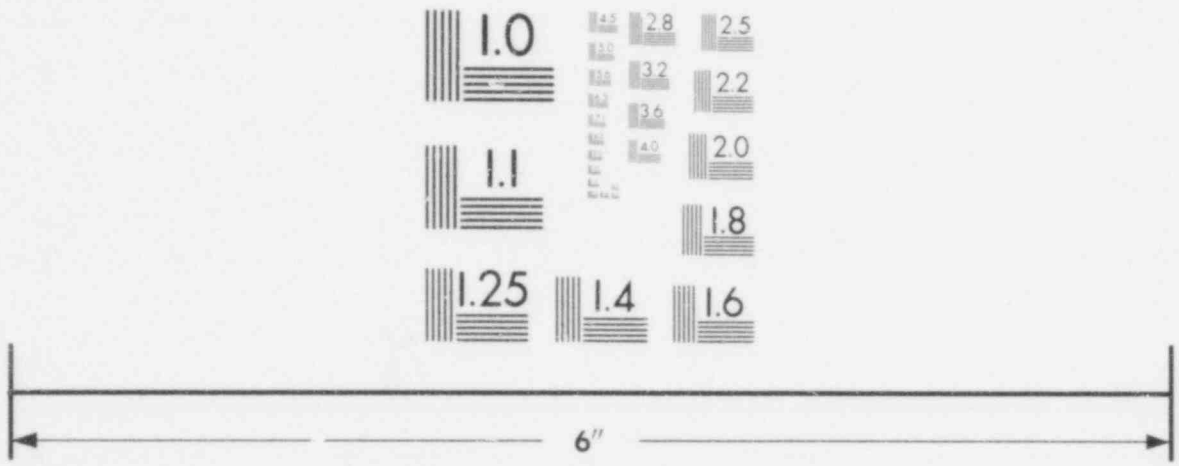

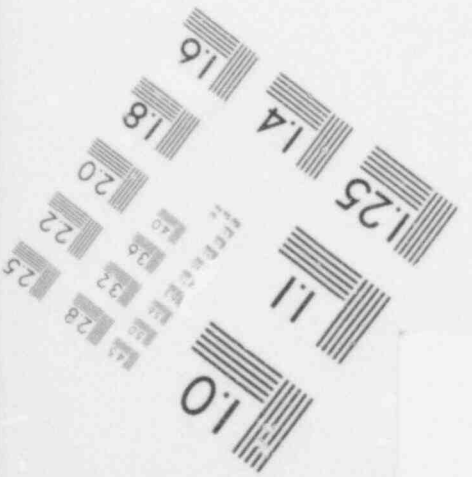

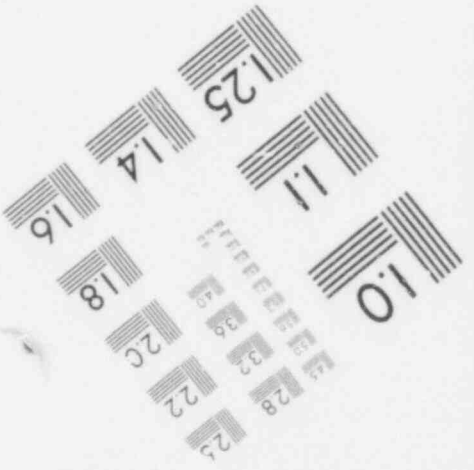

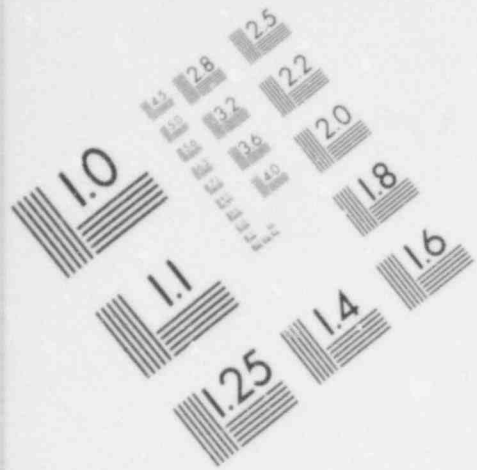

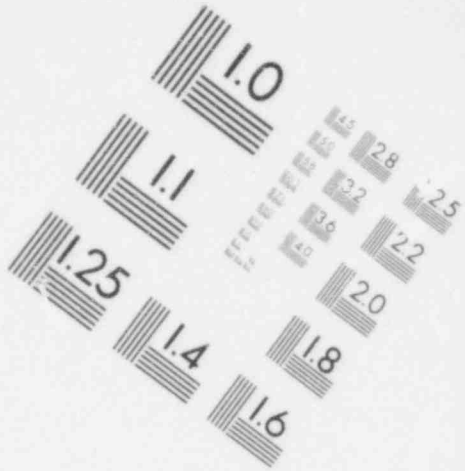

IMAGE EVALUATION
TEST TARGET (MT-3)

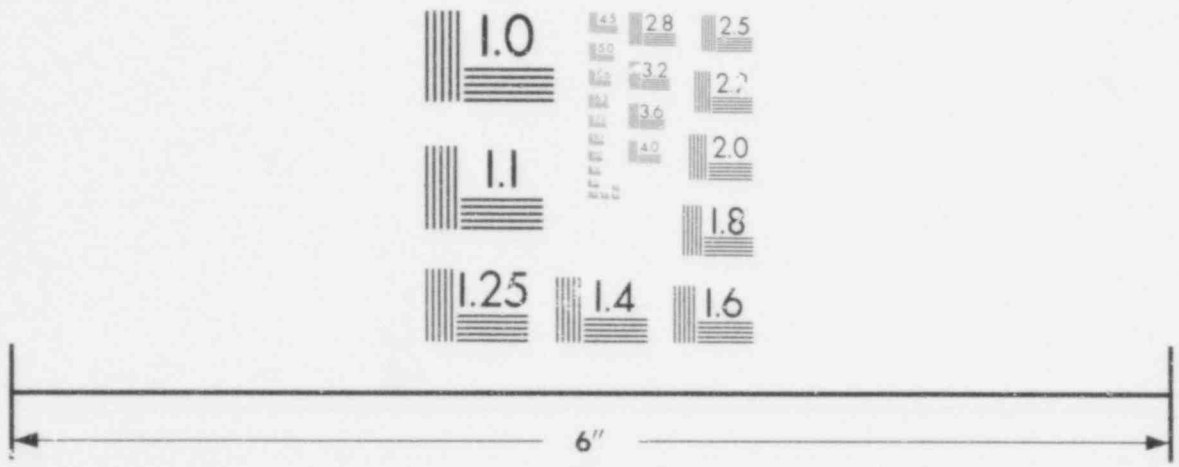

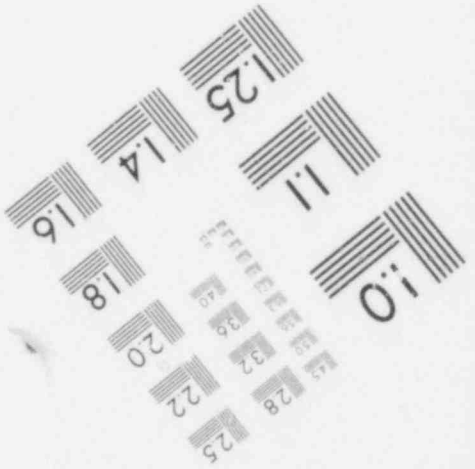

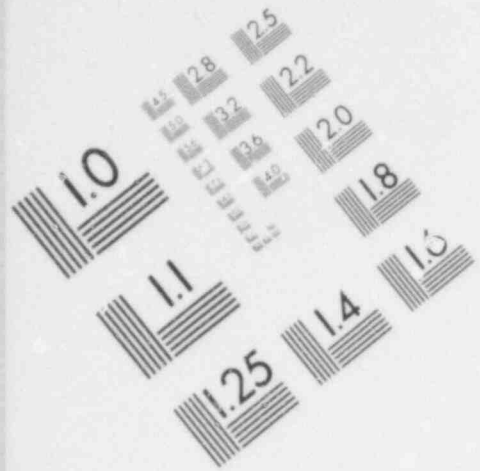

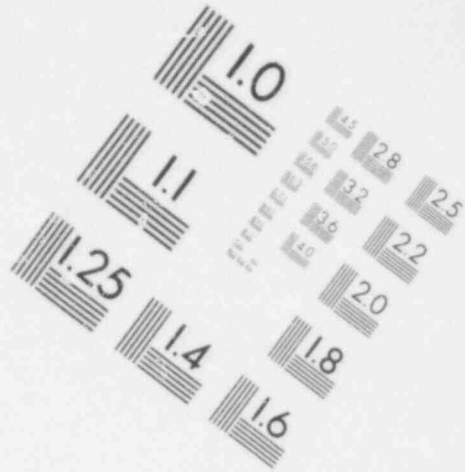

IMAGE EVALUATION TEST TARGET (MT-3)

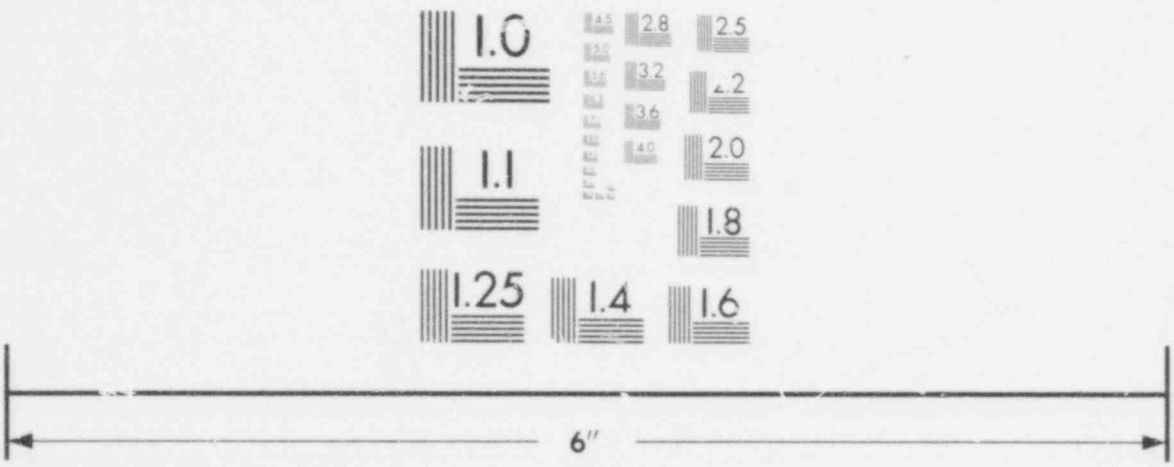

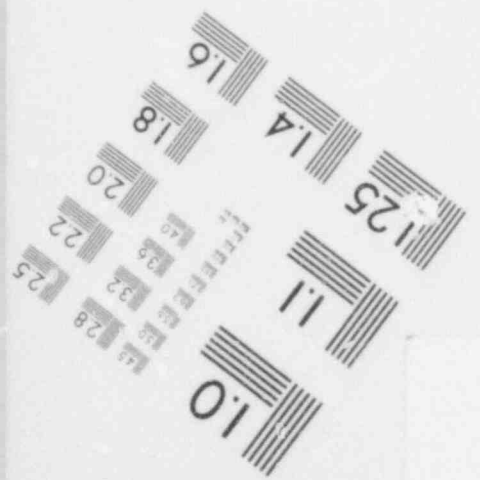

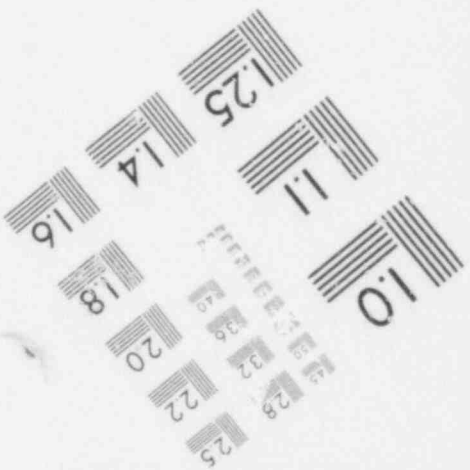

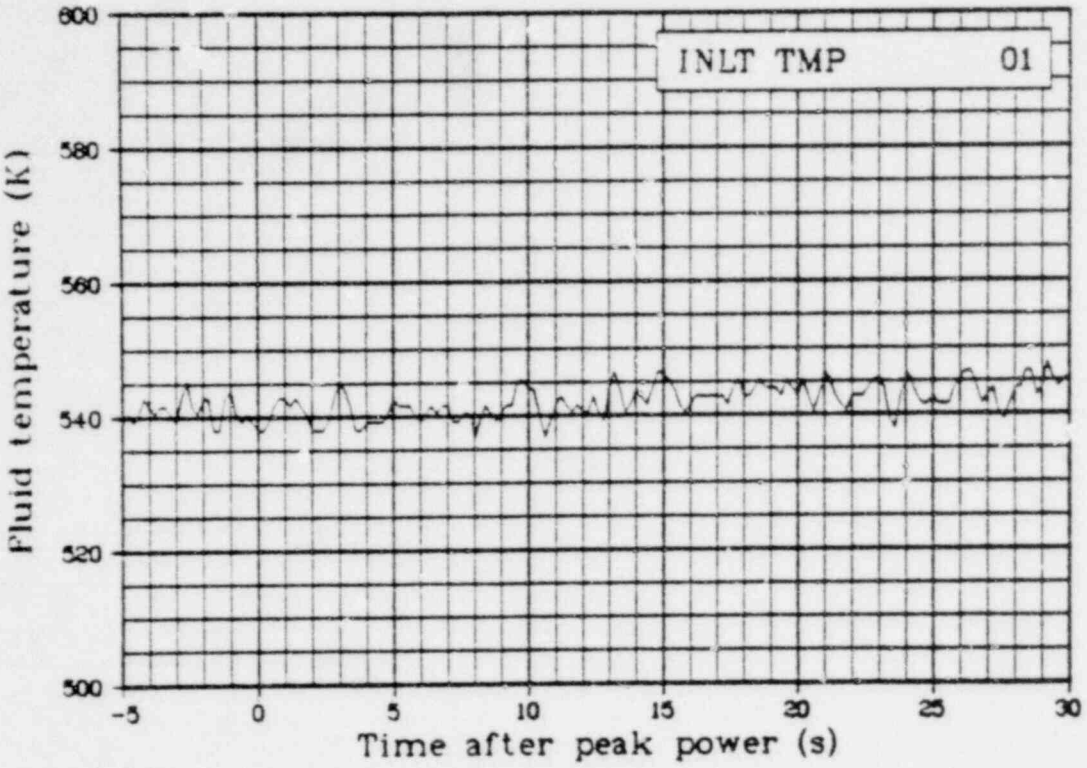

Fig. 23 Fluid temperature of Rod 801-1 coolant inlet (INLT TMP 01), from -5 to 30 s. (QEUD)

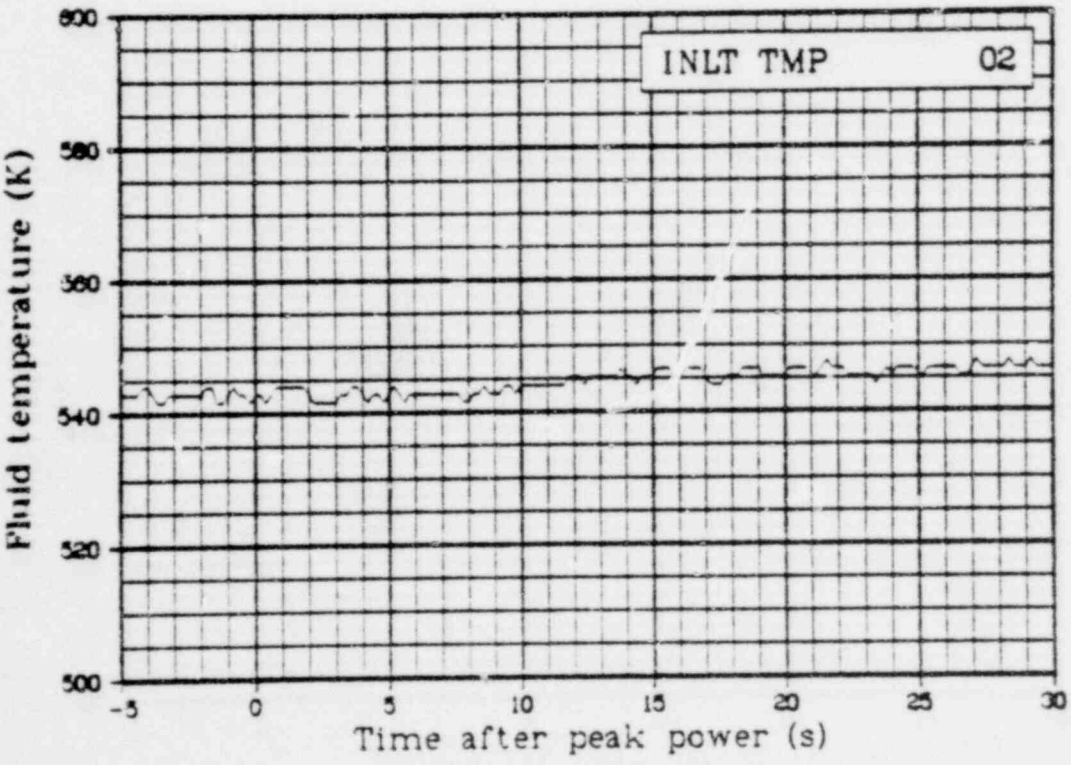

Fig. 24 Fluid temperature of Rod 801-2 coolant inlet (INLT TMP 02), from -5 to 30 s. (QEUD)

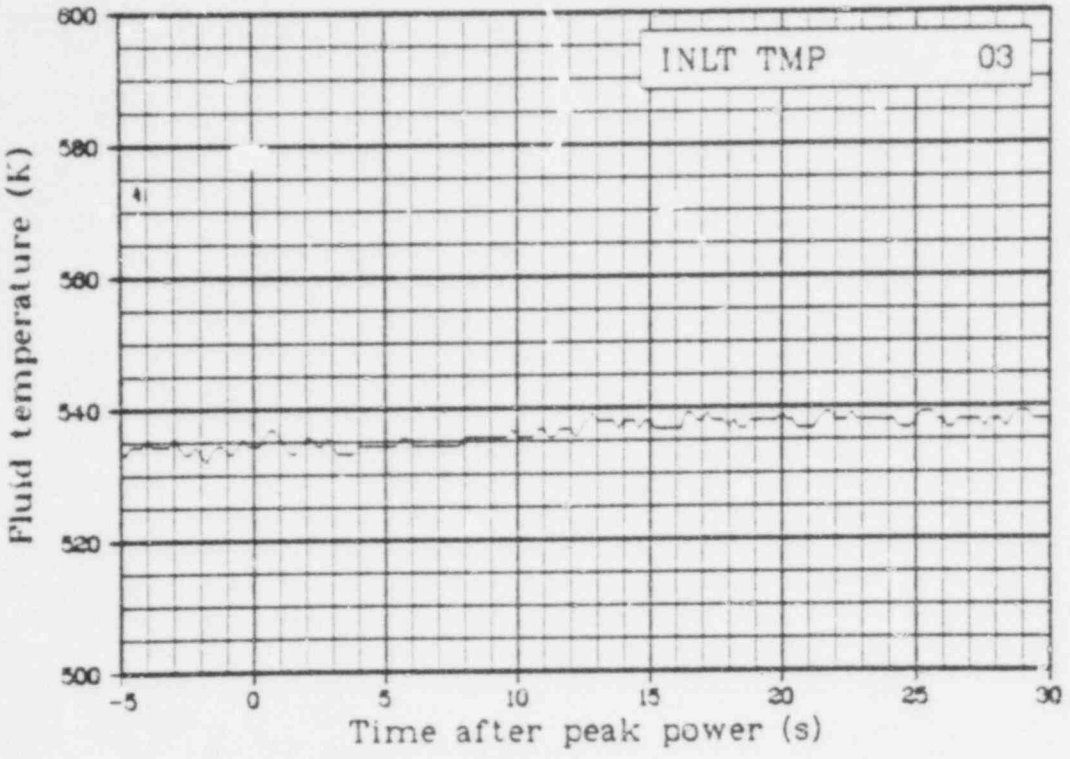

Fig. 25 Fluid temperature of Rod 801-3 coolant inlet (INLT TMP 03), from -5 to 30 s. (QEUD)

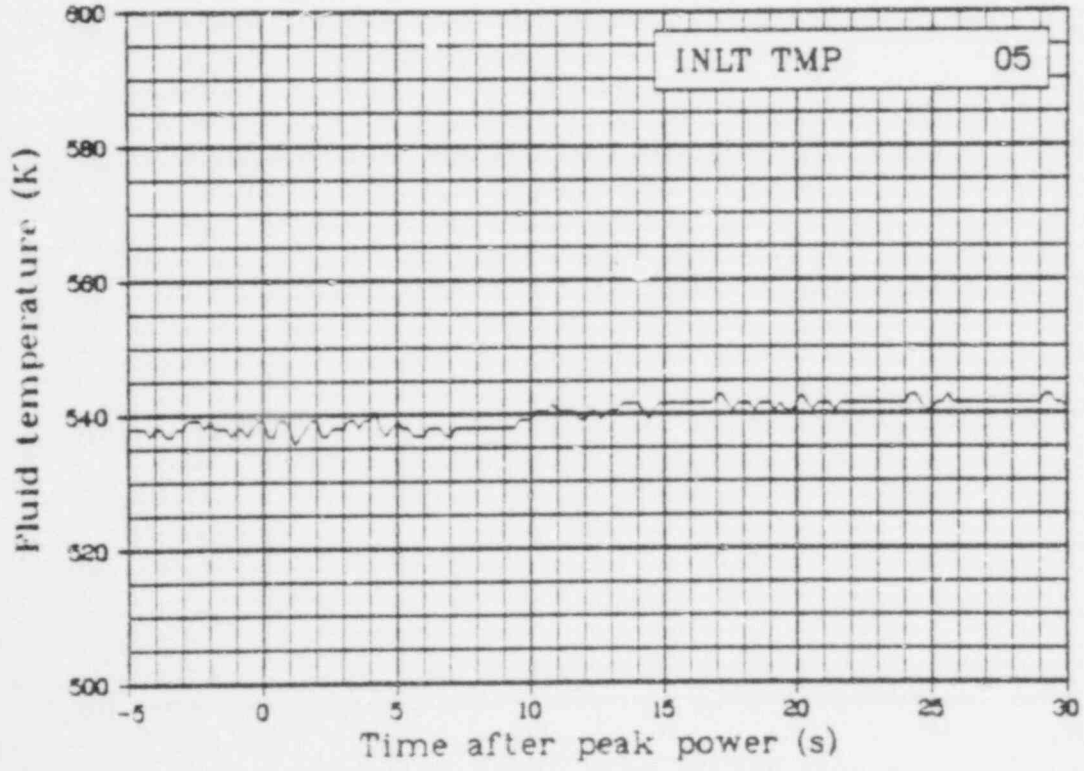

Fig. 26 Fluid temperature of Rod 801-5 coolant inlet (INLT TMP 05), from -5 to 30 s. (QEUD)

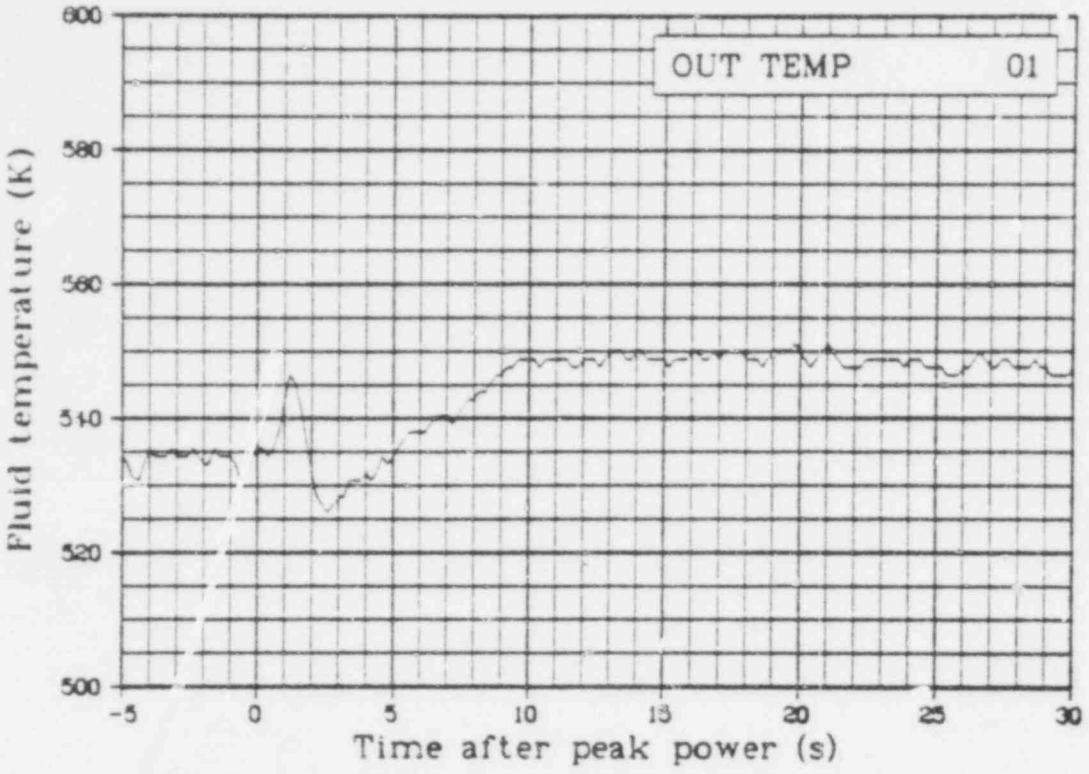

Fig. 27 Fluid temperature of Rod 801-1 coolant outlet (OUT TEMP 01), from -5 to 30 s. (QEUD)

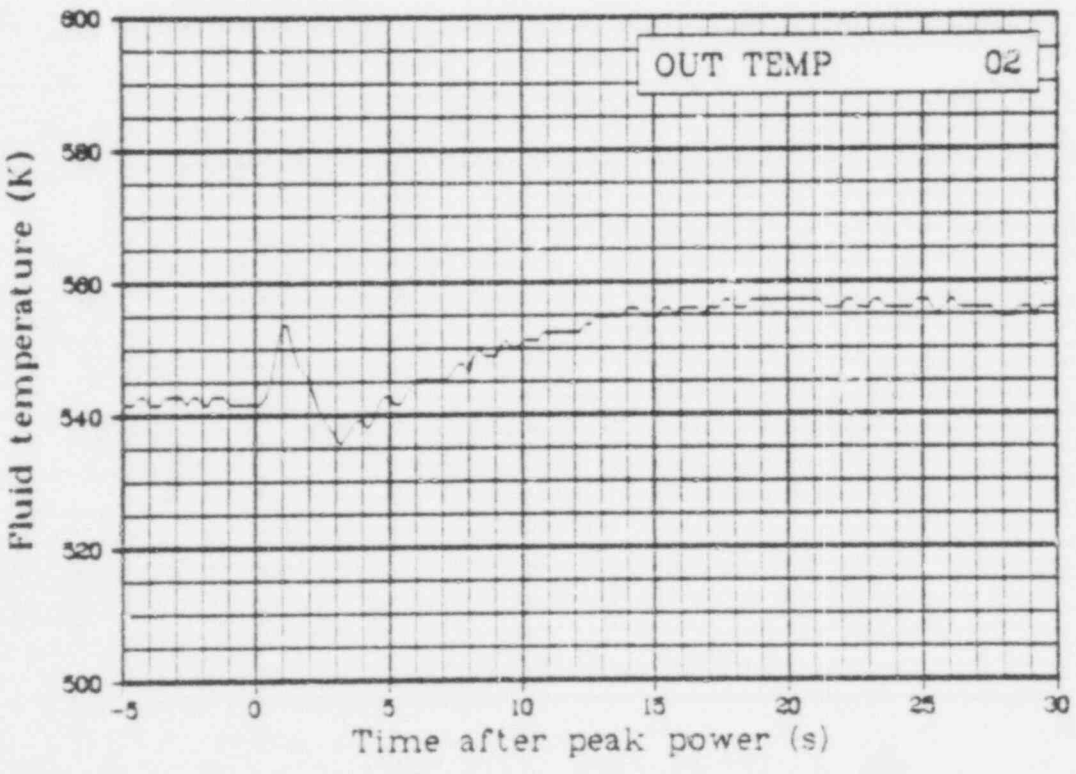

Fig. 28 Fluid temperature of Rod 801-2 coolant outlet (OUT TEMP 02), from 30 s. (QEUD)

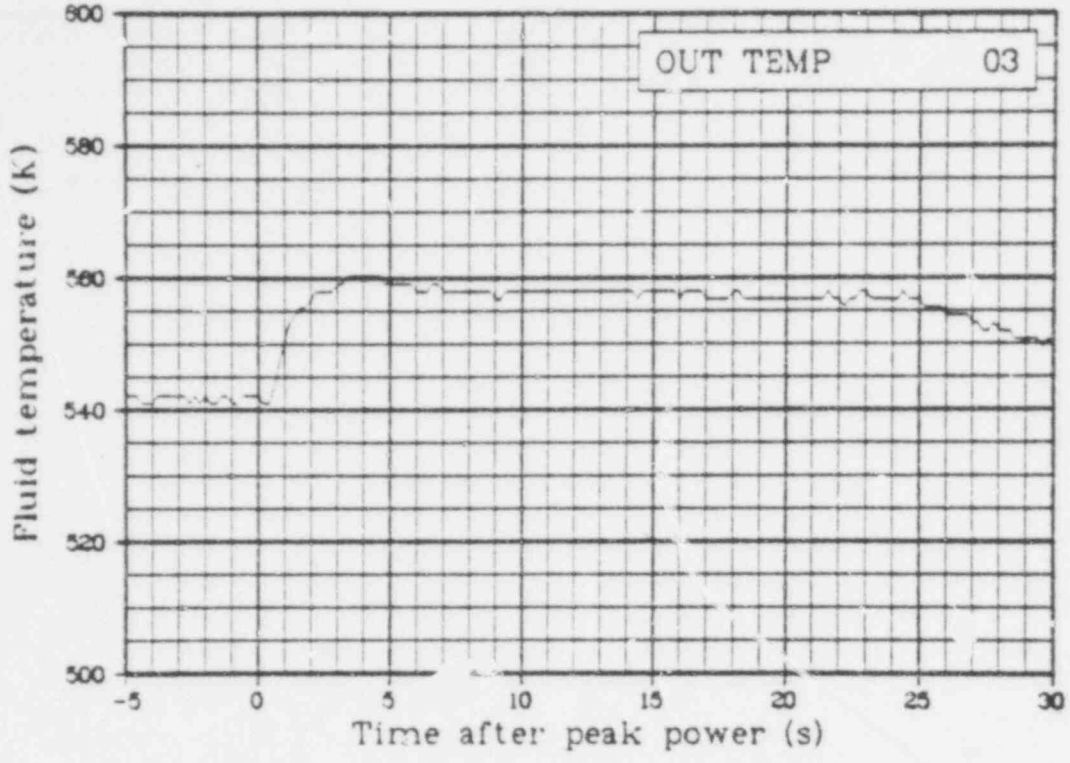

Fig. 29 Fluid temperature of Rod 801-3 coolant outlet (OUT TEMP 03), from -5 to 30 s. (QEUD)

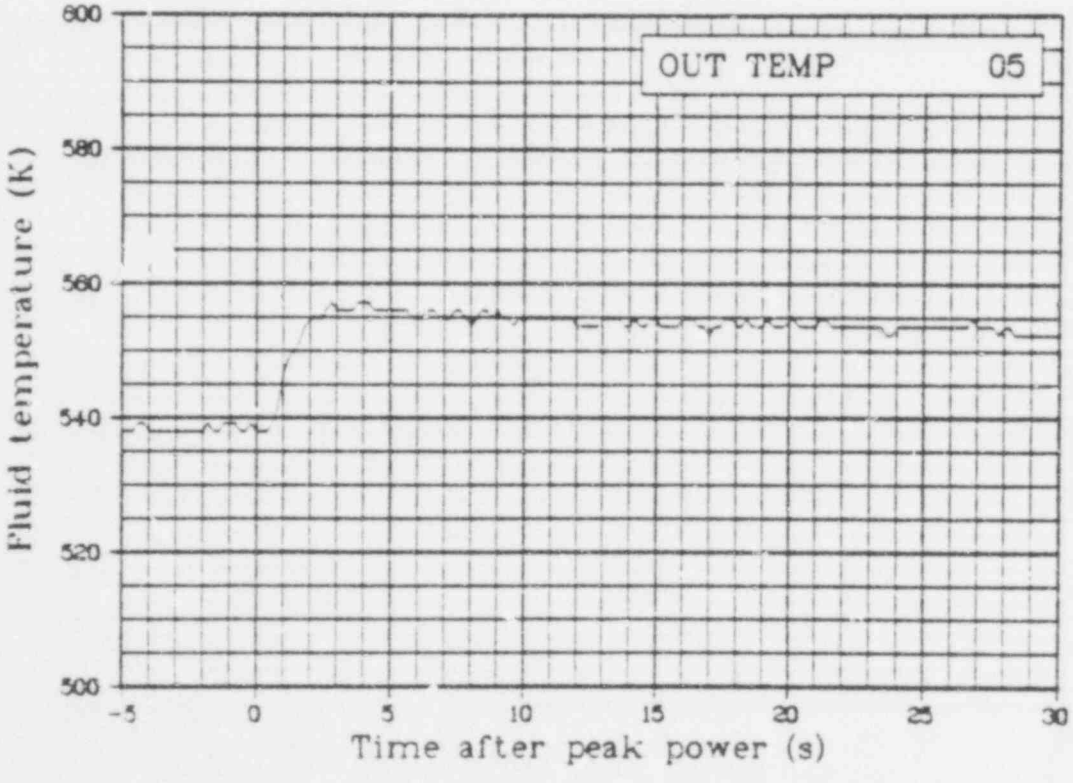

Fig. 30 Fluid temperature of Rod 801-5 coolant outlet (OUT TEMP 05), from -5 to 30 s. (QEUD)

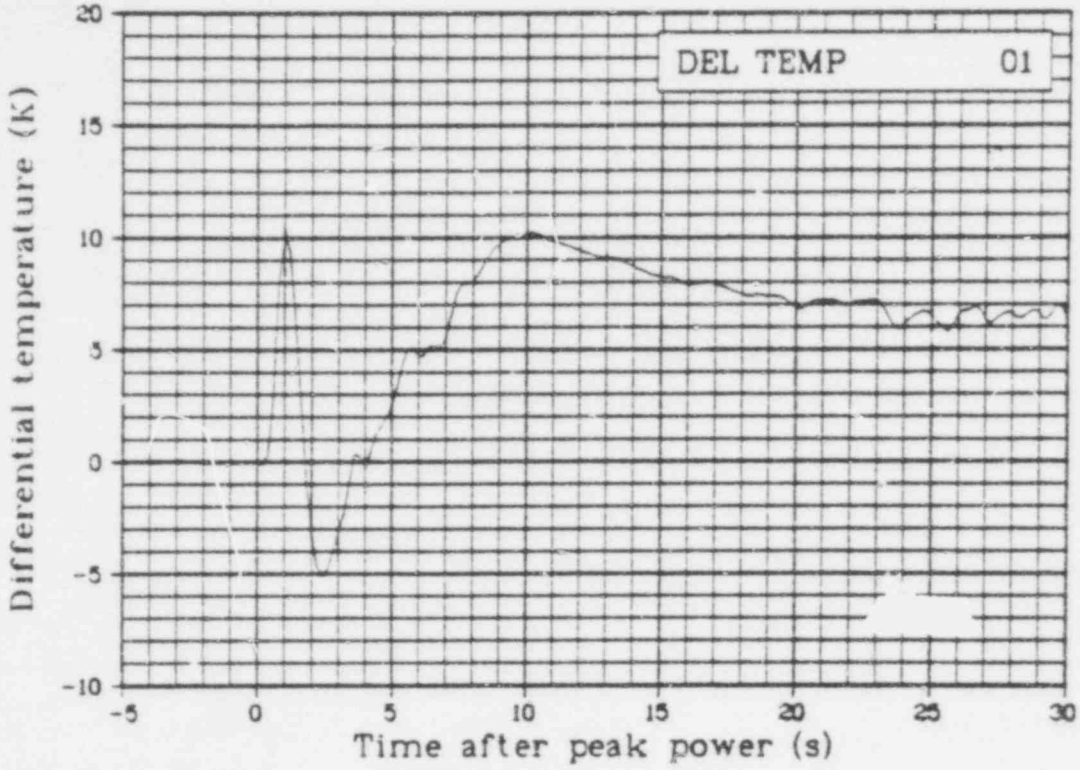

Fig. 31 Differential temperature of Rod 801-1 coolant inlet and outlet (DEL TEMP 01), from -5 to 30 s. (QEUD)

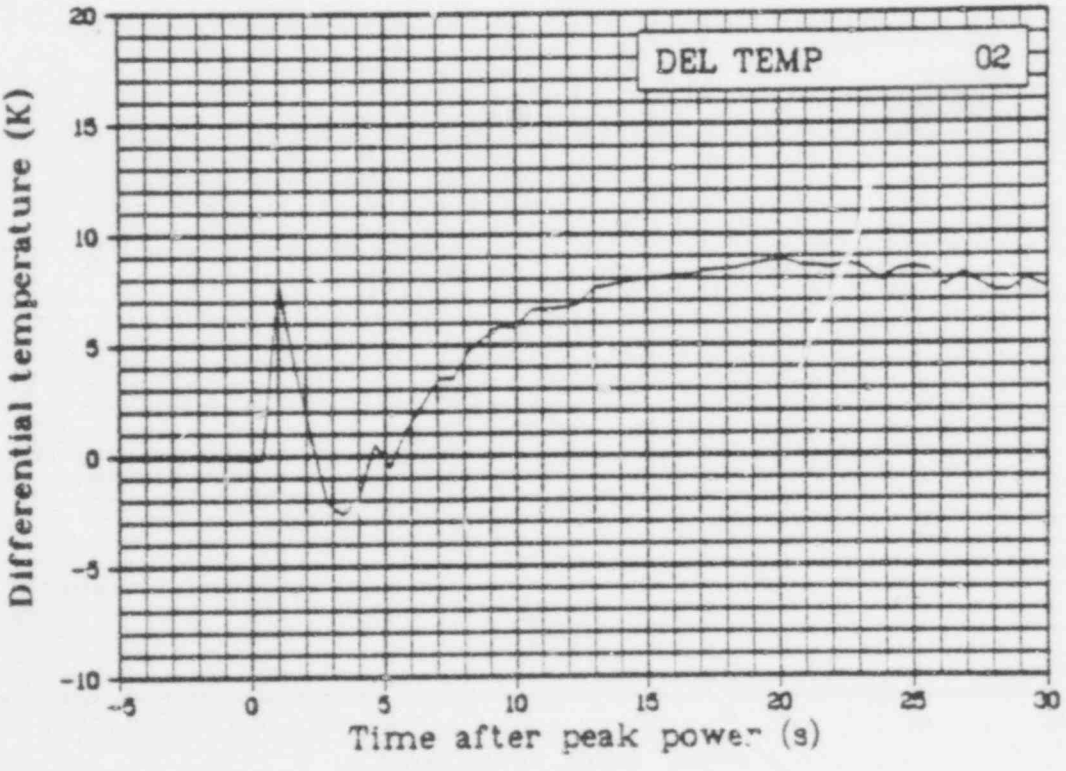

Fig. 32 Differential temperature of Rod 801-2 coolant inlet and outlet (DEL TEMP 02), from -5 to 30 s. (QEUD)

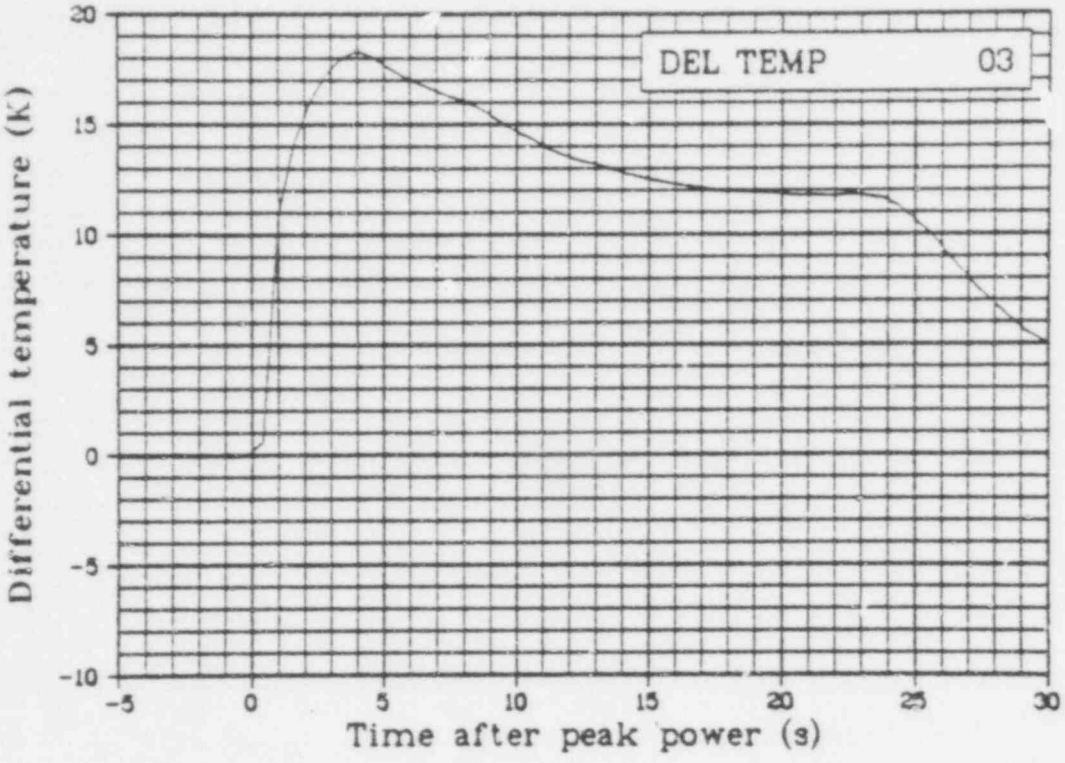

Fig. 33 Differential temperature of Rod 801-3 coolant inlet and outlet (DEL TEMP 03), from -5 to 30 s. (QEUD)

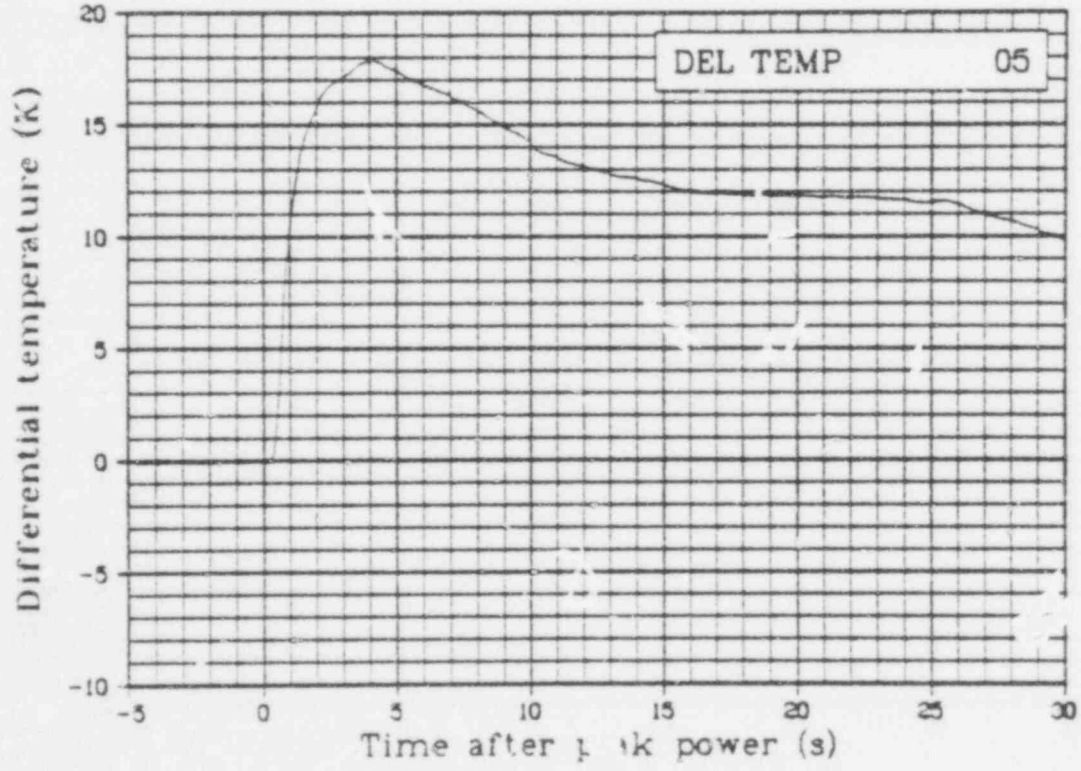

Fig. 34 Differential temperature of Rod 801-5 coolant inlet and outlet (DEL TEMP 05), from -5 to 30 s. (QEUD)

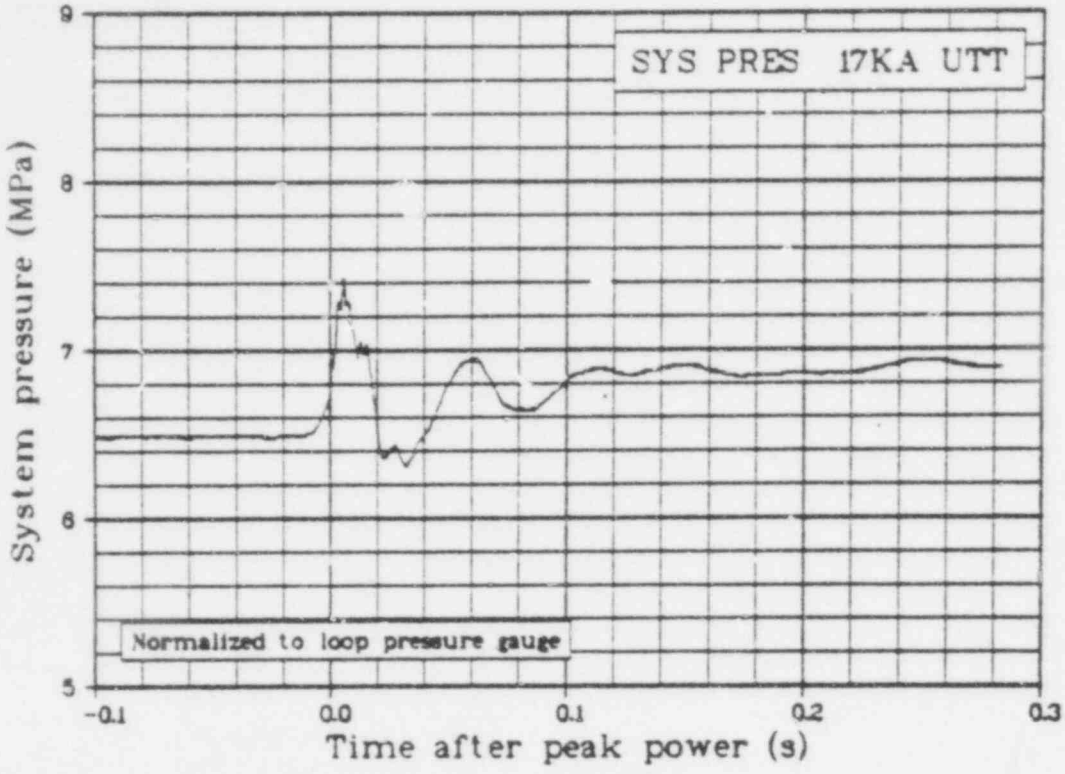

Fig. 35 Absolute pressure in upper test train assembly (SYS PRES 17 KA UTT), from -01 to 0.3 s.

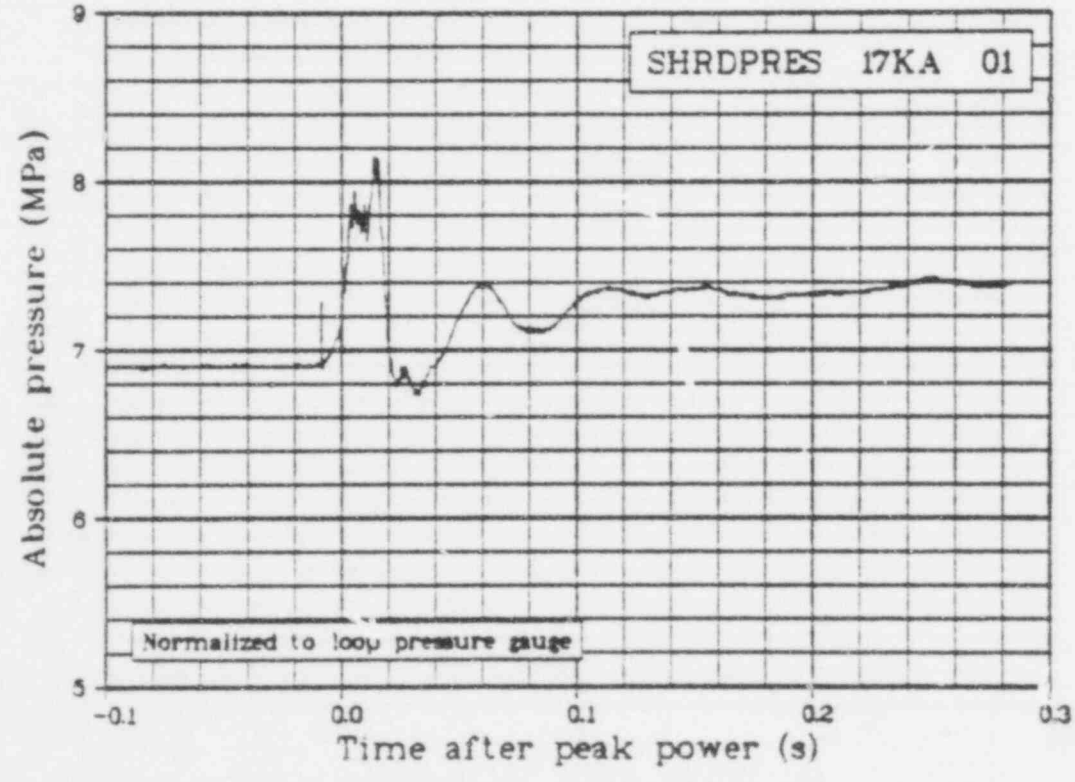

Fig. 36 Absolute pressure inside Rod 801-1 shroud (SHRD PRESS 17 KA 01), from -0.1 to 0.3 s.

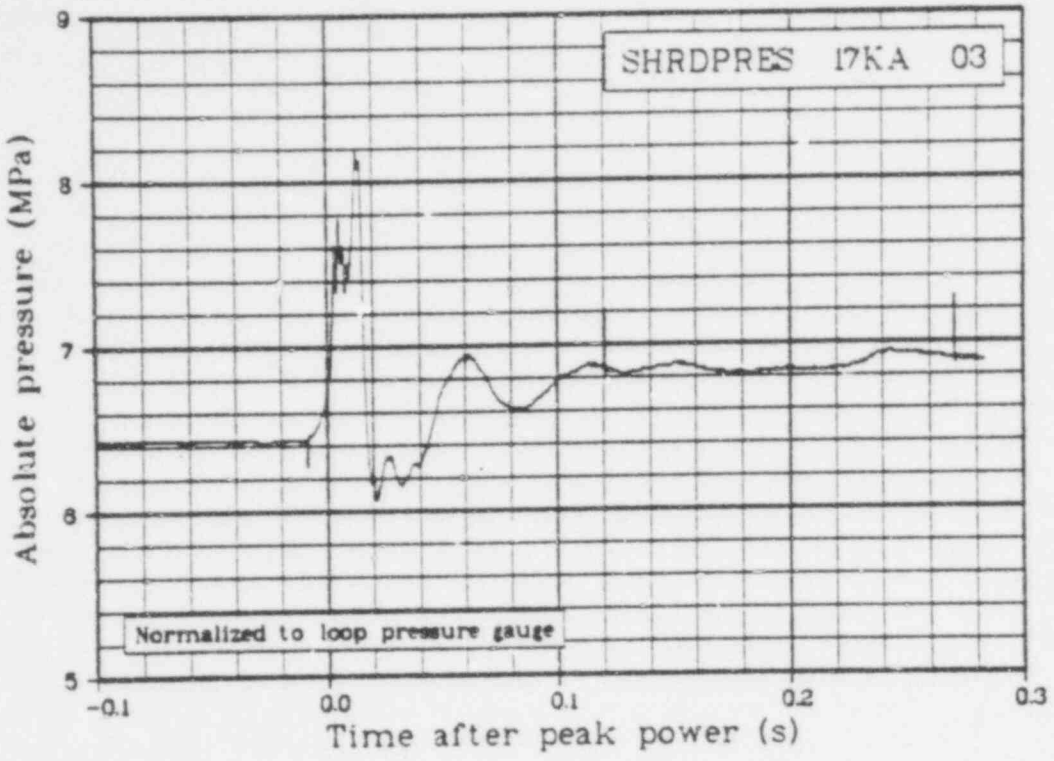

Fig. 37 Absolute pressure inside Rod 801-3 shroud (SHRD PRESS 17 K A 03) from -0.1 to 0.3 s.

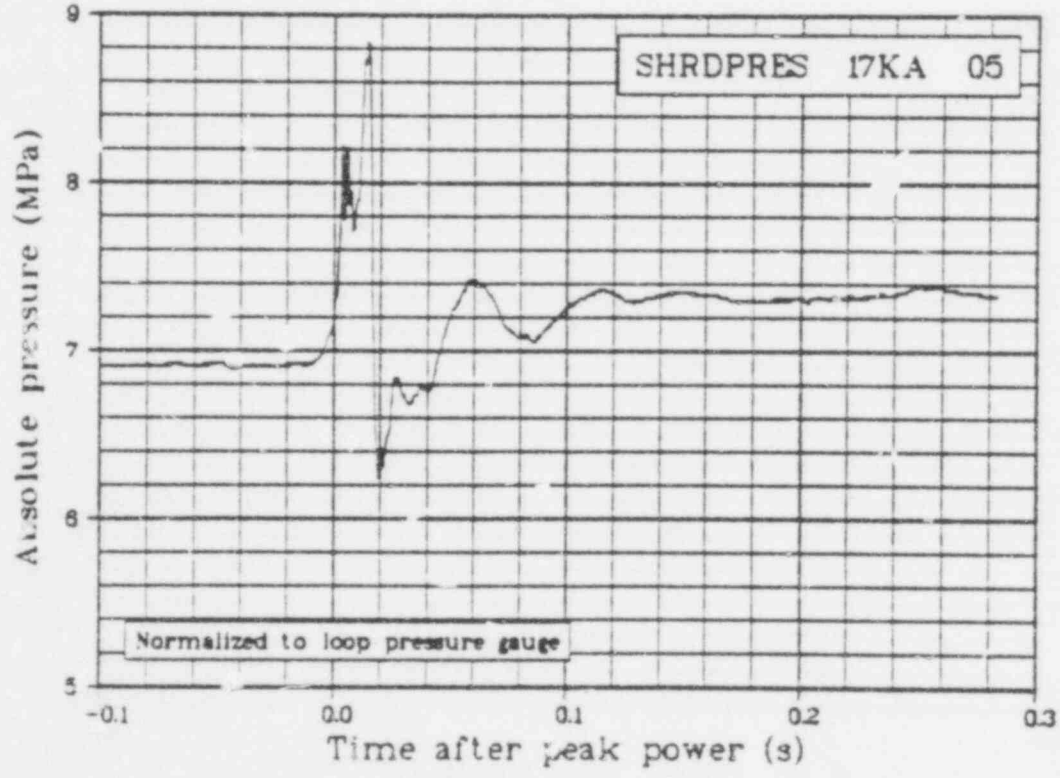

Fig. 38 Absolute pressure inside Rod 801-5 shroud (SHRD PRESS 17 KA 05), from -0.1 to 0.3 s.

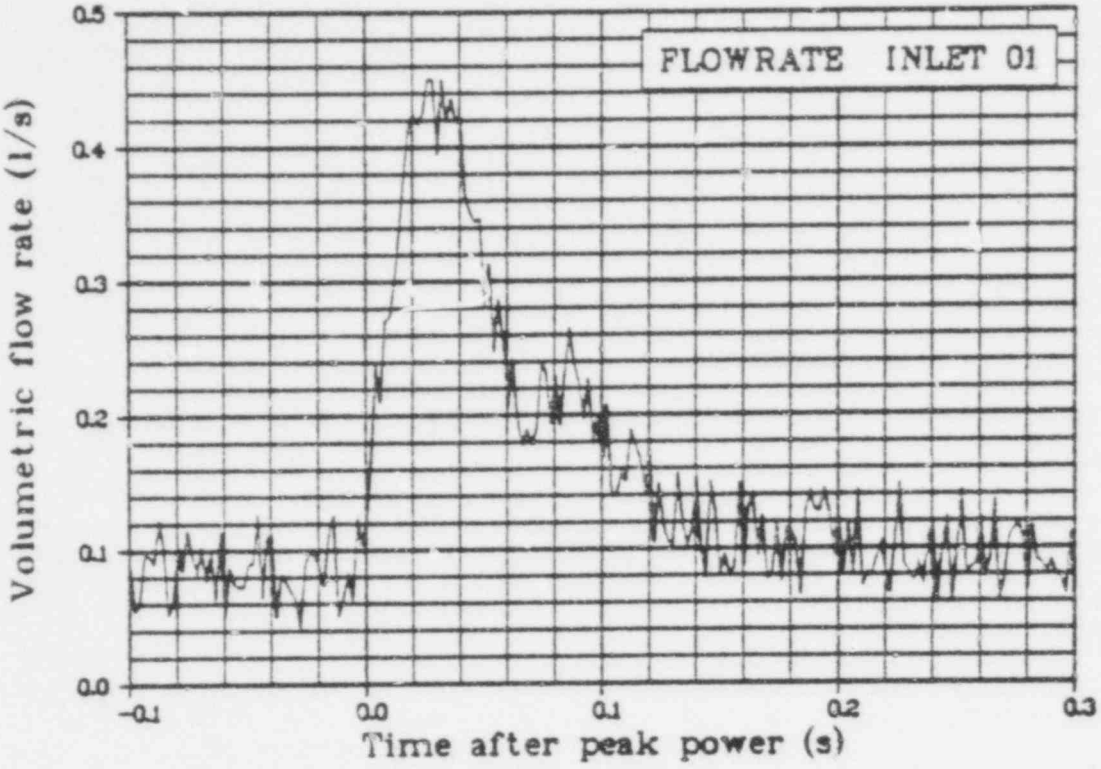

Fig. 39 Volumetric flow rate in Fuel Rod 801-1 shroud inlet (FLOWRATE INLET 01), from -0.1 to 0.3 s.

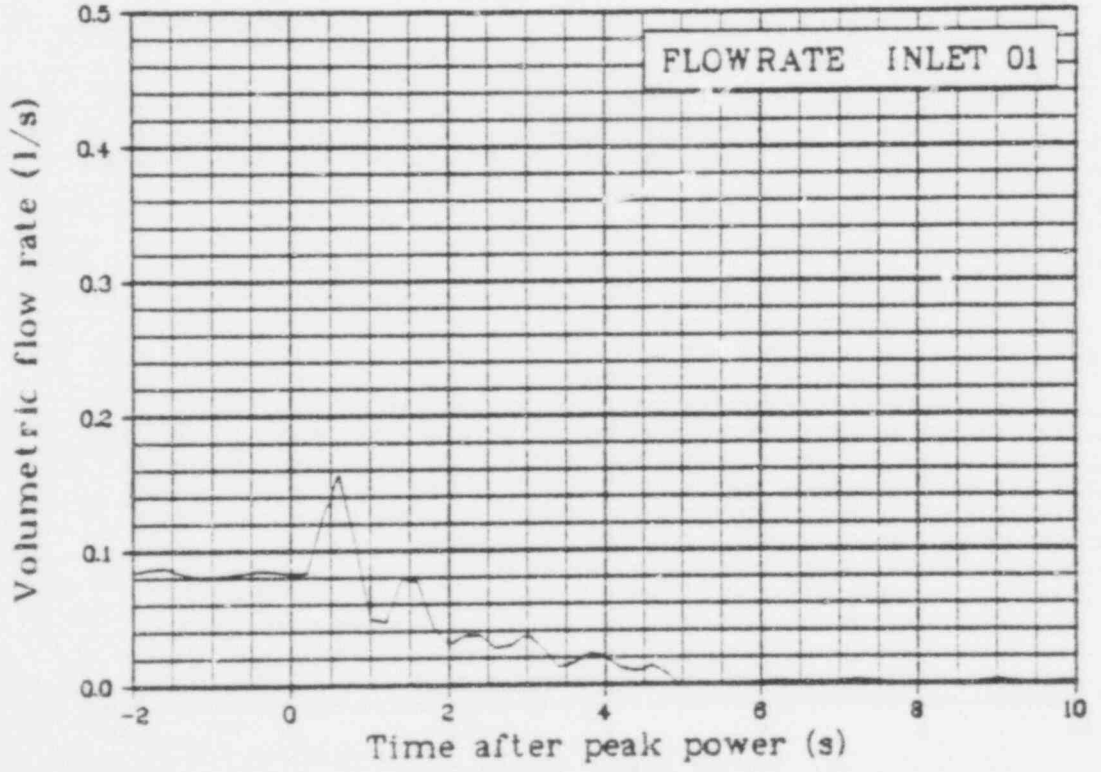

Fig. 40 Volumetric flow rate in Fuel Rod 801-1 shroud inlet (FLOWRATE INLET 01), from -2 to 10 s.

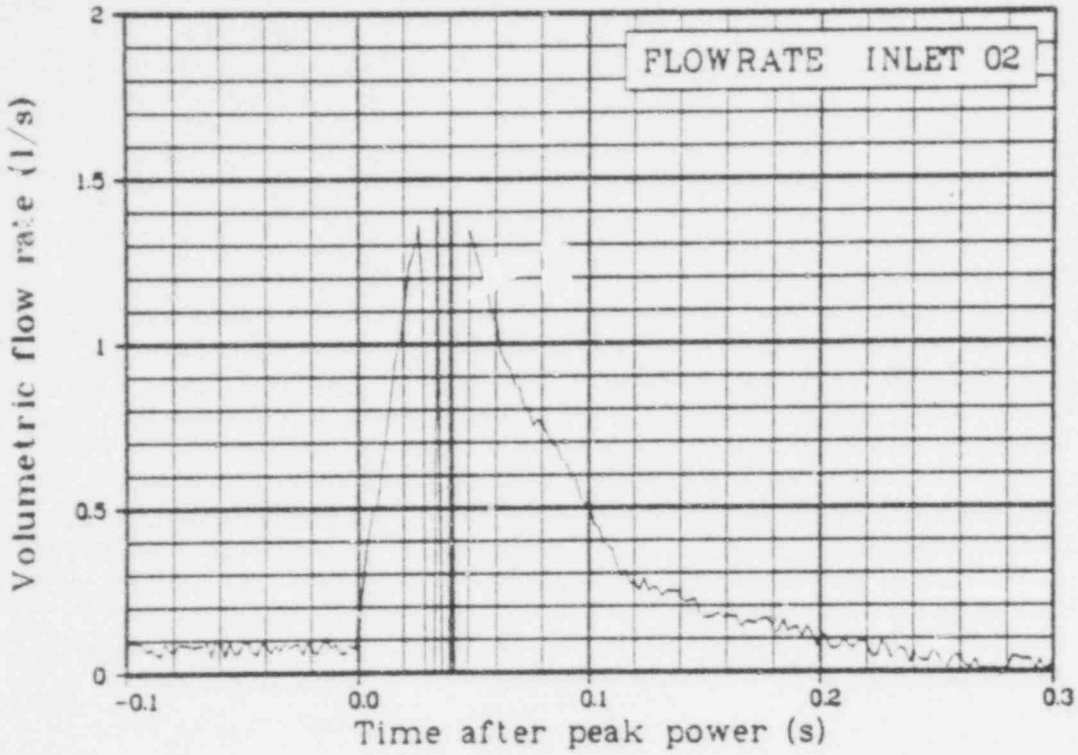

Fig. 41 Volumetric flow rate in Fuel Rod 801-2 shroud inlet (FLOWRATE INLET 02), from -0.1 to 0.3 s.

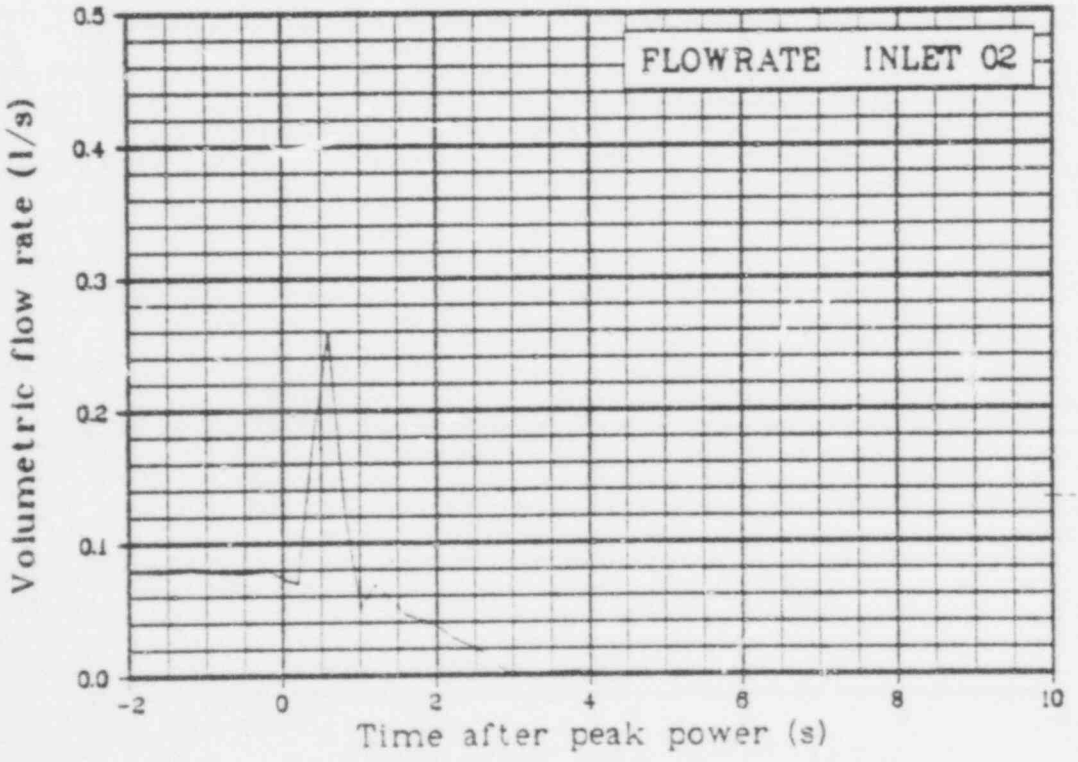

Fig. 42 Volumetric flow rate in Fuel Rod 801-2 shroud inlet (FLOWRATE INLET 02), from -2 to 10 s.

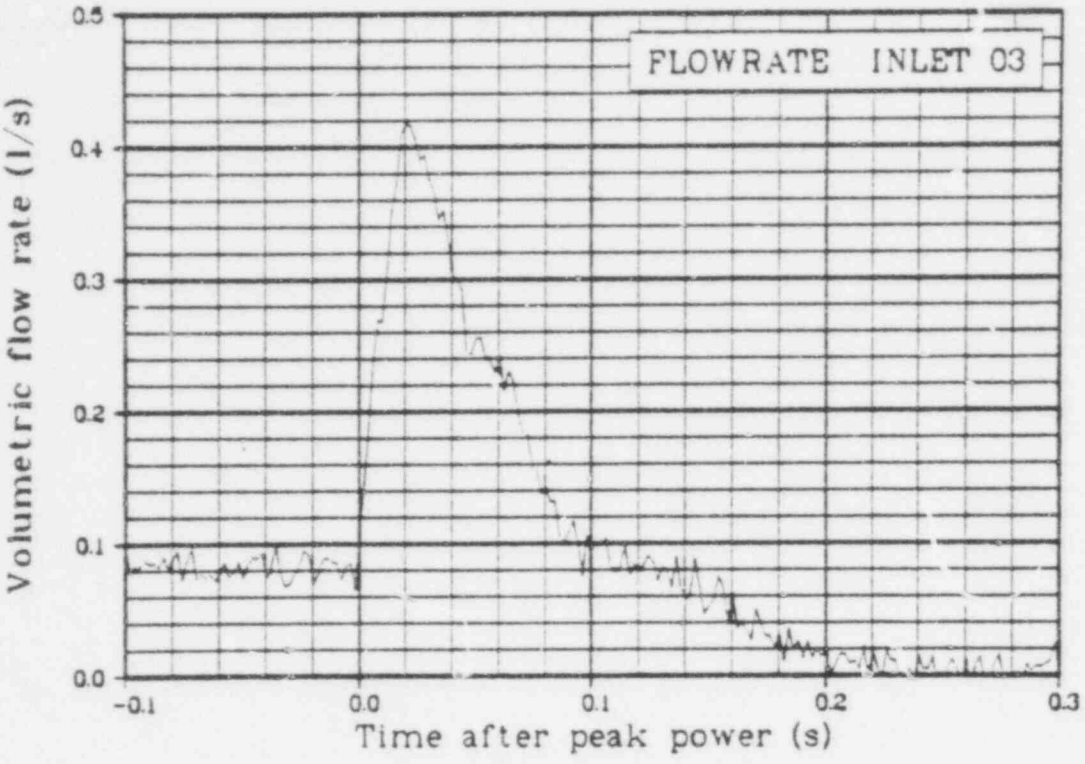

Fig. 43 Volumetric flow rate in Fuel Rod 801-3 shroud inlet (FLOWRATE INLET 03), from -0.1 to 0.3 s.

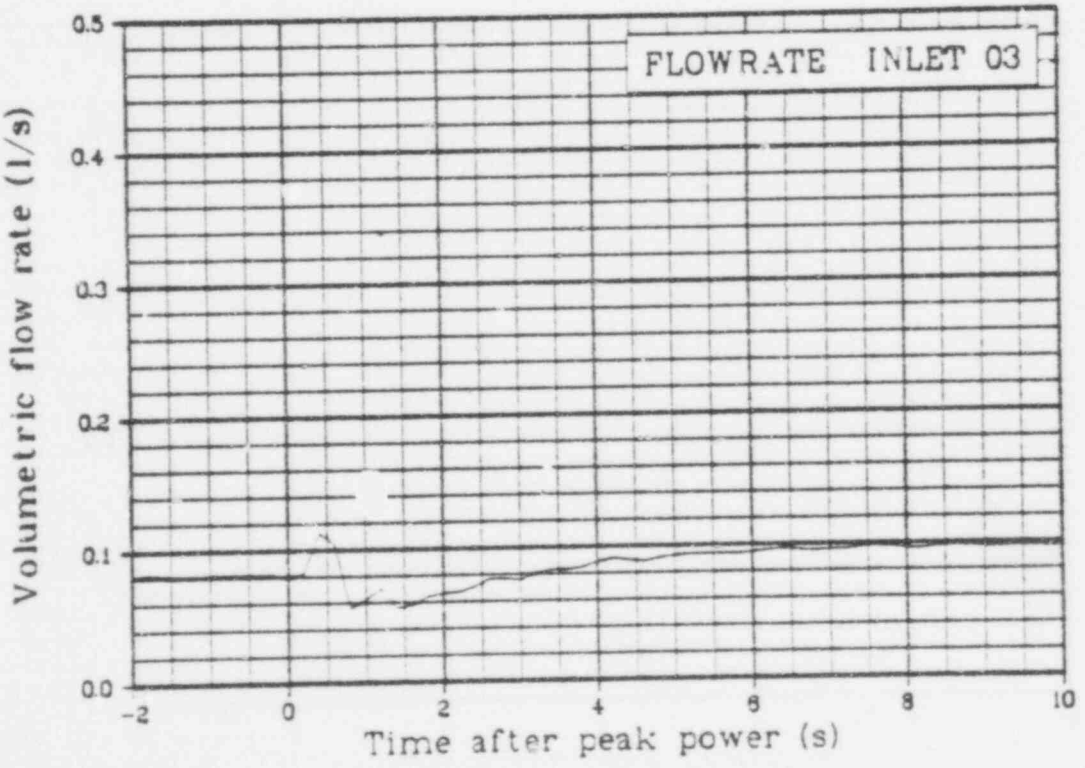

Fig. 44 Volumetric flow rate in Fuel Rod 801-3 shroud inlet (FLOWRATE INLET 03), from -2 to 10 s.

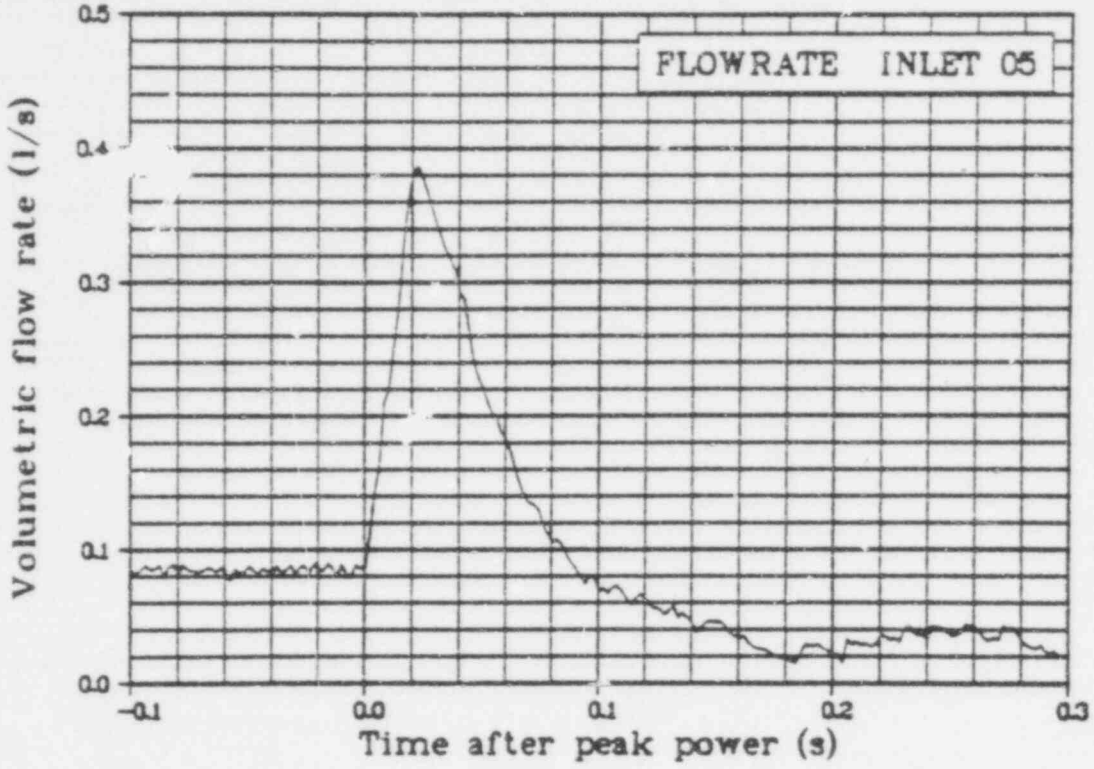

Fig. 45 Volumetric flow rate in Fuel Rod 801-5 shroud inlet (FLOWRATE INLET 05), from -0.1 to 0.3 s.

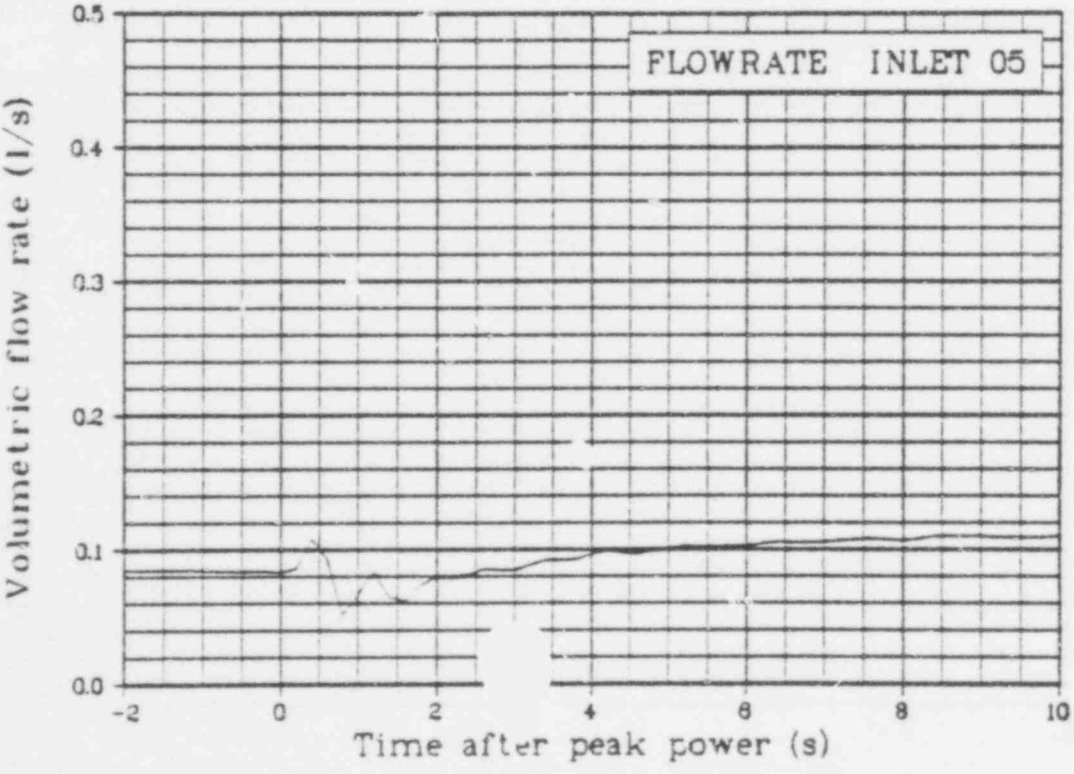

Fig. 46 Volumetric flow rate in Fuel Rod 801-5 shroud inlet (FLOWRATE INLET 05), from -2 to 10 s.

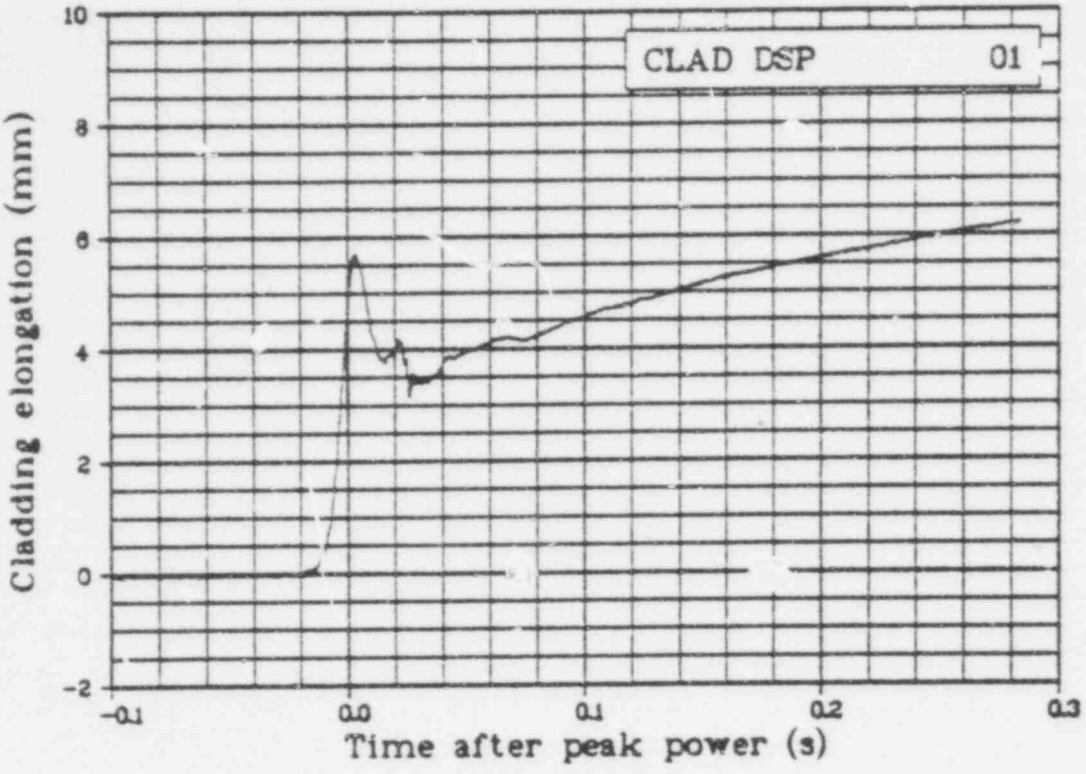

Fig. 47 Cladding elongation of Fuel Rod 801-1 (CLAD DSP 01), from -0.1 to 0.3 s. (QEUD)

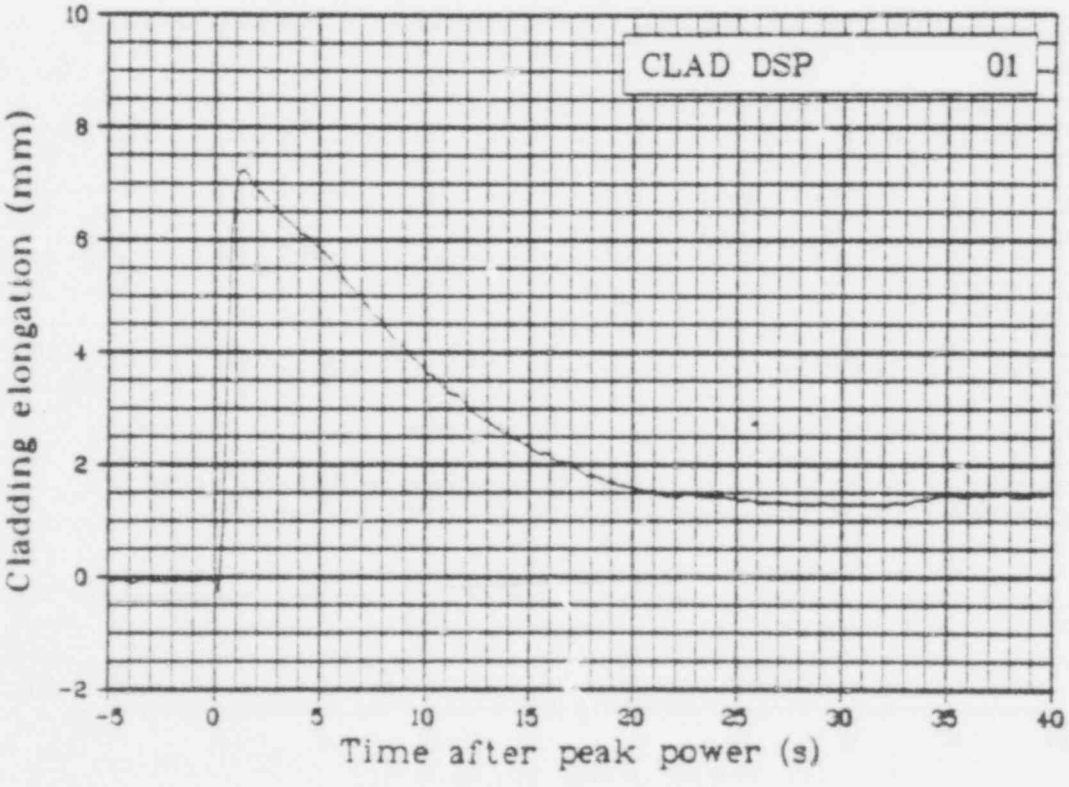

Fig. 48 Cladding elongation of Fuel Rod 801-1 (CLAD DSP 01), from -5 to 40 s. (QEUD)

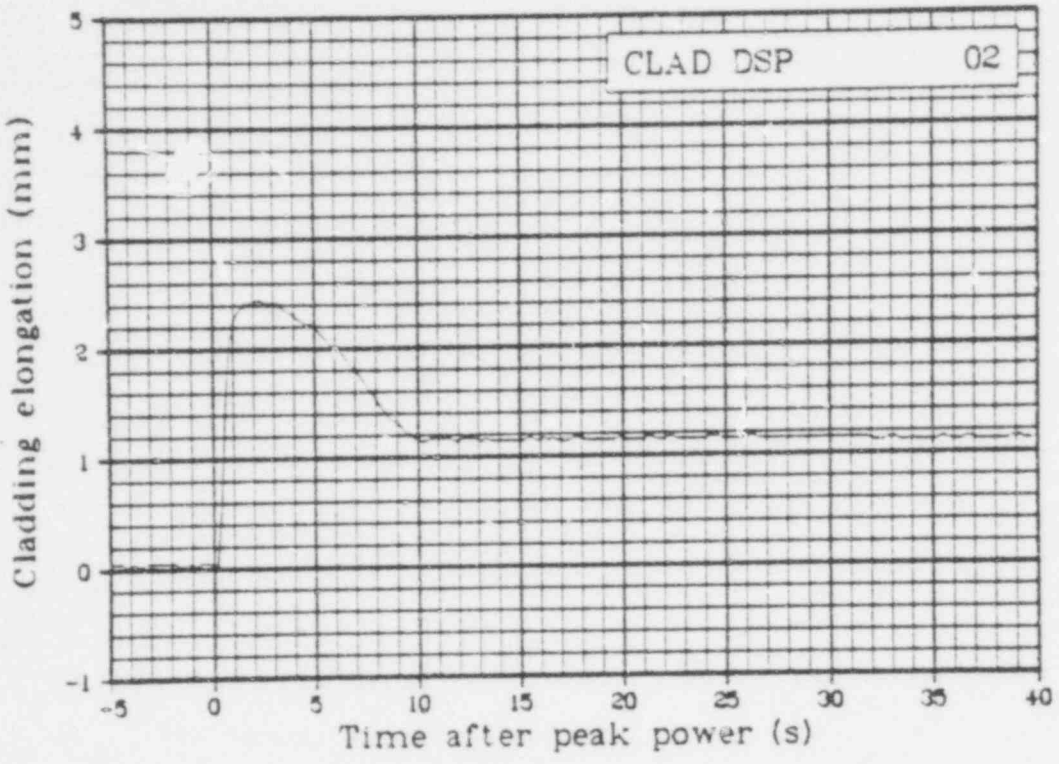

Fig. 49 Cladding elongation of Fuel Rod 801-2 (CLAD DSP 02), from -5 to 40 s. (QEUD)

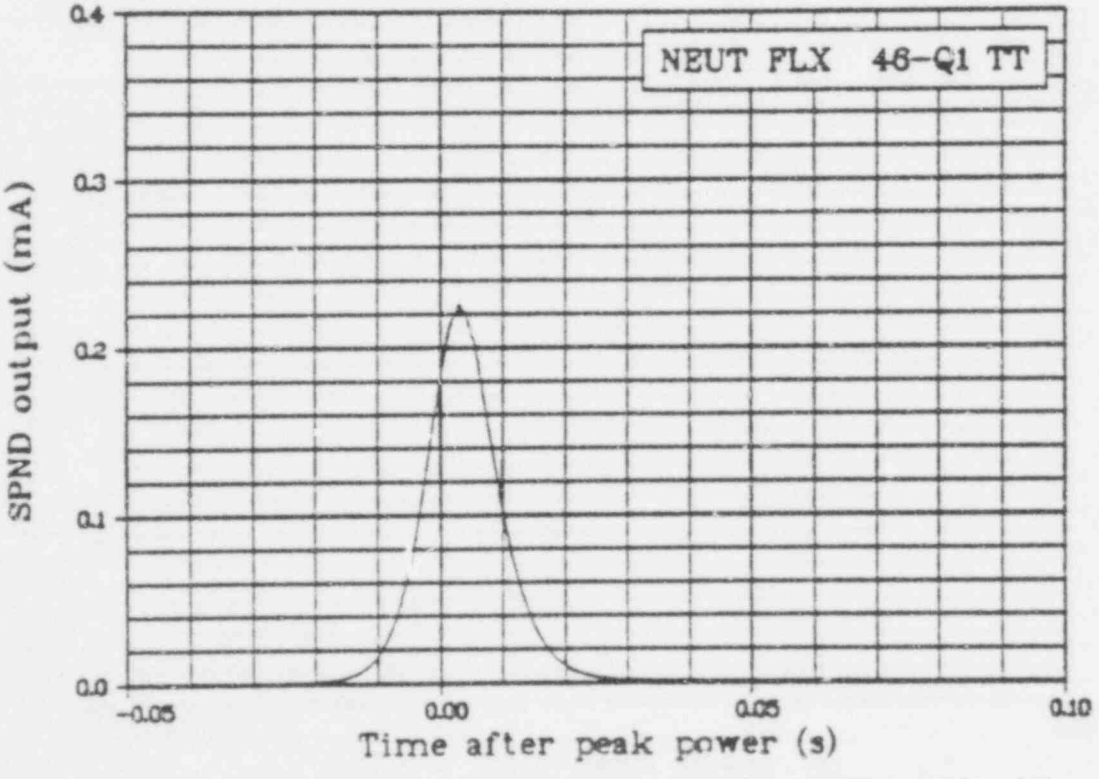

Fig. 50 Neutron flux in Quadrant 1, 0.46 m above fuel stack bottom (NEUT FLX 46-Q1 TT), from -0.05 to 0.10 s.

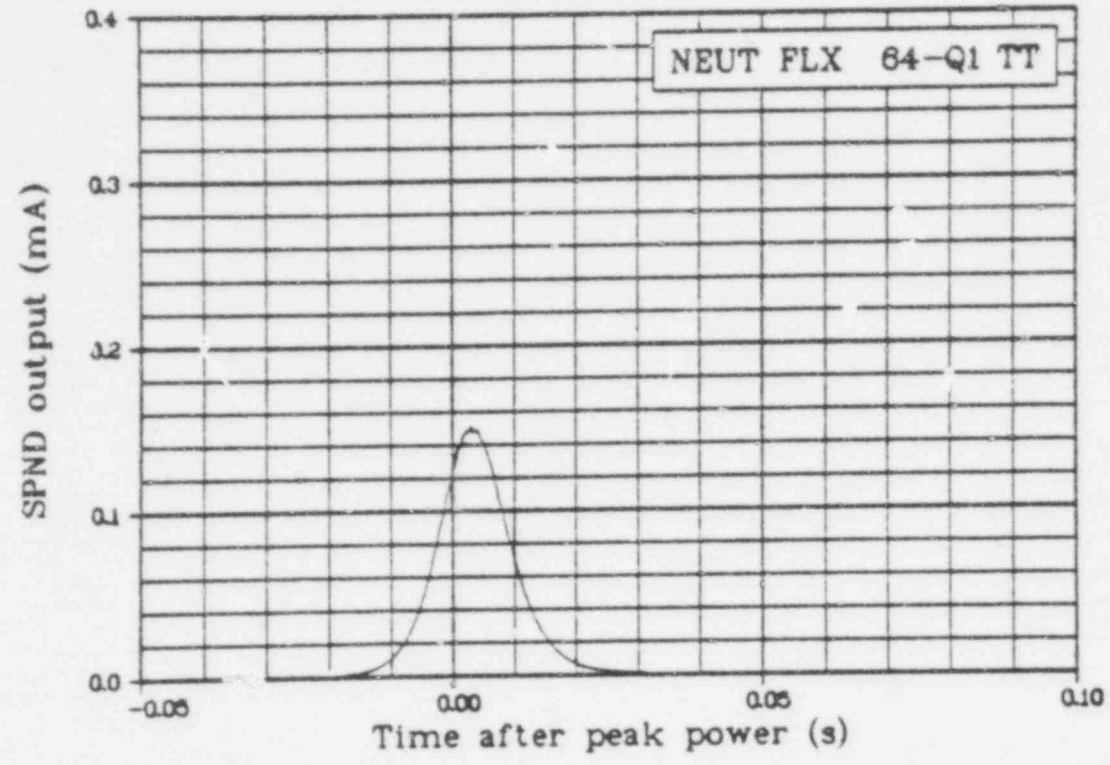

Fig. 51 Neutron flux in Quadrant 1, 0.64 m above fuel stack bottom (NEUT FLX 64-Q1 TT), from -0.05 to 0.10 s.

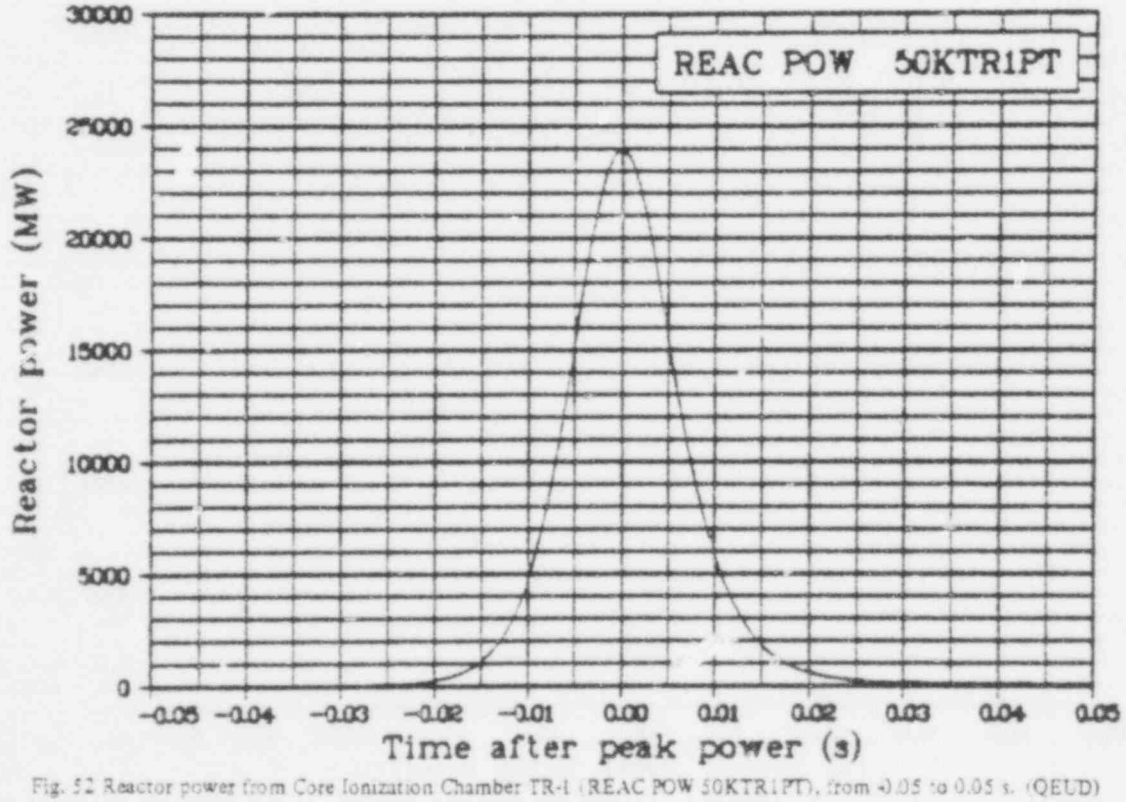

Fig. 52 Reactor power from Core Ionization Chamber TR-1 (REAC POW 50KTR1PT), from -0.05 to 0.05 s. (QEUD)

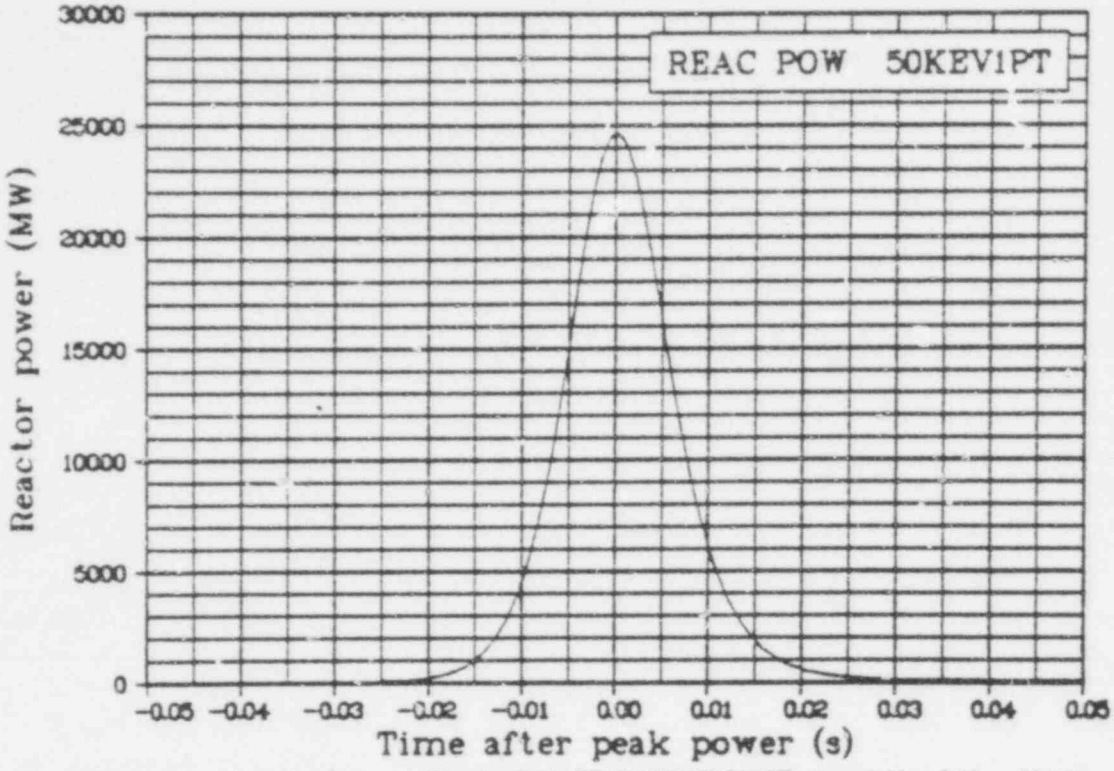

Fig. 53 Reactor power from Core Ionization Chamber EV-1 (REAC POW 50KEV1PT), from -0.05 to 0.05 s. (QEUD)

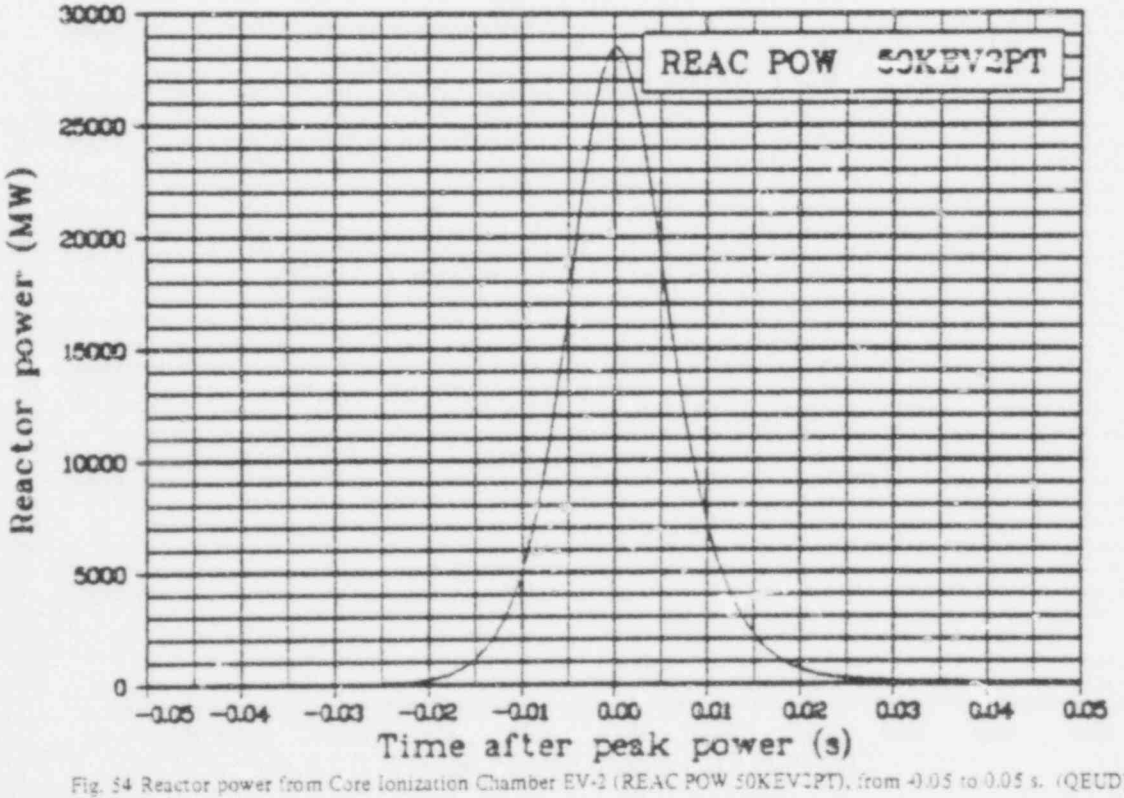

Fig. 54 Reactor power from Core Ionization Chamber EV-2 (REAC POW 50KEV2PT), from -0.05 to 0.05 s. (QEUD)

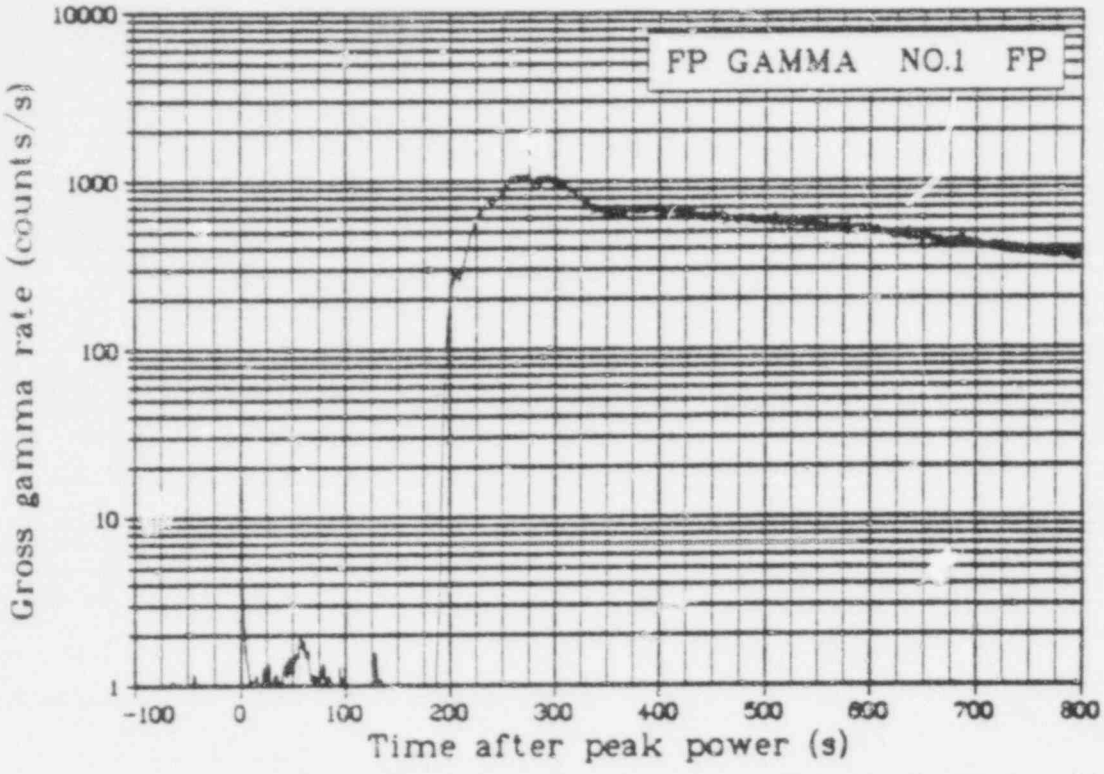

Fig. 55 Gross gamma rate of fission product detector, 150- to 3400-keV region (FP GAMMA NO. 1 FP), from -100 to 800 s.

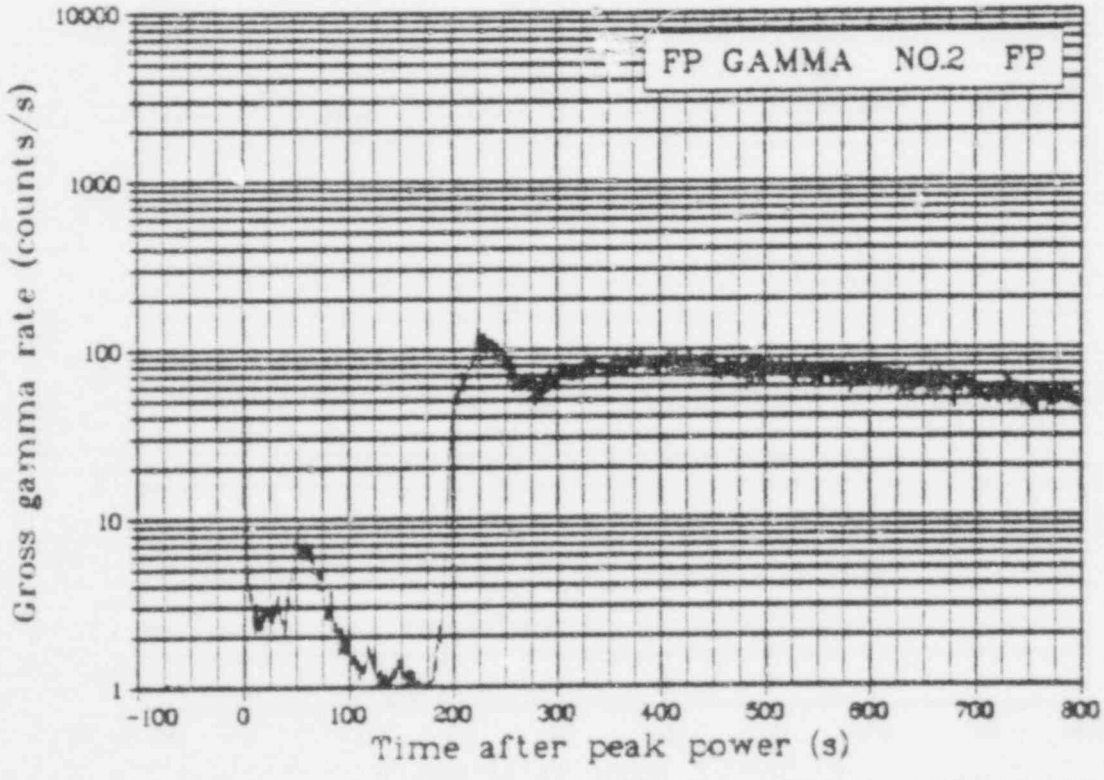

Fig. 56 Gross gamma rate of fission product detector, 150- to 6300-keV region (FP GAMMA NO. 2 FP), from -100 to 800 s.

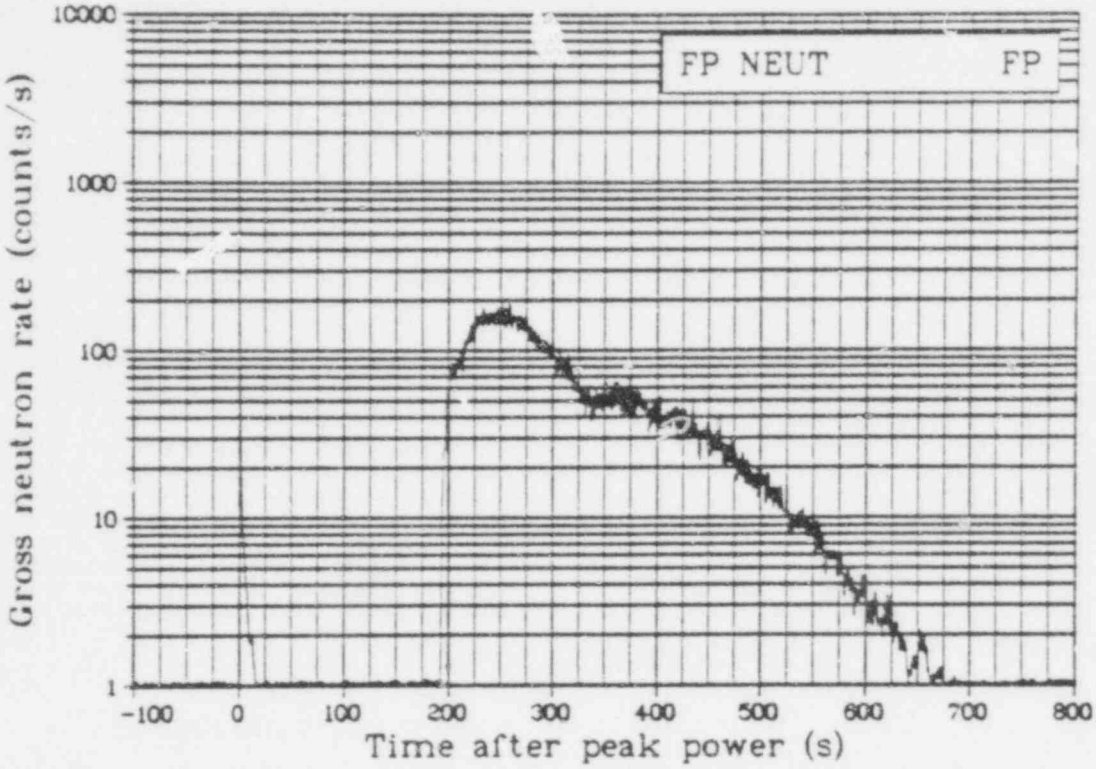

Fig. 57 Gross neutron rate of fission product detector system (FP NEUT FP), from -100 to 800 s.

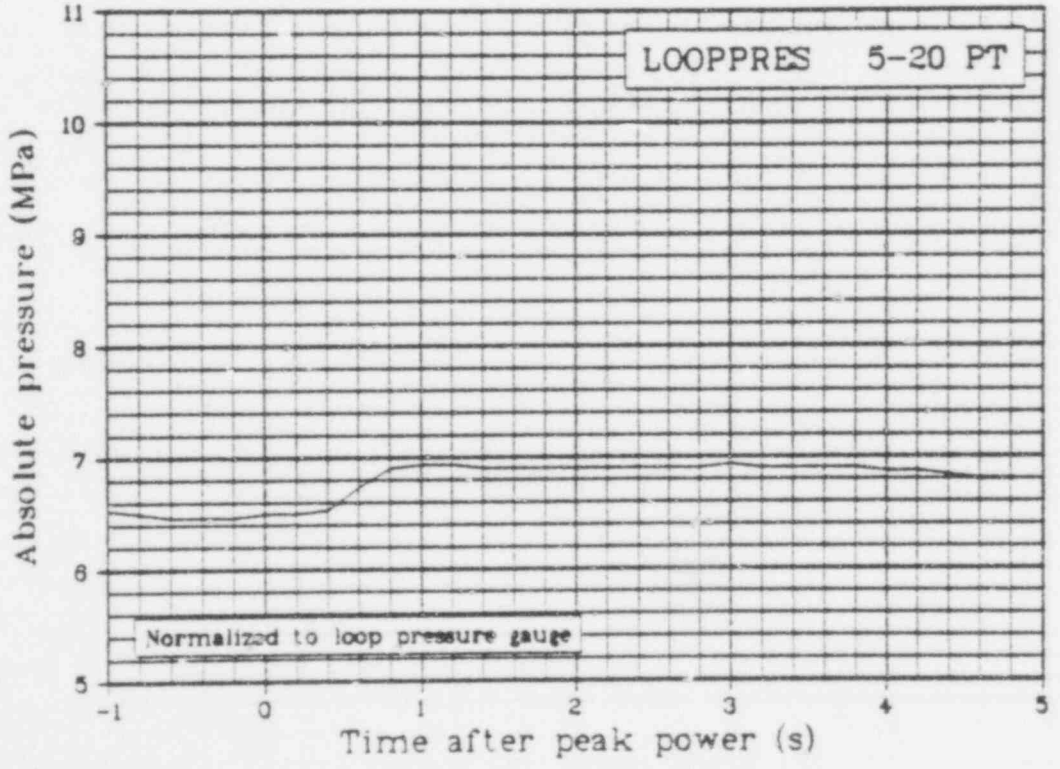

Fig. 58 Absolute pressure in plant loop system from Transducer 20 (LOOPPRES 5-20 PT), from -1 to 5 s.

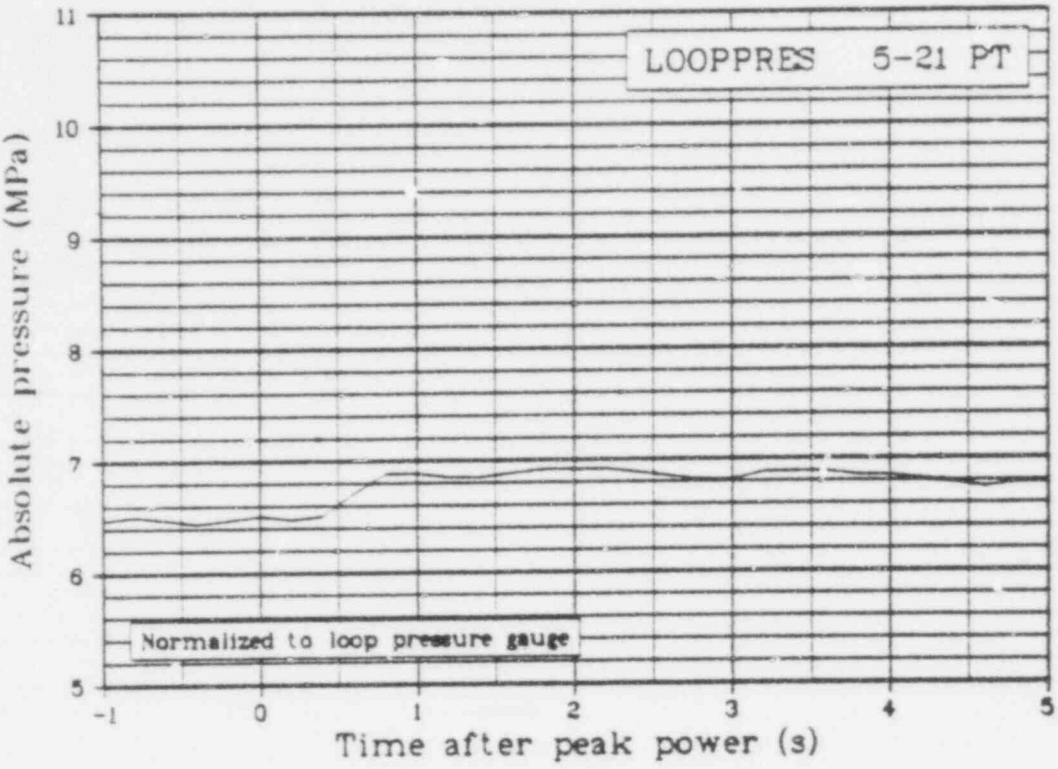

Fig. 59 Absolute pressure in plant loop system from Transducer 21 (LOOPPRES 5-21 PT), from -1 to 5 s.

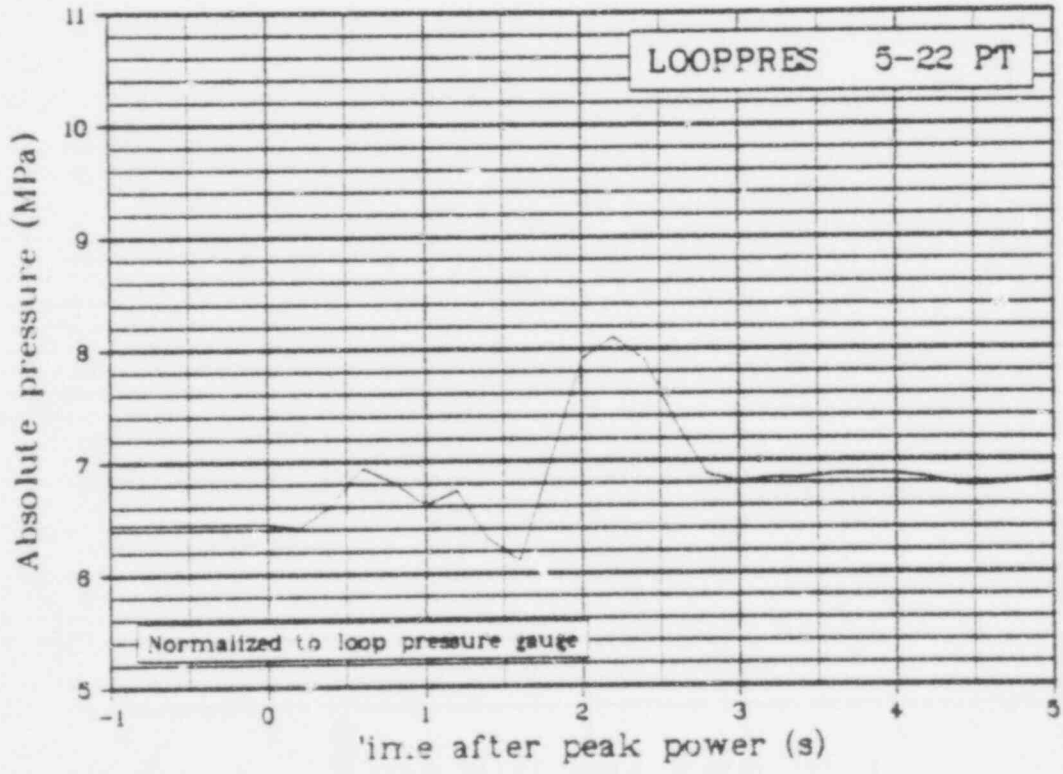

Fig. 60 Absolute pressure in plant loop system from Transducer 22 (LOOPPRES 5-22 PT), from -1 to 5 s.

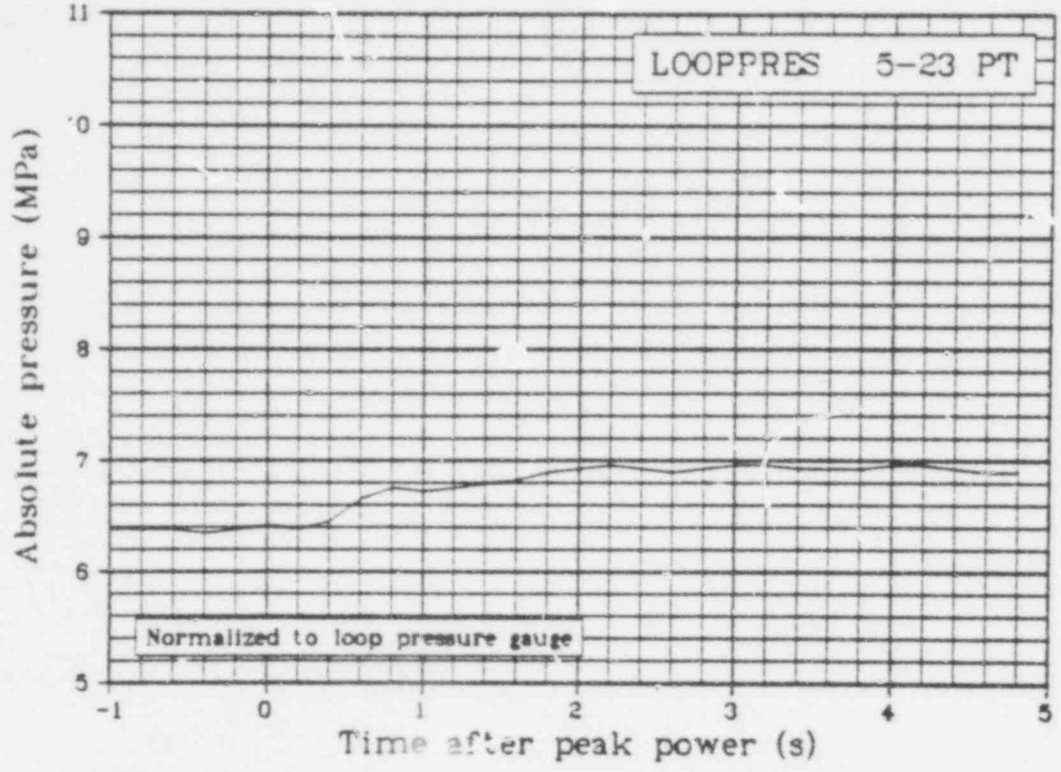

Fig. 61 Absolute pressure in plant loop system from Transducer 23 (LOOPPRES 5-23 PT), from -1 to 5 s.

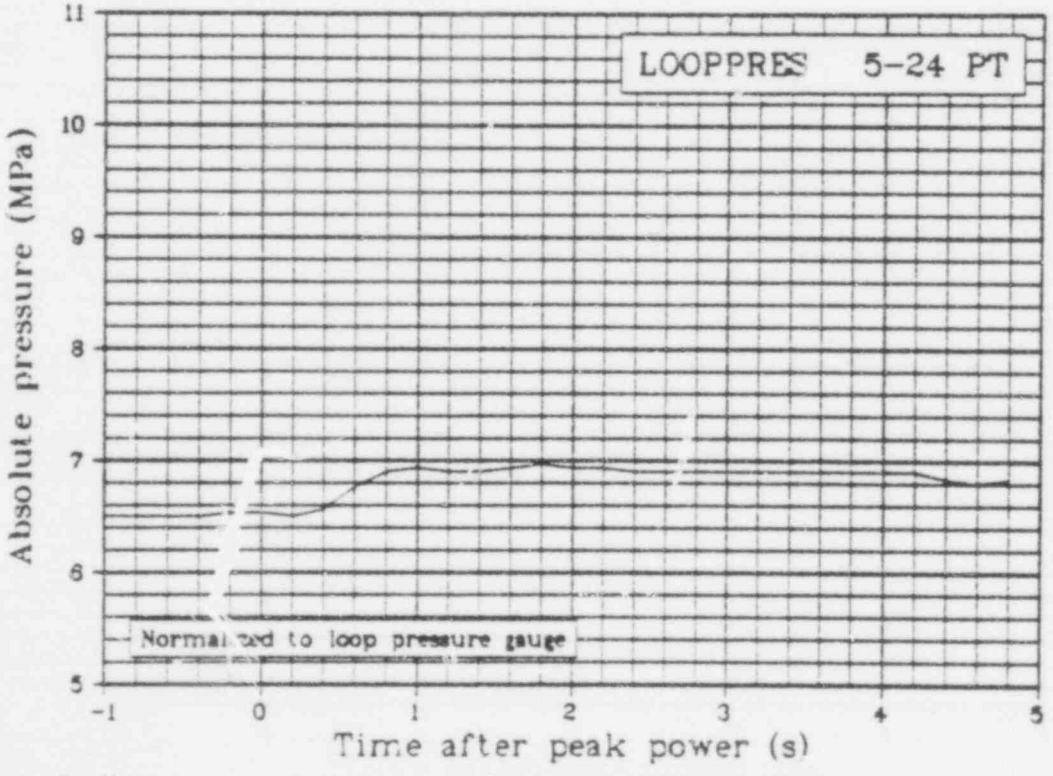

Fig. 62 Absolute pressure in plant loop system from Transducer 24 (LOOPPRES 5-24 PT), from -1 to 5 s.

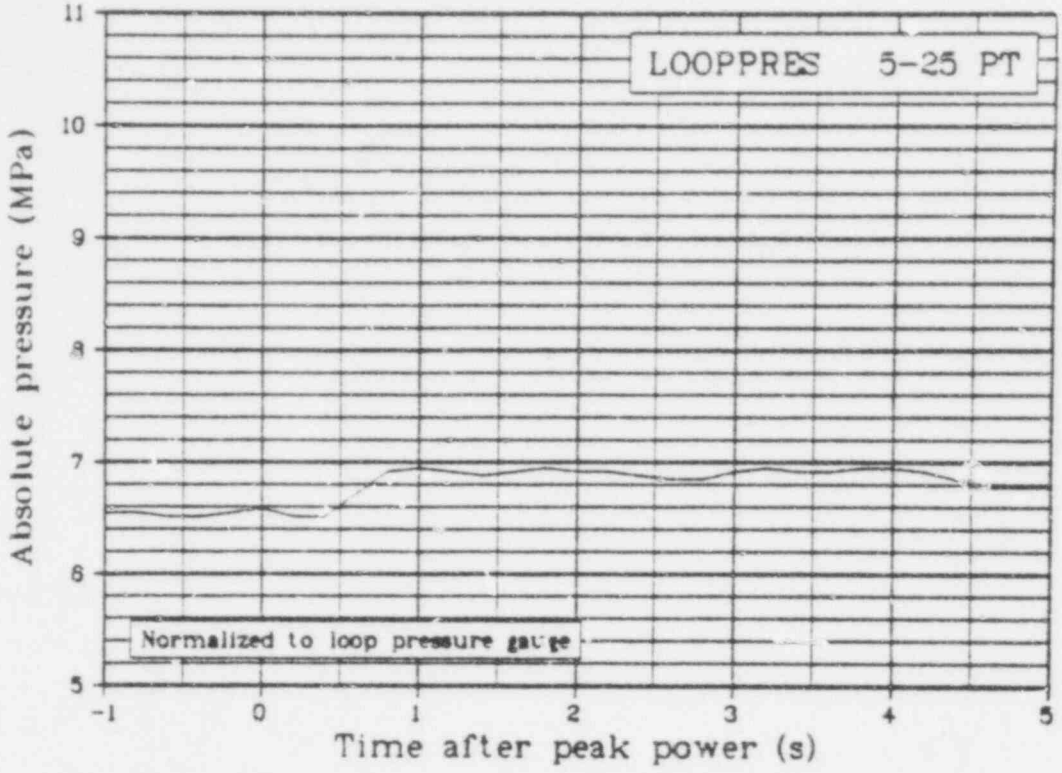

Fig. 63 Absolute pressure in plant loop system from Transducer 25 (LOOPPRES 5-25 PT), from -1 to 5 s.

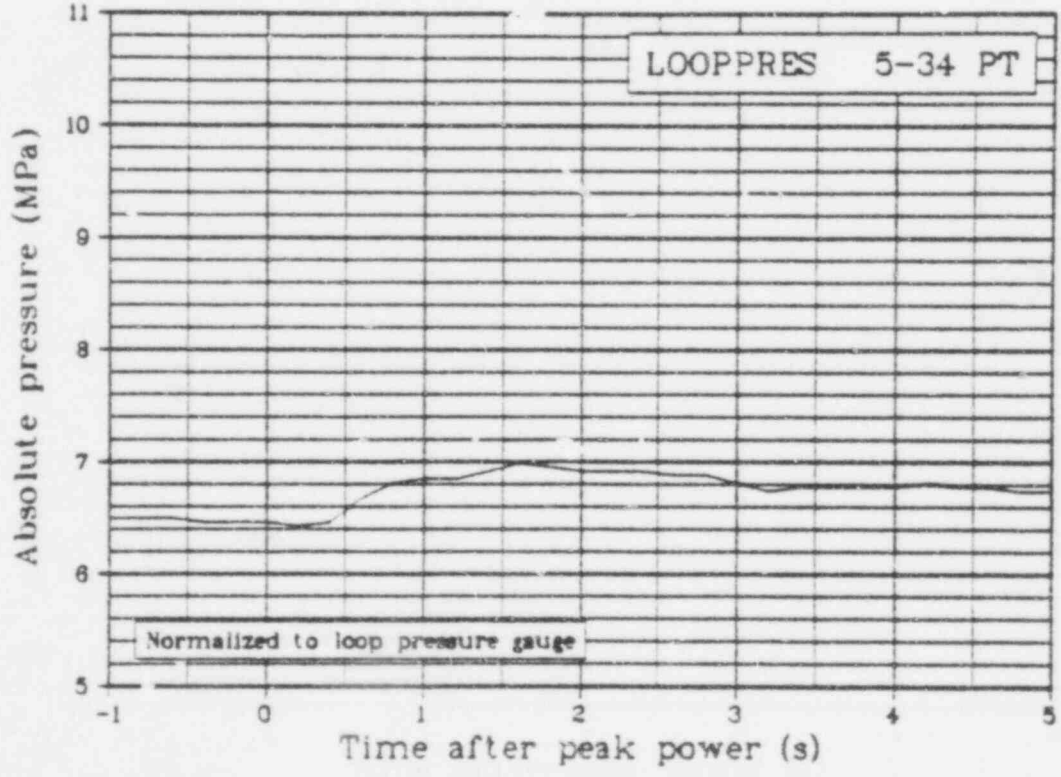

Fig. 64 Absolute pressure in plant loop system from Transducer 34 (LOOPPRES 5-34 PT), from -1 to 5 s.

V. REFERENCE

1. *Characteristics of UO_2-Zircaloy Fuel Rod Materials from Saxton Reactor for Use in the Power Burst Facility*, ANCR-NUREG-1321 (September 1976).

APPENDIX A

POSTTEST DATA ADJUSTMENTS AND QUALIFICATION

APPENDIX A

POSTTEST DATA ADJUSTMENTS AND QUALIFICATION

Many of the instrumentation transducers used during the conduct of Test RIA 1-1 are recognized to have the potential for responding erroneously, in varying degrees, to extraneous environmental stimuli such as pressure, temperature, neutron flux, gamma radiation, vibration, and mechanical strain. In addition, the data acquisition and recording system and the signal conditioning equipment may also have contributed unwanted or distorted signals to the measurement channel while the transducer output was being processed and recorded.

Although the errors introduced into the data by these spurious secondary inputs generally do not exceed the specified error ranges of the transducers, significant improvement in measurement accuracy can be achieved if the secondary sensitivity can be identified and removed. Since the exact values of the spurious inputs to which different transducers might be sensitive cannot be easily predicted and are sometimes inconvenient to measure, secondary effects have been accounted for by correcting the data after the test.

Data acquired at the PBF during the performance of the Thermal Fuels Behavior Program testing are appraised by a data integrity review committee for quality and validity. The appraisal process determines whether the measurement channel output represents the phenomenon being measured. The data review and examination process ascertains that verified calibration equations have been applied and that offsets and corrections have also been applied to remove any identifiable spurious secondary effects from the data. As a result of the review and examination by the review committee, each measurement is assigned one or more of the following classifications as a function of time.

(1) Qualified engineering unit data (QEUD). These data represent the phenomenon measured within the defined uncertainty limits. These data must meet the following criteria: (a) verified calibrations and all corrections have been applied, (b) independent data was used for comparison with this data and agreement was found between the data during the period of interest within specified uncertainty limits, (c) verified engineering unit conversion equations have been applied, and (d) uncertainty limits have been established and can be verified.

(2) Restrained. These data represent the phenomenon measured with one or more of the following constraints: (a) verified calibrations have been applied but not all corrections have been made, (b) offsets and corrections cannot be adequately determined, and (c) uncertainty limits have been established but cannot be adequately verified.

(3) Trend. These data have been verified to represent the relative changes in the phenomenon but do not necessarily represent the absolute level in the measured phenomenon due to: (a) instrument calibrations do not adequately represent the environment measured by the transducer, (b) the calibration and performance of the DARS are questionable but known errors have been eliminated, (c) uncertainty limits cannot be adequately quantified, (d) transducer performance is questionable but relatively correct, or (e) no corrections can be made to adequately compensate for environmental effects. The data have met the following criteria: (a) instrument and DARS calibrations have been applied, (b) wild points have been removed, (c) data have been appropriately filtered, and (d) relative uncertainty limits have been defined.

(4) Failed. Data are irretrievable due to a transducer, signal conditioning, or data channel failure or inadequate rejection of extraneous noise, transient, or frequencies.

Voltage insertion calibrations are made on all measurement channels at the start and conclusion of each test period in the PBF. The corrections and offsets applied to the data are based on pretest and posttest calibrations performed on all measurement channels. The linear offset adjustments and electronic gain changes applied to Test RIA 1-1 data per the review committee approval are presented in Table A-I.

TABLE A-I

POSTTEST DATA ADJUSTMENTS

Measurement	Offset Correction		Electronic Gain Correction	
	Preconditioning and Power Calibration	Power Burst	Preconditioning and Power Calibration	Power Burst
Fuel Rods				
FUEL TEMP 79 03	0	0	0.98	0.98
PLNM TMP 03	0	0	1.0	1.0
CLAD TMP 46-18001	62.6 K	14.0 K	1.0	1.0
CLAD TMP 79-0 01	52.6 K	7.0 K	1.02	1.0
CLAD TMP 46-0 03	73.6 K	0	1.0	1.0
CLAD TMP 79-18003	62.6 K	7.0 K	1.0	1.0
ROD PRES 6.9 KA 01	5.45 MPa	5.1 MPa	1.0	1.0
ROD PRES 6.9 KA 03	7.0 MPa	8.0 MPa	1.0	1.0
Test Train				
INLT TMP 01	0	0	1.0	1.0
INLT TMP 02	-3.0 K	-3.0 K	1.0	1.0
INLT TMP 03	0	0	1.01	1.01
INLT TMP 04/05	-1.0 K	-1.0 K	1.01	1.01
OUT TEMP 01	0	0	1.015	1.015
OUT TEMP 02	0	0	1.01	1.01
OUT TEMP 03	0	0	1.005	1.005
OUT TEMP 04/05	-1.0 K	-1.0 K	1.01	1.01
DEL TEMP 01	-0.9 K	-0.3 K	1.0	1.0
DEL TEMP 02	0	-0.7 K	1.0	1.0
DEL TEMP 03	-2.0 K	0.8 K	1.0	1.0
DEL TEMP 04/05	0.25 K	-0.6 K	1.0	1.0
SYS PRES 69 EG UTT	0.66 MPa		1.02	
SYS PRES 17 KA UTT	0.76 MPa	0.58 MPa	1.0	1.0
SYS PRES SCHAV UTT	-6.78 MPa		1.0	
SHRDPRES 17 KA 01	-1.59 MPa	0	1.0	1.0
SHRDPRES 17 KA 02	2.71 MPa		1.02	1.0
SHRDPRES 17 KA 03	-2.43 MPa	-1.3	1.02	
SHRDPRES 17 KA 04/05	5.27 MPa	0	1.0	1.0

TABLE A-I (continued)

Measurement	Offset Correction		Electronic Gain Correction	
	Preconditioning and Power Calibration	Power Burst	Preconditioning and Power Calibration	Power Burst
Test Train (continued)				
FLOWRATE INLET 01	0	0	1.0	1.0
FLOWRATE INLET 02	0	0	1.0	1.0
FLOWRATE INLET 03	0	0	1.0	1.0
FLOWRATE INLET 04/05	0	0	1.0	1.0
CLAD DSP 01	2.04 mm	6.75 mm	1.0	1.0
CLAD DSP 02	3.01 mm	7.3 mm	1.0	1.0
CLAD DSP 03				
CLAD DSP 04/05	2.90 mm		1.0	
NEUT FLX 9-Q1 TT	0		1.0	
NEUT FLX 27-Q1 TT	0		1.0	
NEUT FLX 46-Q1 TT	0	0	1.0	1.0
NEUT FLX 64-Q1 TT	0	0	1.26	0.95
NEUT FLX 82-Q1 TT	0		1.0	
NEUT FLX 9-Q3 TT	0		1.0	
NEUT FLX 27-Q3 TT	0		1.0	
NEUT FLX 46-Q3 TT	0		1.0	
NEUT FLX 64-Q3 TT	0		1.0	
NEUT FLX 82-Q3 TT	0		1.0	
Plant				
REAC POW 50TR1PT	0.002 MW		1.0	
REAC POW 50KTR1PT		0.2 GW		1.0
REAC POW 50TR2PT	0		1.0	
REAC POW 50KTR2PT				
REAC POW 50EV1PT	0	0	1.0	
REAC POW 50KEV1PT		0.2 GW		1.0
REAC POW 50EV2PT	0		1.0	
REAC POW 50KEV2PT		-1.3 GW		1.0
FP GAMMA NO. 1 FP	0	0	1.0	1.0
FP GAMMA NO. 2 FP		0		1.0
FP GAMMA NO. 3 FP				
FP NEUT FP	0	0	1.0	1.0
LOOP PRES 5-20 PT		-2.03 MPa		1.0
LOOP PRES 5-21 PT		-1.46 MPa		1.0
LOOP PRES 5-22 PT		-1.57 MPa		1.0
LOOP PRES 5-23 PT		1.44 MPa		-1.0

TABLE A-I (continued)

Measurement	Offset Correction		Electronic Gain Correction	
	Preconditioning and Power Calibration	Power Burst	Preconditioning and Power Calibration	Power Burst
Plant (continued)				
LOOP PRES 5-24 PT		1.02 MPa		1.0
LOOP PRES 5-25 PT		-1.01 MPa		1.0
LOOP PRES 5-34 PT		2.47 MPa		1.0
LOOP PRES 5-35 PT				

APPENDIX B

UNCERTAINTY ANALYSIS

APPENDIX B

UNCERTAINTY ANALYSIS

Analyses have been performed on selected representative data from the power burst phase of Test RIA 1-1 to provide a guide to the uncertainty associated with data measurements in the PBF system. Three possible sources of data measurement error were analyzed – conversion to engineering unit uncertainties, bias uncertainties due to offset applications, and random variations in the data. These sources are not inclusive of all the uncertainties that may exist in most measurements and therefore should not be considered indicative of the total uncertainty levels in the Test RIA 1-1 data.

(1) Conversion to engineering unit uncertainties. During the calibration and development of engineering unit conversion polynomials, a value for the standard deviation (σ) of each measurement was determined.

The first column of Table B-I lists these 2-σ deviations assigned to each measurement.

(2) Bias uncertainties for applied offsets. All data in this report were reviewed to determine the quality and validity of the data. Each measurement was compared with redundant or similar measurements, calculated values, and initial conditions to determine the required offsets or adjustments. The bias uncertianties are the expected errors in the offsets that were applied to the data. These 2-σ deviations are listed in the second column of Table B-I.

(3) Random variations in the data. Representative data from Test RIA 1-1 have been selected to provide a guide to variations in the data determined from analysis of the data itself. The selected data traces were empirically fitted with a linear difference equation, which was subject to a white noise input at each sampling time point. The object of the empirical fitting procedure was to characterize the white noise, which was taken to represent the random variability. The procedures for fitting the difference equation are discussed in depth in Reference B-1. A data trace was often segmented and different equations were fitted to each segment with statistical correlations between successive observations accounted for by the fitting procedure. The white noise input was assumed to arise from a normally distributed population. The standard deviation of the white noise as derived from the fitting procedures was taken as an estimate of the random uncertainty standard deviation, and has

TABLE B-I

MEASUREMENT UNCERTAINTIES FOR TEST RIA 1-1

	Engineering Unit Conversion Uncertainties (2σ)	Bias for Applied Offsets (2σ)	Figure Showing Random Uncertainty for Selected Data
Fuel Rods			
FUEL TMP 79 03	±25.7 K	±3.0 K	B-1
PLNM TMP 03	± 1.47 K	±2.0 K	
CLAD TMP 46-18001	± 1.06 K	±2.0 K	B-2, B-3
CLAD TMP 79-0 01	± 1.06 K	±2.0 K	B-4, B-5
CLAD TMP 46-0 03	± 1.06 K	±2.0 K	B-6, B-7
CLAD TMP 79-18003	± 1.06 K	±2.0 K	B-8, B-9
ROD PRES 6.9 KA 01	NA	None	
ROD PRES 6.9 KA 03	NA		
Test Train			
INLT TMP 01	± 1.47 K	±1.0 K	B-12
INLT TMP 02	± 1.47 K	±1.0 K	B-13
INLT TMP 03	± 1.47 K	±1.0 K	
INLT TMP 04/05	± 1.47 K	±1.0 K	
OUT TEMP 01	± 1.47 K	±1.0 K	B-14
OUT TEMP 02	± 1.47 K	±1.0 K	B-15
OUT TEMP 03	± 1.47 K	±1.0 K	
OUT TEMP 04/05	± 1.47 K	±1.0 K	
DEL TEMP 01	± 0.92 K	±0.1 K	B-16
DEL TEMP 02	± 0.06 K	±0.1 K	B-17
DEL TEMP 03	± 0.17 K	±0.1 K	
DEL TEMP 04/05	± 0.53 K	±0.1 K	
SYS PRES 69EG UTT	NA	±0.1 MPa	
SYS PRES 17KA UTT	NA	±0.1 MPa	B-18
SYS PRES SCHAV UTT	NA	±0.1 MPa	
SHRD PRES 17KA 01	± 0.15 MPa	±0.1 MPa	B-19
SHRD PRES 17KA 02	± 0.15 MPa	±0.1 MPa	
SHRD PRES 17KA 03	± 0.18 MPa	±0.1 MPa	
SHRD PRES 17KA 04/05	± 0.09 MPa	±0.1 MPa	

TABLE B-I (continued)

	Engineering Unit Conversion Uncertainties (2σ)	Bias for Applied Offfsets (2σ)	Figure Showing Random Uncertainty for Selected Data
Test Train (continued)			
FLOWRATE INLET 01	$\pm$ 1.23 x 10^{-3} l/s	$\pm$0.005 l/s	B-10
FLOWRATE INLET 02	$\pm$ 1.05 x 10^{-3} l/s	$\pm$0.005 l/s	D-11
FLOWRATE INLET 03	$\pm$ 2.04 x 10^{-3} l/s	$\pm$0.005 l/s	
FLOWRATE INLET 04/05	$\pm$ 1.79 x 10^{-3} l/s	$\pm$0.005 l/s	
CLAD DSP 01	NA	$\pm$0.02 mm	
CLAD DSP 02	NA	$\pm$0.02 mm	
CLAD DSP 03	NA	$\pm$0.02 mm	
CLAD DSP 04/05	NA	$\pm$0.02 mm	
NEUT FLX 9-Q1 TT	NA	0	
NEUT FLX 27-Q1 TT	NA	0	
NEUT FLX 46-Q1 TT	NA	0	
NEUT FLX 64-Q1 TT	NA	0	
NEUT FLX 82-Q1 TT	NA	0	
NEUT FLX 9-Q3 TT	NA	0	
NEUT FLX 27-Q3 TT	NA	0	
NEUT FLX 46-Q3 TT	NA	0	
NEUT FLX 64-Q3 TT	NA	0	
NEUT FLX 82-Q3 TT	NA	0	
Plant			
REAC POW 50TR1PT	NA	$\pm$0.0005 MW	
REAC POW 50KTR1PT	NA	$\pm$0.01 GW	
REAC POW 50TR2PT	NA	0	
REAC POW 50KTR2PT	NA	$\pm$0.01 GW	
REAC POW 50EV1PT	NA	0	
REAC POW 50KEV1PT	NA	$\pm$0.01 GW	
REAC POW 50EV2PT	NA	0	
REAC POW 50KEV2PT	NA	$\pm$0.01 GW	
FP GAMMA NO. 1 FP	NA	None	
FP GAMMA NO. 2 FP	NA	None	
FP GAMMA NO. 3 FP	NA	None	
FP NEUT FP	NA	None	

TABLE B-I (continued)

			Engineering Unit Conversion Uncertainties (2σ)	Bias for Applied Offfsets (2σ)	Figure Showing Random Uncertainty for Selected Data
Plant (continued)					
LOOPPRES	5-20	PT	0.182 MPa	±0.1 MPa	
LOOPPRES	5-21	PT	0.159 MPa	±0.1 MPa	
LOOPPRES	5-22	PT	0.160 MPa	±0.1 MPa	
LOOPPRES	5-23	PT	0.150 MPa	±0.1 MPa	
LOOPPRES	5-24	PT	0.207 MPa	±0.1 MPa	
LOOPPRES	5-25	PT	0.128 MPa	±0.1 MPa	
LOOPPRES	5-34	PT	0.117 MPa	±0.1 MPa	
LOOPPRES	5-35	PT	0.113 MPa	±0.1 MPa	

been plotted as an upper and lower uncertainty band. Since these 2σ bands were found to be small, they are presented in this appendix in Figures B-1 through B-19 without the corresponding data which fit within the error bands. If any filtering process is applied to the original data the random uncertainty obtained from the original data would no longer precisely apply.

The values listed in Table B-I and the random uncertainty plots correspond to $1.96\,\sigma$ which represents a 95% confidence level.

The method used to estimate the random component of the uncertainty was observed to tend to reflect the total noise content of the data that arises from sample repeatability, electrical noise, the measured event, and extraneous phenomenon occurring during the test. To rigorously characterize the separate random components of a measurement would be difficult, although one or more of these components could possibly be filtered from the noise which was used to determine the random uncertainty.

Other random and systematic uncertainties exist in the data but they could not be adequately analyzed for this report. These uncertainties include measurement dependent and independent uncertainties. A detailed and comprehensive measurement independent uncertainty analysis of the PBF measurement system is currently in progress.

The measurement dependent uncertainties are the most difficult to analyze and will probably never be rigorously presented in an experiment data report (EDR).

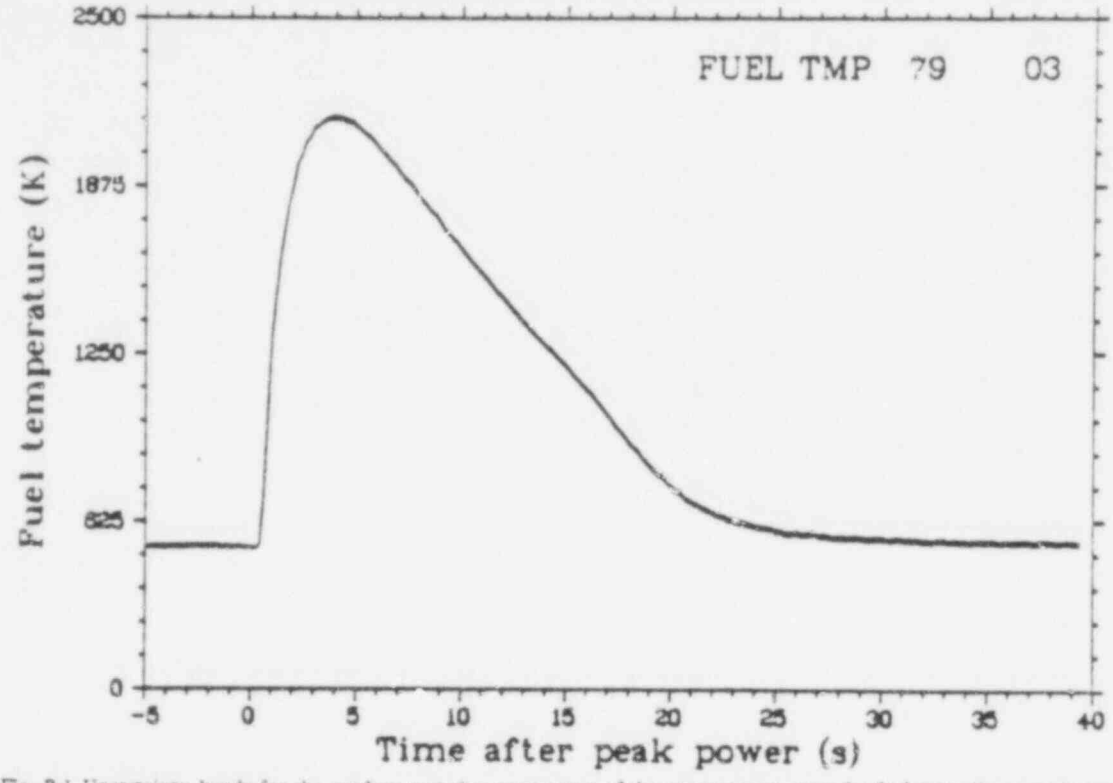

Fig. B-1 Uncertainty bands for the random variation component of the measurement error for fuel centerline temperature in Rod 801-3, 0.79 m above fuel stack bottom (FUEL TMP 79 03), from -5 to 40 s.

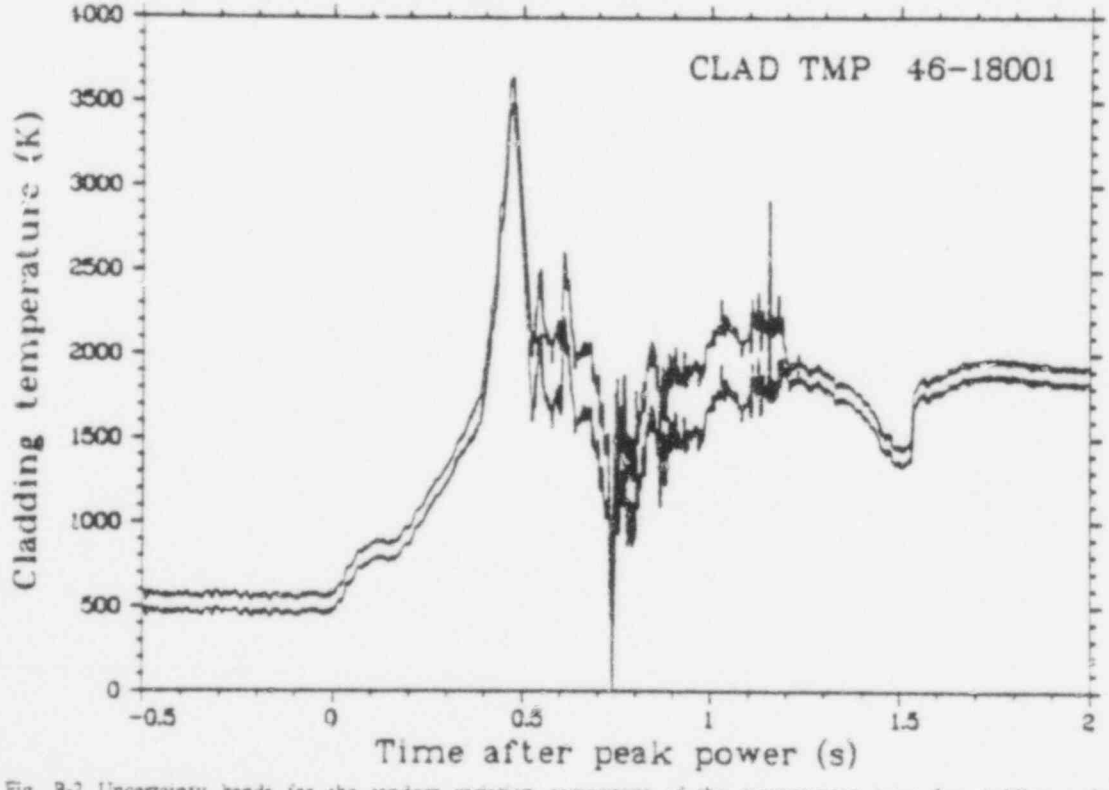

Fig. B-2 Uncertainty bands for the random variation component of the measurement error for cladding surface temperature of Rod 801-1, 0.46 m above fuel stack bottom (CLAD TMP 46-18001), from -0.5 to 2 s.

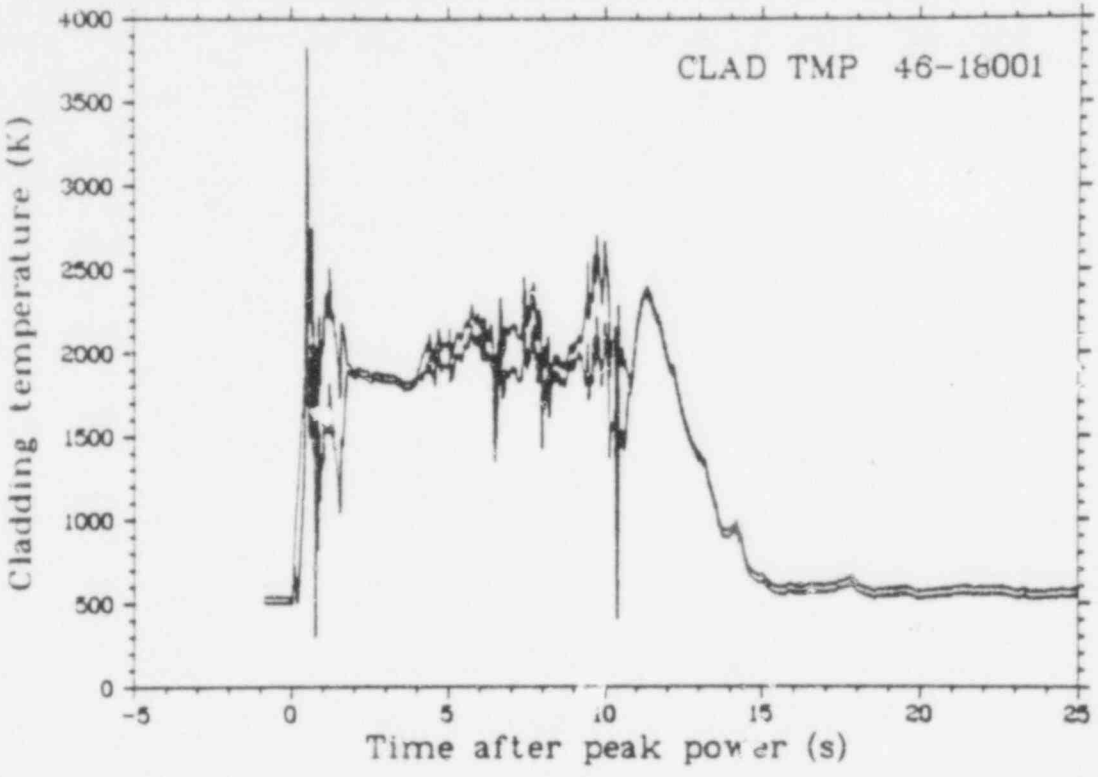

Fig. B-3 Uncertainty bands for the random variation component of the measurement error for cladding surface temperature of Rod 801-1, 0.46 m above fuel stack bottom (CLAD TMP 46-18001), from -5 to 25 s.

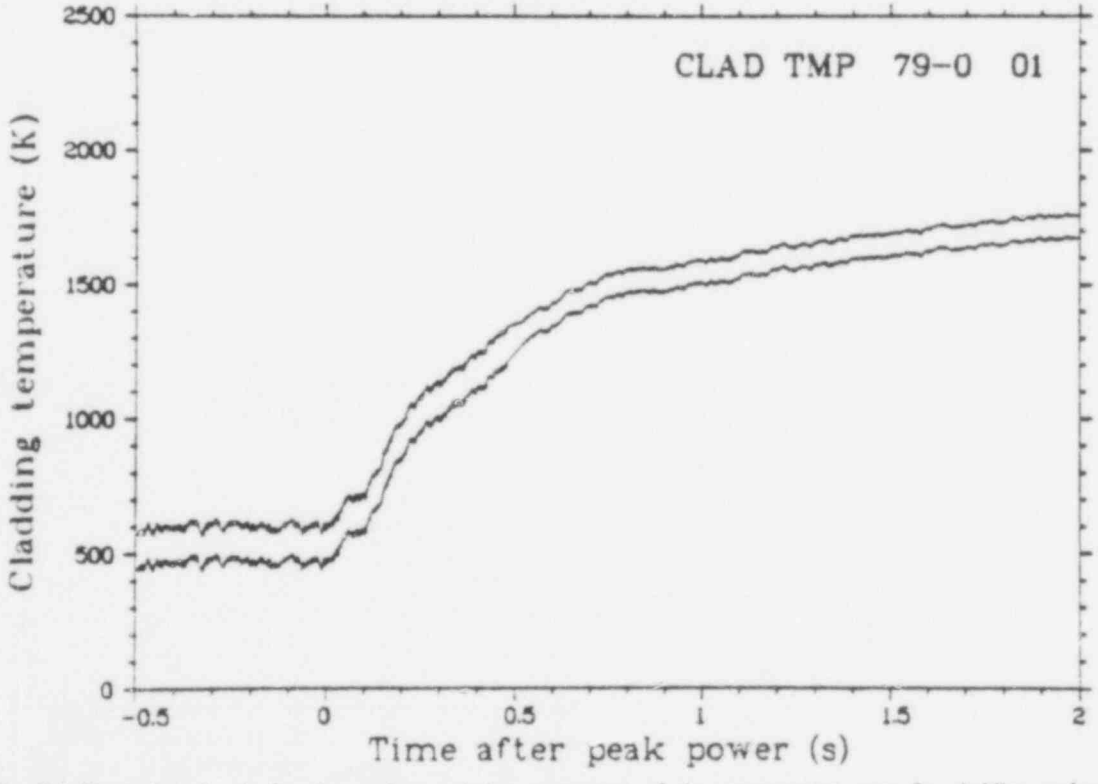

Fig. B-4 Uncertainty bands for the random variation component of the measurement error for cladding surface temperature of Rod 801-1, 0.79 m above fuel stack bottom (CLAD TMP 79-0 01), from -0.5 to 2 s.

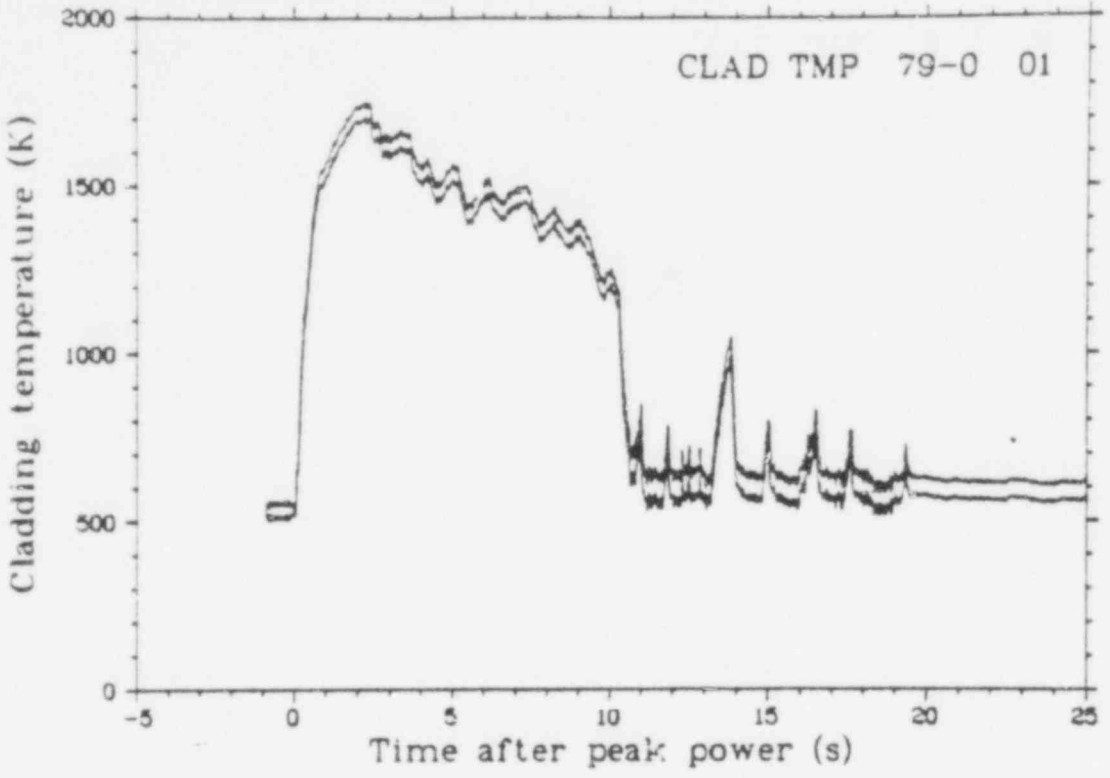

Fig. B-5 Uncertainty bands for the random variation component of the measurement error for cladding surface temperature of Rod 801-1, 0.79 m above fuel stack bottom (CLAD TMP 79-0 01), from -5 to 25 s.

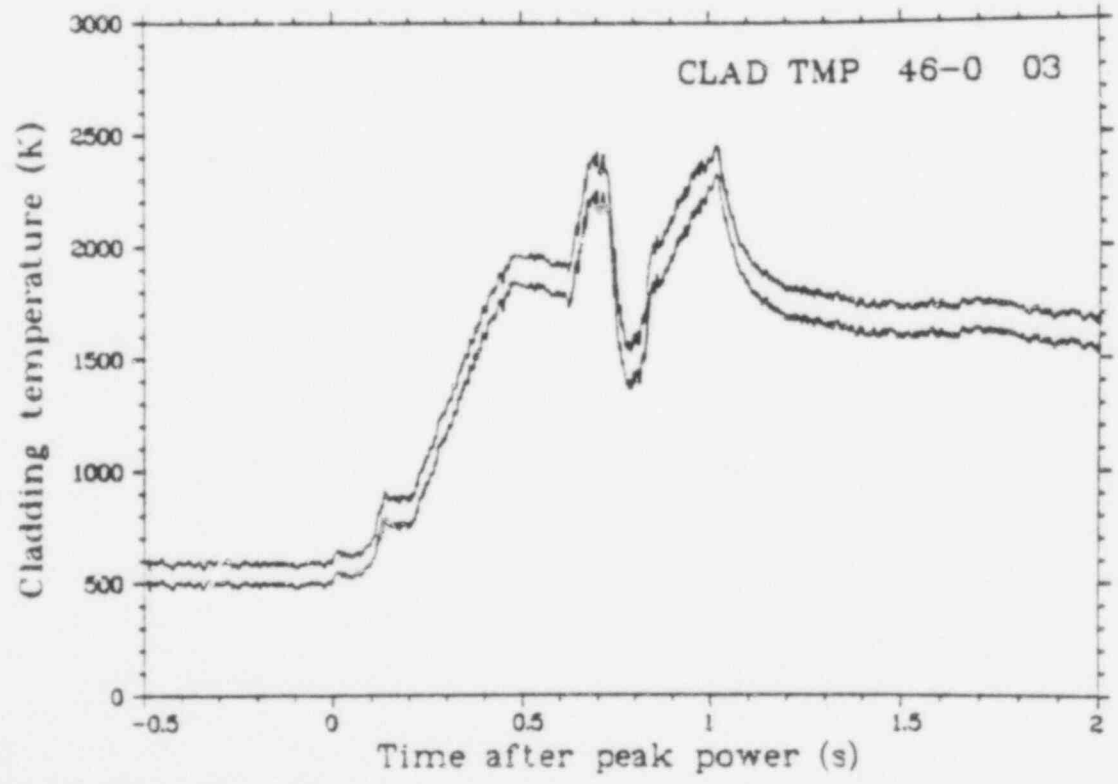

Fig. B-6 Uncertainty bands for the random variation component of the measurement error for cladding surface temperature of Rod 801-3, 0.46 m above fuel stack bottom (CLAD TMP 46-0 03), from -0.5 to 2 s.

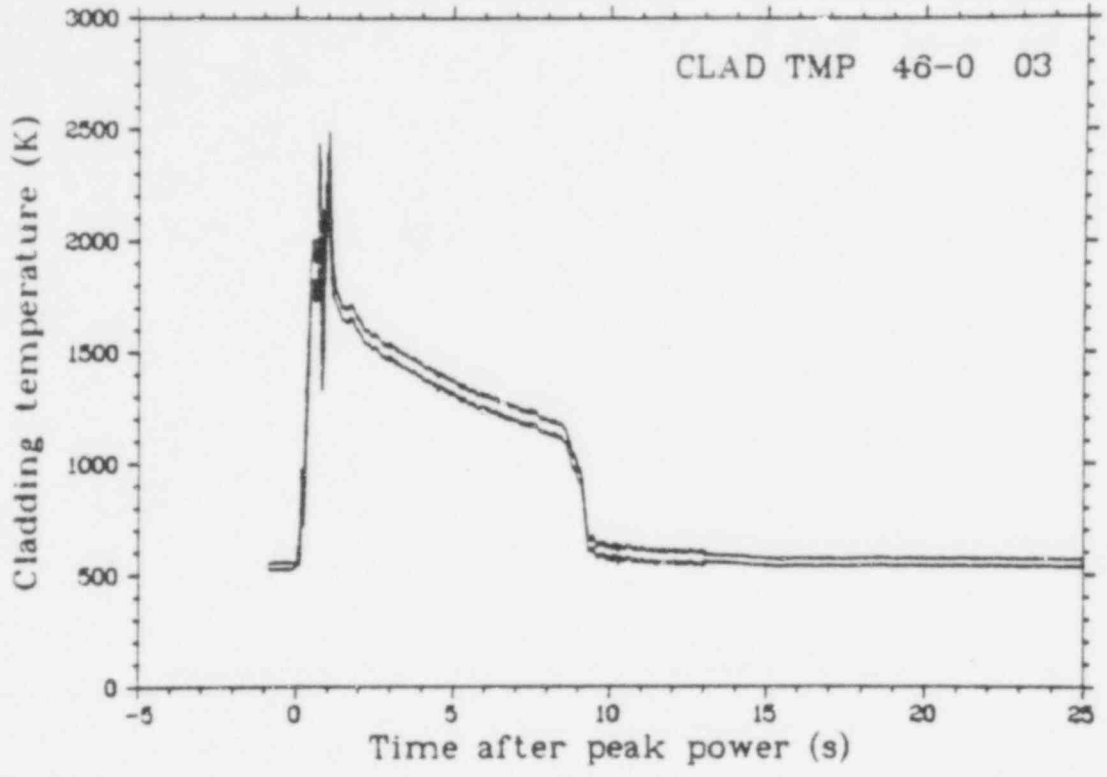

Fig. B-7 Uncertainty bands for the random variation component of the measurement error for cladding surface temperature of Rod 801-3, 0.46 m above fuel stack bottom (CLAD TMP 46-0 03), from -5 to 25 s.

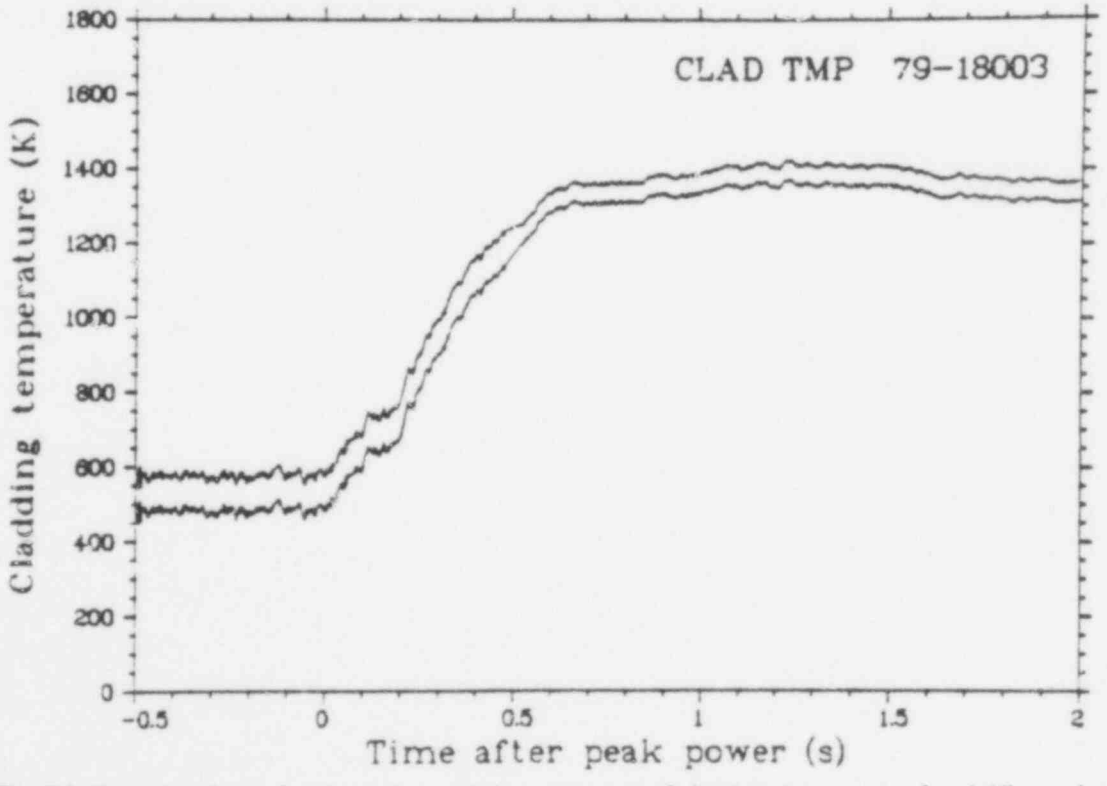

Fig. B-8 Uncertainty bands for the random variation component of the measurement error for cladding surface temperature of Rod 801-3, 0.79 m above fuel stack bottom (CLAD TMP 79-18003), from -0.5 to 2 s.

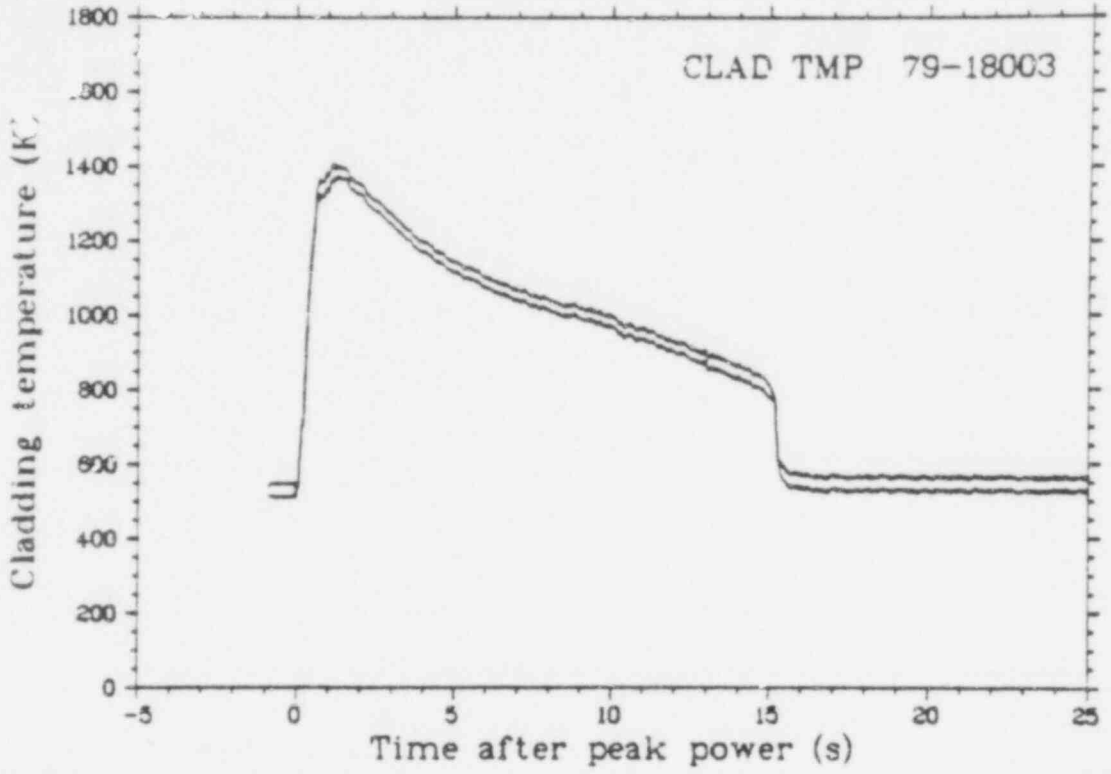

Fig. B-9 Uncertainty bands for the random variation component of the measurement error for cladding surface temperature of Rod 801-3, 0.79 m above fuel stack bottom (CLAD TMP 79-18003), from -5 to 25 s.

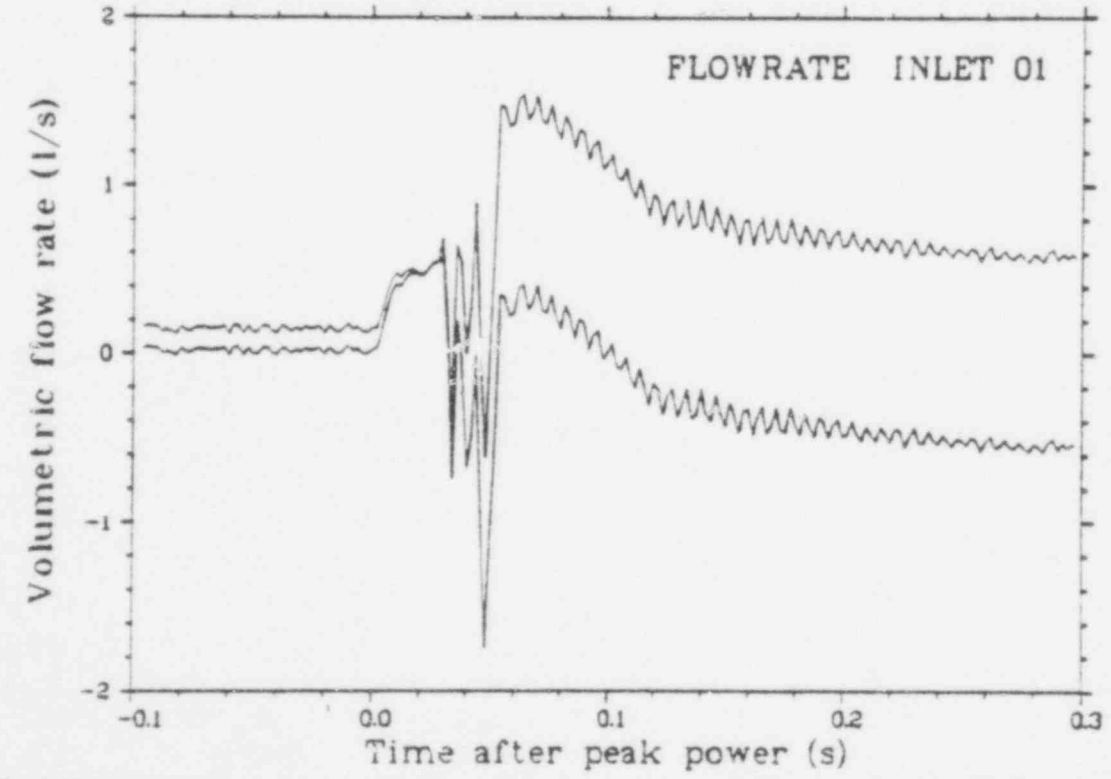

Fig. B-10 Uncertainty bands for the random variation component of the measurement error for volumetric flow rate in Fuel Rod 801-1 shroud inlet (FLOWRATE INLET 01), from -0.1 to 0.3 s.

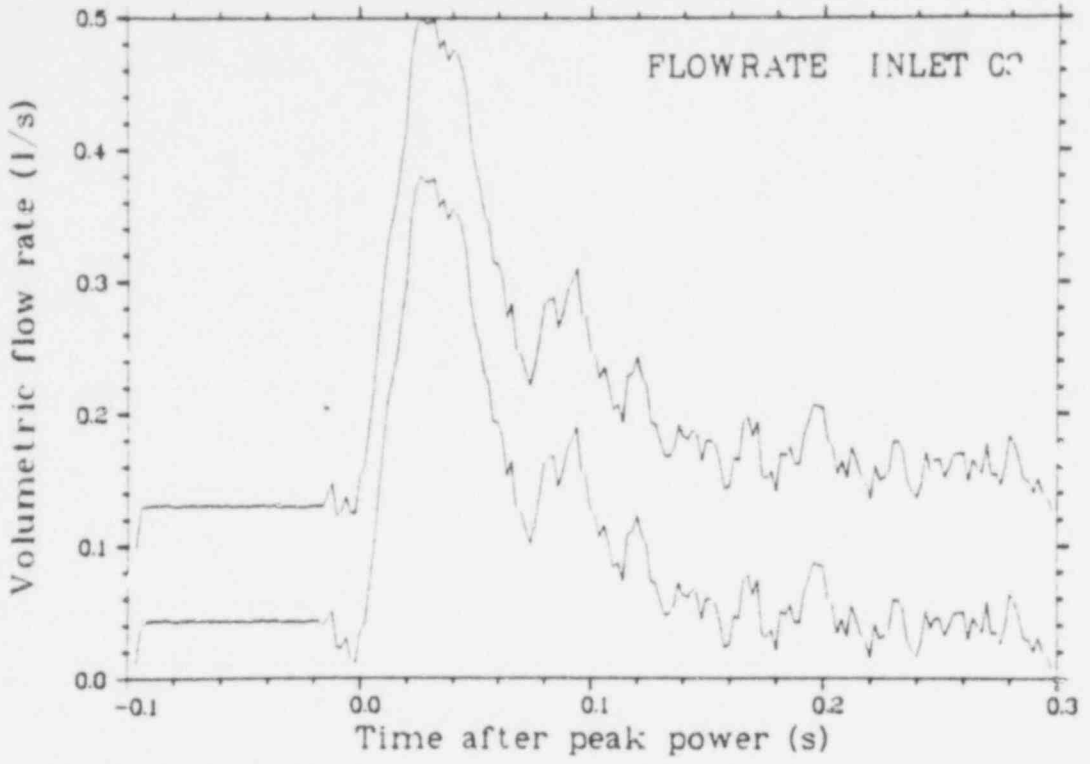

Fig. B-11 Uncertainty bands for the random variation component of the measurement error for volumetric flow rate in Fuel Rod 801-2 shroud inlet (FLOWRATE INLET 02), from -0.1 to 0.3 s.

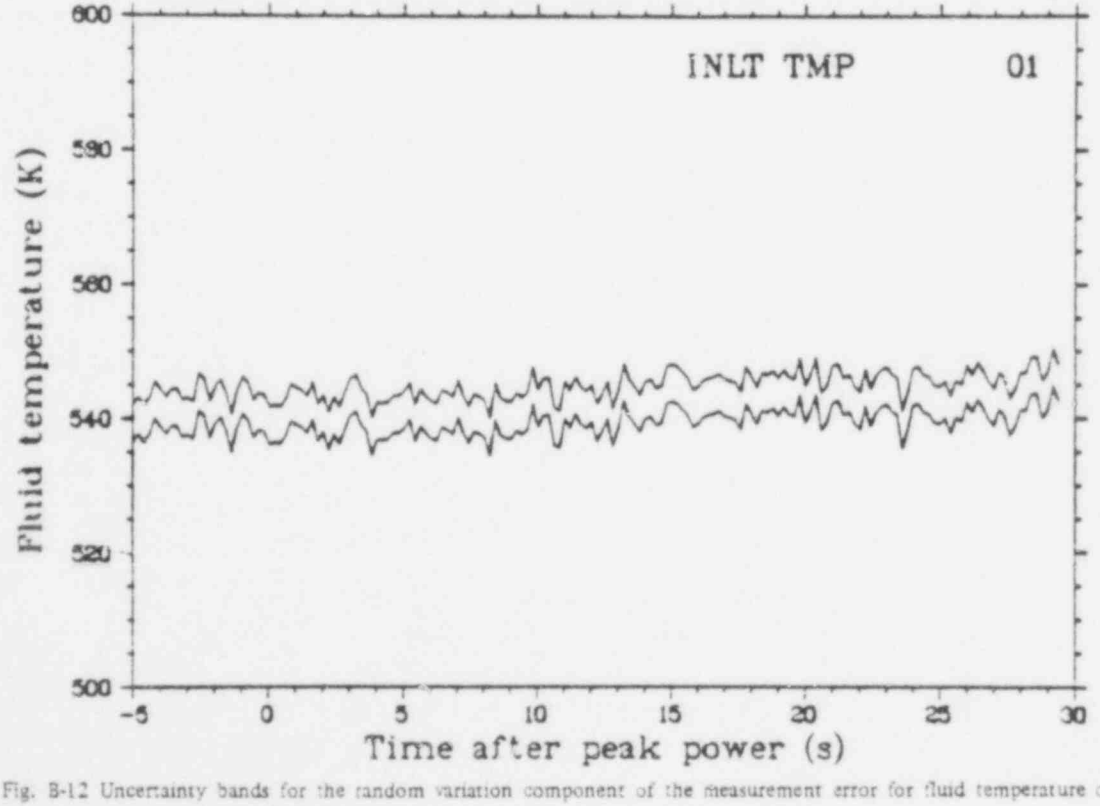

Fig. B-12 Uncertainty bands for the random variation component of the measurement error for fluid temperature of Rod 801-1 coolant inlet (INLT TMP 01), from -5 to 30 s.

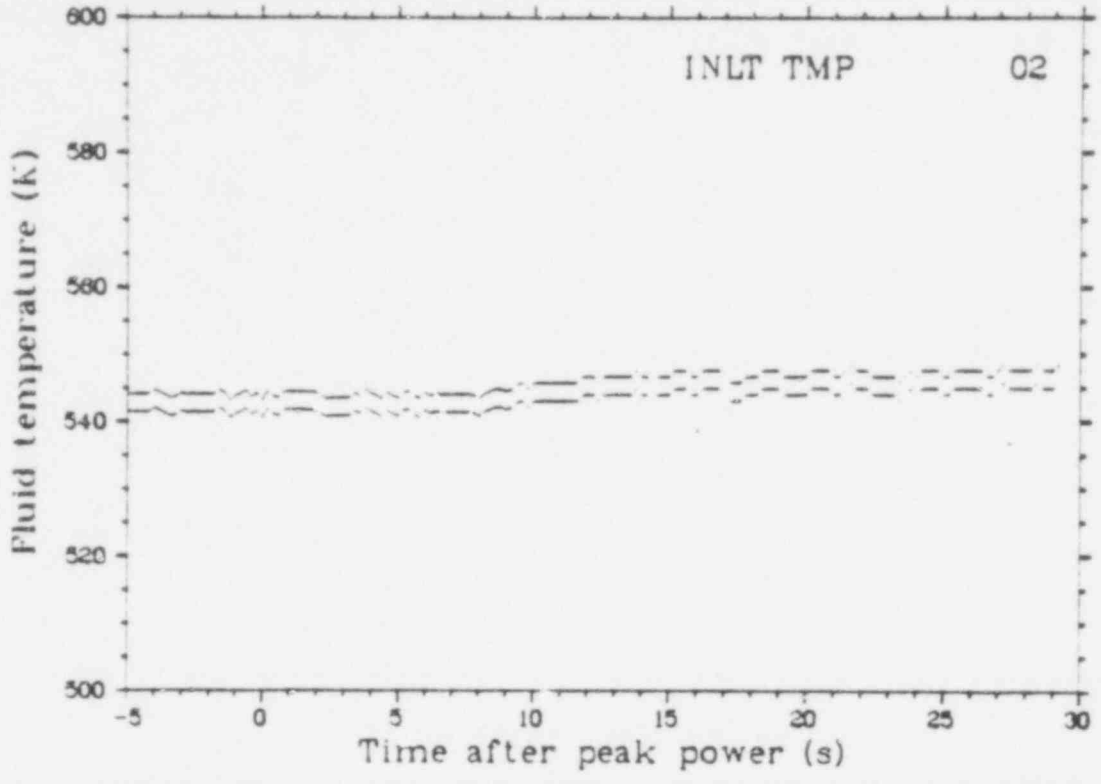

Fig. B-13 Uncertainty bands for the random variation component of the measurement error for fluid temperature of Rod 801-2 coolant inlet (INLT TMP 02), from -5 to 30 s.

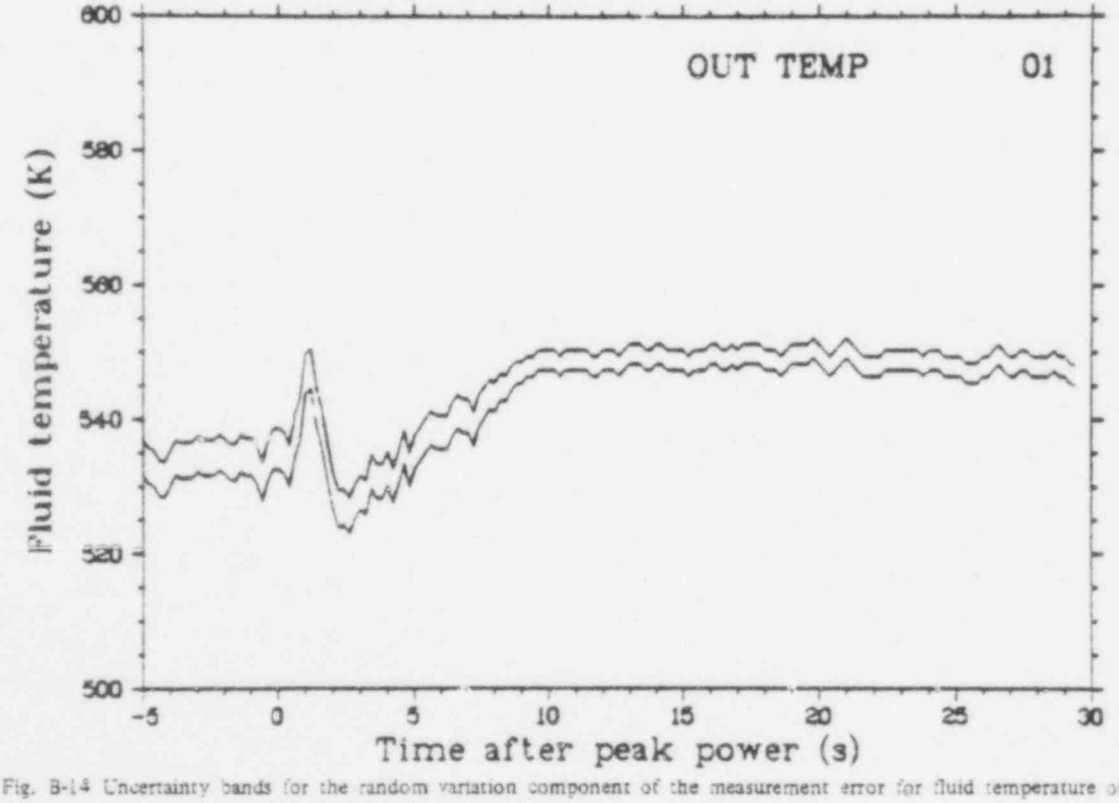

Fig. B-14 Uncertainty bands for the random variation component of the measurement error for fluid temperature of Rod 801-1 coolant outlet (OUT TEMP 01), from -5 to 30 s.

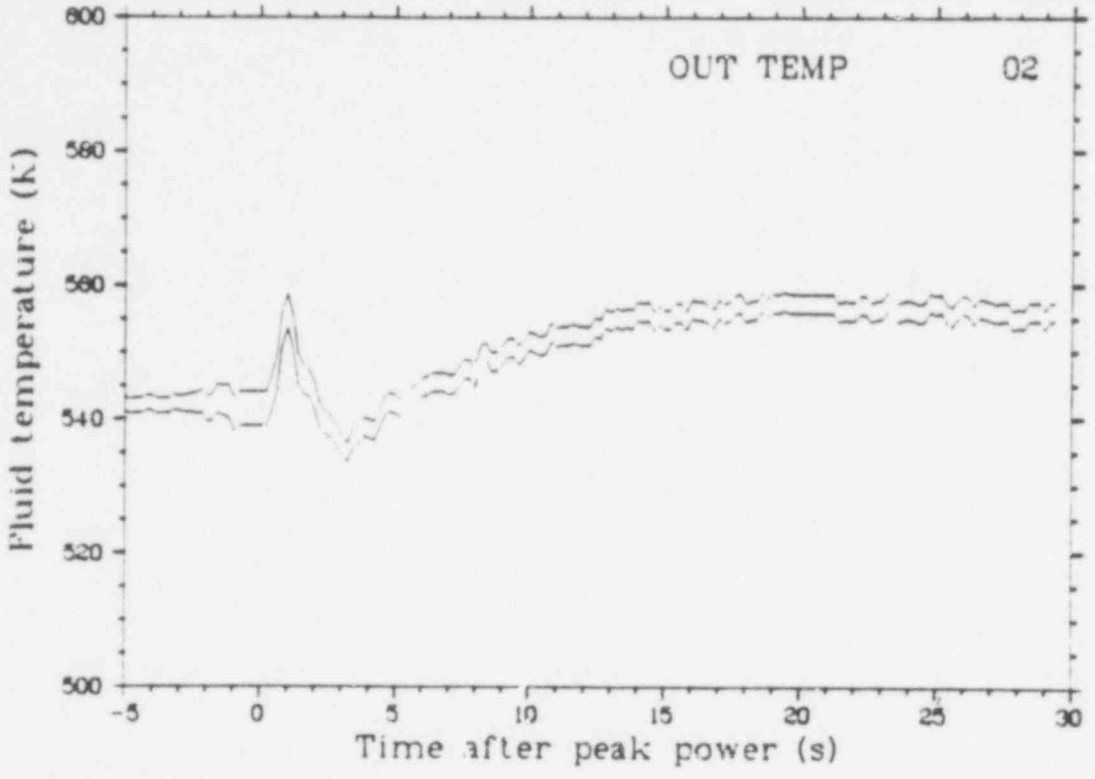

Fig. B-15 Uncertainty bands for the random variation component of the measurement error for fluid temperature of Rod 801-2 coolant outlet (OUT TEMP 02), from -5 to 30 s.

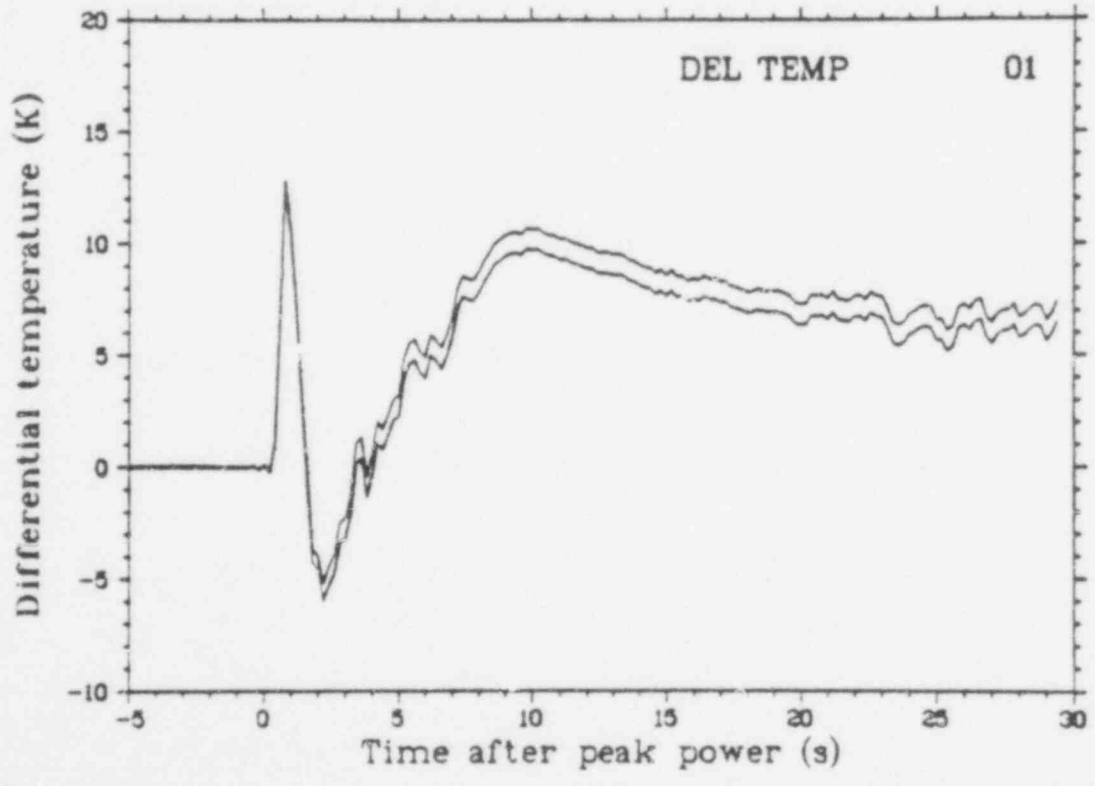

Fig. B-16 Uncertainty bands for the random variation component of the measurement error for differential temperature of Rod 801-1 coolant inlet and outlet (DEL TEMP 01), from -5 to 30 s.

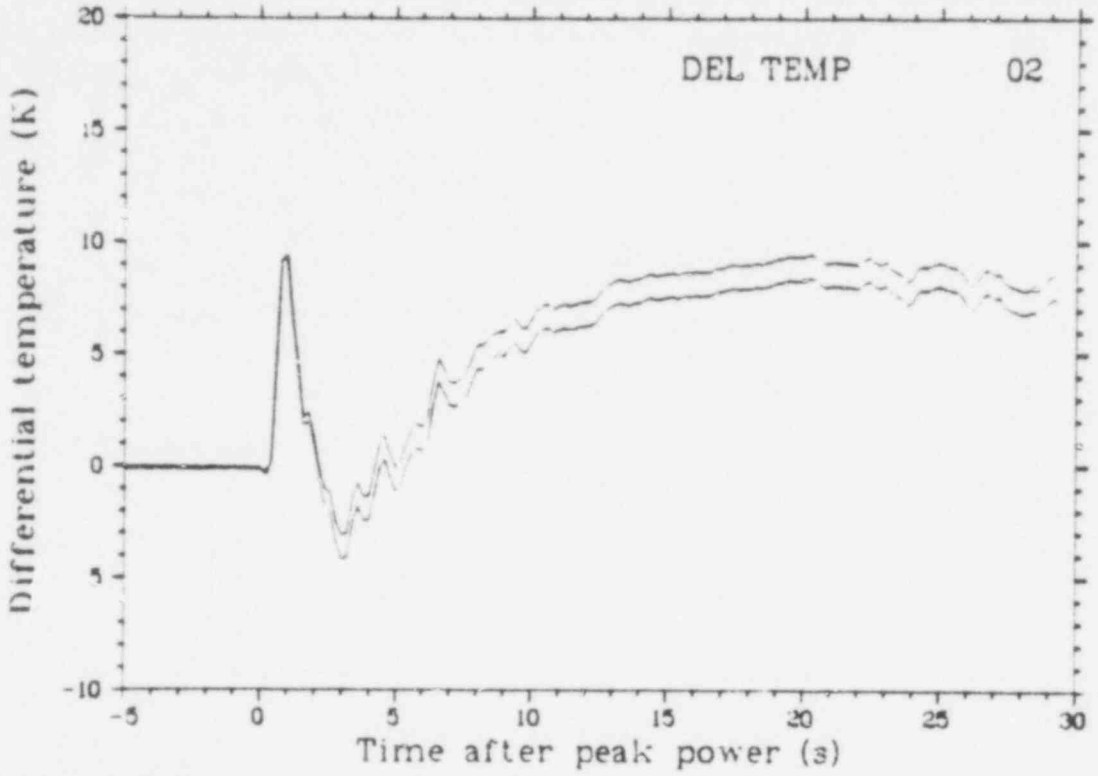

Fig. B-17 Uncertainty bands for the random variation component of the measurement error for differential temperature of Rod 801-2 coolant inlet and outlet (DEL TEMP 02), from -5 to 30 s.

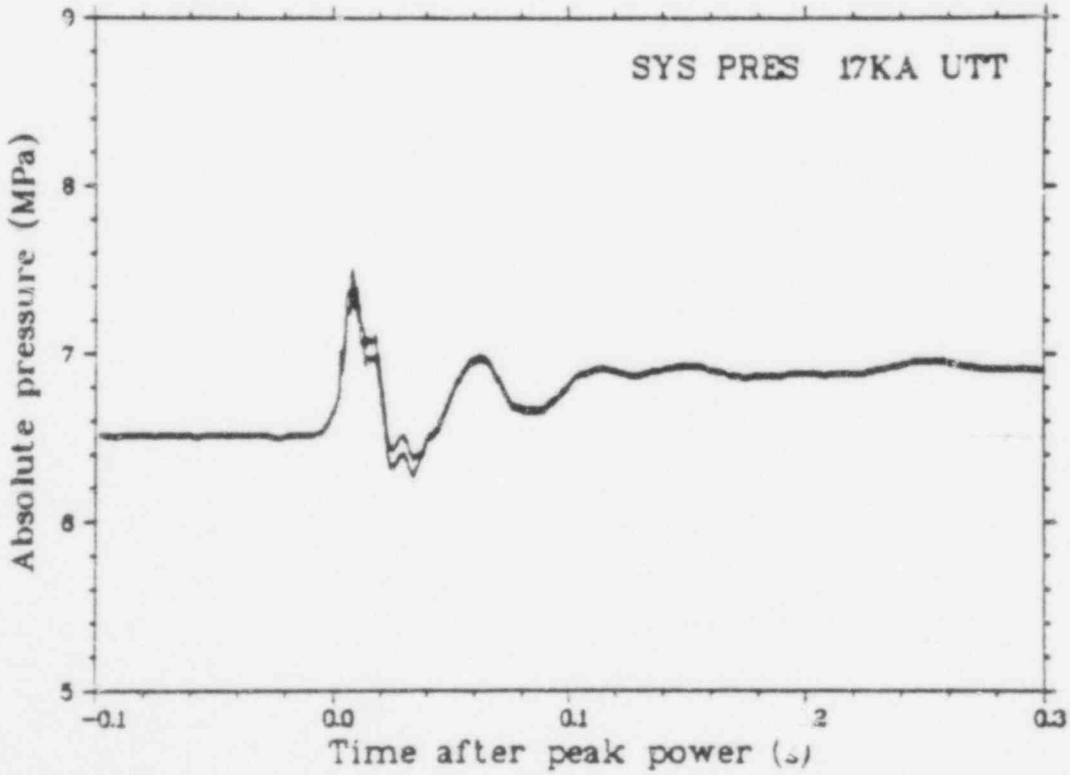

Fig. B-18 Uncertainty bands for the random variation component of the measurement error for absolute pressure in upper test train assembly (SYS PRES 17KA UTT), from -0.1 to 0.3 s.

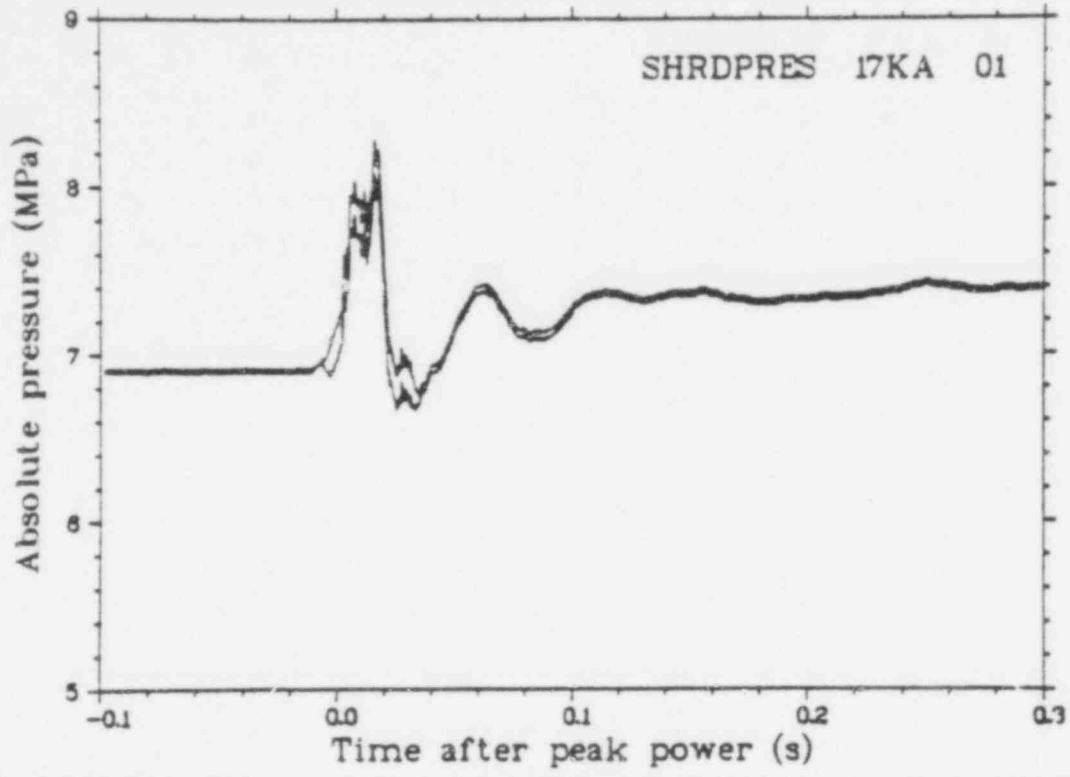

Fig. B-19 Uncertainty bands for the random variation component of the measurement error for absolute pressure inside Rod 801-1 shroud (SHRD PRESS 17KA 01), from -0.1 to 0.3 s.

REFERENCE

B-1 G. E. P. Box and B. M. Jenkins, *Time Series Analysis – Forecasting and Control*, San Francisco: Holden-Day, 1970.

DISTRIBUTION RECORD FOR NUREG/CR-0516
(TREE-1236)

Internal Distribution

1 - R. J. Beers, ID

2 - P. E. Litteneker, ID

3-5 - INEL Technical Library

6-8 - Author

9-50 - Special Internal

External Distribution

51-52 - Saul Levine, Director
Office of Nuclear Regulatory Research, NRC
Washington, D. C. 20555

53-58 - Special External

59-355 - Distribution under R3, Water Reactor Safety Research - Fuel Behavior.